AD-A112 117 MICHIGAN UNIV ANN ARBOR ELECTRON PHYSICS LAB F/G 9/5
NEAR-MILLIMETER-WAVE SOLID-STATE SOURCES--LIMITATIONS AND CONTR--ETC(U)
JAN 82 D F PETERSON, G I HADDAD, Y S HWANG DAAG29-79-G-0034
UNCLASSIFIED ARO-15951.1-EL NL

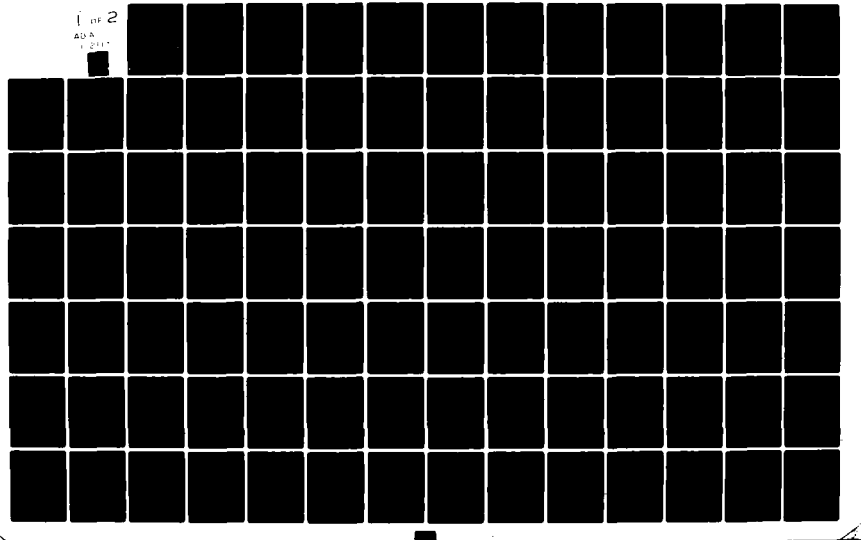

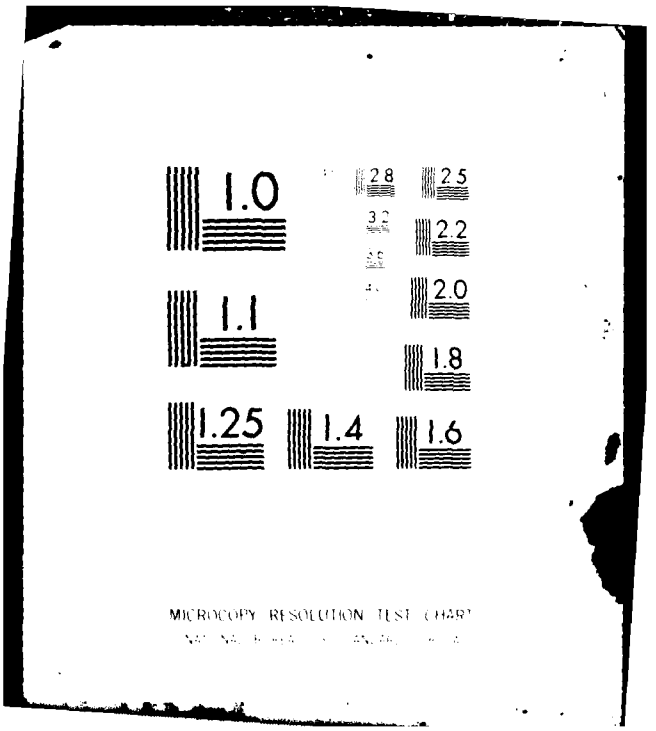
1.0
1.1
1.25
1.4
1.6
2.8
2.5
2.2
2.0
1.8
MICROCOPY RESOLUTION TEST CHART

NEAR-MILLIMETER-WAVE SOLID-STATE SOURCES-- LIMITATIONS AND CONTROL OF PULSED AND INJECTION-LOCKED IMPATT DIODE MILLIMETER-WAVE OSCILLATORS

Final Report

D. F. Peterson
G. I. Haddad
Y. S. Hwang

January 1982

U. S. Army Research Office

Grant No. DAAG29-79-G-0034

Electron Physics Laboratory
Department of Electrical and Computer Engineering
The University of Michigan
Ann Arbor, MI 48109

UNCLASSIFIED

SECURITY CLASSIFICATION OF THIS PAGE (When Data Entered)

REPORT DOCUMENTATION PAGE

READ INSTRUCTIONS BEFORE COMPLETING FORM

1. REPORT NUMBER	2. GOVT ACCESSION NO. AD-A112117
	3. RECIPIENT'S CATALOG NUMBER
4. TITLE (and Subtitle) NEAR-MILLIMETER-WAVE SOLID-STATE SOURCES--LIMITATIONS AND CONTROL OF PULSED AND INJECTION-LOCKED IMPATT DIODE MILLIMETER-WAVE OSCILLATORS	5. TYPE OF REPORT & PERIOD COVERED Final Report 1 Dec 1978 - 30 Nov 1981
	6. PERFORMING ORG. REPORT NUMBER
7. AUTHOR(s) D. F. Peterson, G. I. Haddad, Y. S. Hwang	8. CONTRACT OR GRANT NUMBER(s) DAAG29-79-G-0034
9. PERFORMING ORGANIZATION NAME AND ADDRESS Electron Physics Laboratory The University of Michigan Ann Arbor, MI 48109	10. PROGRAM ELEMENT, PROJECT, TASK AREA & WORK UNIT NUMBERS
11. CONTROLLING OFFICE NAME AND ADDRESS U. S. Army Research Office Post Office Box 12211 Research Triangle Park, NC 27709	12. REPORT DATE January 1982
	13. NUMBER OF PAGES 110
14. MONITORING AGENCY NAME & ADDRESS(if different from Controlling Office)	15. SECURITY CLASS. (of this report) Unclassified
	15a. DECLASSIFICATION/DOWNGRADING SCHEDULE

16. DISTRIBUTION STATEMENT (of this Report)

Approved for public release; distribution unlimited.

17. DISTRIBUTION STATEMENT (of the abstract entered in Block 20, if different from Report)

NA

18. SUPPLEMENTARY NOTES

The view, opinions, and/or findings contained in this report are those of the author(s) and should not be construed as an official Department of the Army position, policy, or decision, unless so designated by other documentation.

19. KEY WORDS (Continue on reverse side if necessary and identify by block number)

Millimeter wavelengths	Turn-on transient
Oscillators	Turn-on jitter
IMPATT diodes	Injection locking
Pulsed oscillators	Quasi-statics
Frequency chirp	IMPATT and circuit impedance

20. ABSTRACT (Continue on reverse side if necessary and identify by block number)

The limitations and control of pulsed IMPATT diode millimeter-wavelength oscillators are described. A quasi-static oscillator model is established for characterizing amplitude and frequency behavior during pulsed operation in response to external influences such as bias current, temperature, optical injection, locking signal injection and RF circuit. The effect of these external parameters in oscillator turn-on, turn-off, frequency chirp during the pulse, and start-up jitter are given for a millimeter-wavelength oscillator using a Si double-drift diode. Methods of controlling

DD FORM 1 JAN 73 1473 EDITION OF 1 NOV 65 IS OBSOLETE

UNCLASSIFIED

SECURITY CLASSIFICATION OF THIS PAGE (When Data Entered)

20. ABSTRACT CONTINUED

the pulsed behavior are also presented for this oscillator example. The effect of device and circuit parameters on performance are also given.

FOREWORD

This technical report on near millimeter-wave solid-state sources deals primarily with the limitations and control of pulsed IMPATT-diode millimeter-wavelength oscillators for radar systems and other applications. Additional work performed under this grant, dealing with optical effects in millimeter-wave IMPATT devices is included as a supplement ("Optical Effects in Millimeter-Wave IMPATT Diodes," by M. Y. Burmawi, Technical Report No. 153, Electron Physics Laboratory, Department of Electrical and Computer Engineering, The University of Michigan, Ann Arbor, October 1981).

TABLE OF CONTENTS

LIST OF ILLUSTRATIONS

SECTION 1. INTRODUCTION

1.1 Millimeter-Wave Applications of IMPATT Diodes

IMPATT devices provide an extremely important source of solid-state power generation, particularly in the millimeter-wave frequency range from 30 to 300 MHz (10- to 1-mm wavelength). While atmospheric absorption caused by a combination of water vapor and oxygen molecular resonances[1] are significant in this region of the spectrum, relatively transparent windows exist at 35, 94, 140 and 225 GHz where the advantages of millimeter-wave systems are possible. These advantages are large data bandwidth, small antenna size, low detection probability, and high anti-jam capability[2].

Millimeter-waves have applications in radar, communication and medicine. Millimeter-wave radar systems make use of a variety of coherent, noncoherent pulse, pulse doppler FM-CW and pulse compression techniques. The size, reliability, and power generating capability of IMPATT devices are particularly well suited to many of these applications.

1.2 Pulsed Oscillators and Their Applications

A fundamental problem with all solid-state devices including IMPATT diodes is the reduction in their power generating capability as frequency increases (pf^2 = constant). RF power generated from the active device becomes limited at millimeter-wave frequencies. For CW operation the maximum current density, and hence power output, is limited thermally, while pulsed operation can increase this peak

power depending on the pulsewidth and duty cycle. For very short pulsewidth and low duty cycle as required in many millimeter-wave pulsed applications, the generated power is no longer thermally limited. The current density can be increased to obtain more power until space charge effects cause power and efficiency to decline. Since the diode output power increases with current density, pulsed operation is often required to generate the power levels necessary in this frequency range. Other problems of the pulsed oscillator include turn-on jitter in the leading edge envelope of the output power and power variation (AM) and frequency chirp (FM) during the pulse.

Pulsed oscillators are used as transmitters in pulsed radar systems. Resolution and maximum range are two of the important parameters of radar systems, and the range resolution of a radar set is determined by pulsewidth. High resolution requires short pulsewidth with stable, clean operation of the transmitter oscillator. The maximum range (r_{max}) attainable depends on the reflecting properties of the object as well as the characteristics of the radar. The effectiveness of the transmitter in making r_{max} large is measured by the product of peak power and pulsewidth (the energy of each pulse transmitted).

1.3 Goals of the Present Study

Significant research has been done on the device properties and design criteria for optimizing the output power. However, additional work is required for improved understanding of device-circuit interaction, noise reduction techniques, and methods to control the oscillator frequency, particularly in pulsed operation.

The purpose of this study is to develop an oscillator model which can be used to investigate the behavior of pulsed and CW oscillators. Analytical equations, adequate device characterization, RF circuit models, bias circuit considerations, and computer simulations are used to study the starting transients and behavior of the pulsed IMPATT oscillators.

With this model, a more comprehensive understanding of oscillator properties primarily in the millimeter-wave frequency range can be achieved. These properties are transient and dynamic effects in pulsed and injection locked oscillators, the relation of circuit to oscillator behavior and design criteria for stable ("clean") operation, the effect of external influences (such as bias current, bias circuit, RF circuit, temperature and light) on device behavior and performance as oscillators. Techniques and device design to control the post turn-on transients are important and require further study.

In Section 2 an oscillator model is developed, and the equations governing the behavior of oscillators and device junction temperature are given. Device parameters (device admittance, thermal resistance and thermal time constant) and circuit admittance presented to the device which are required for the oscillator analysis are discussed briefly. The usefulness of this model to predict the behavior of pulsed oscillators and their limitations is described. Turn-on, post turn-on and turn-off transients of a pulsed IMPATT oscillator are demonstrated through an example.

In Section 3 the dependence of oscillator turn-on transients on the device and circuit parameters is investigated. Effects of bias current, RF circuit, bias circuit, injection locking, photon injection and

ambient temperature on the frequency response, RF power buildup and generated output power of a millimeter-wave IMPATT oscillator are described.

In Section 4 techniques to control the oscillation frequency of pulsed and CW oscillators are described. Techniques and examples including bias current compensation, optical injection compensation and injection locking to control the post turn-on transients of pulsed oscillators are presented.

SECTION 2. MODEL FOR CHARACTERIZING THE OSCILLATOR STATICS AND DYNAMICS

2.1 Analysis of the Oscillator Model

It is the purpose of this section to develop a simple oscillator model such that the static and dynamic behavior of a free-running or injection locked pulsed oscillator can be investigated. Although only the IMPATT diode oscillators are discussed, this analysis can be applied to any two-terminal active device or three-terminal device (such as BJT, FET) in an appropriate circuit.

The IMPATT device exhibits negative resistance when its bias current exceeds the threshold level, and the circuit can be designed to utilize this negative-resistance property. For CW operation, the diode is usually biased with constant current instead of constant voltage, while a constant current or constant voltage source with finite impedance may be used under pulsed operation. The bias circuit dictates the bias current passing through the diode and the dc voltage across it. Therefore, dynamic behavior of pulsed oscillators is affected by the bias circuit.

Part of the dc power delivered to the diode converts to ac power, and the remainder of the dc power generates heat. The generated heat in turn contributes to the increase of device temperature. Since the device admittance is dependent upon junction temperature, the oscillator frequency and output power will vary accordingly as a result of the device-circuit interaction. Thus the turn-on, post turn-on and turn-off transients of pulsed oscillators can be obtained by solving

the oscillator equation, the thermal equation and the bias circuit equation simultaneously.

Oscillator Equation

In order to produce oscillation at microwave frequency, the active device must exhibit negative resistance. For the IMPATT diode, the negative-resistance conditions can be achieved by applying adequate dc bias current to the diode. The rest of the oscillator can then be properly designed to make use of the negative-resistance property and obtain oscillation at the desired frequency. The equivalent circuit of an oscillator[3] consists of the large-signal model of the diode admittance Y_d, the equivalent circuit of the microwave circuit admittance Y_c, and injection current I_1 as shown in Fig. 2.1. For a free-running oscillator ($I_1 = 0$), the behavior is governed by the solution of the following equation:

$$Y_d(V_{RF}, I_{dc}, I_{op}, T, s) + Y_c(s) = 0 \quad , \qquad (2.1)$$

where Y_d = the IMPATT diode admittance (mho),

Y_c = the circuit admittance seen from the device (mho),

V_{RF} = the RF voltage across the diode (V),

I_{dc} = the diode bias current (A),

I_{op} = the photon injection current (A),

and the natural frequency ($s = \sigma + j\omega$) is the result of device-circuit interaction.

In the complex frequency s-plane, if $Y_d(s) + Y_c(s)$ has any zeros in the right-half plane ($\sigma > 0$), then the entire circuit is unstable, and the RF voltage will grow in time. The growth rate $\sigma[V_{RF}(t), I_{dc}(t), I_{op}(t), T(t)]$ and frequency $f[V_{RF}(t), I_{dc}(t), I_{op}(t), T(t)]$ are given by the solution of Eq. 2.1. The relation between RF

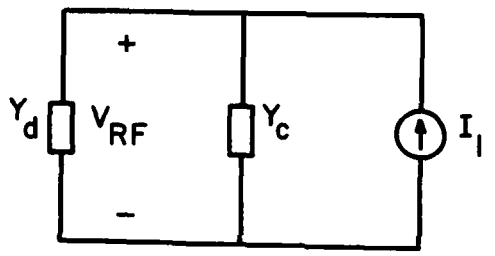

FIG. 2.1 OSCILLATOR EQUIVALENT CIRCUIT USED TO STUDY THE BEHAVIOR OF A FREE-RUNNING OR INJECTION LOCKED OSCILLATOR.

voltage and growth rate is given by

$$\frac{1}{V_{RF}} \frac{dV_{RF}}{dt} = \sigma[V_{RF}(t), I_{dc}(t), I_{op}(t), T(t)] \quad . \qquad (2.2)$$

Thermal Equation

To turn on an oscillator, a certain amount of bias current is applied to the device resulting in the generation of heat. The generated heat has to be removed to keep the temperature down which in turn allows more bias current and the generation of additional output power. Since heat generation is proportional to the electric field,[1] most of the heat is generated in the space charge region and removed through the semiconductor, metal contact and heatsink. The temperature response of the device is governed by the following equation:

$$\frac{dT}{dt} + \frac{T - T_a}{\tau_{th}} = \frac{R_{th} \cdot P_d}{\tau_{th}} \quad , \qquad (2.3)$$

where T = the junction temperature of the device,

T_a = the ambient temperature,

τ_{th} = the device thermal time constant, and

P_d = the dissipated power which is related to the dc power delivered to the diode P_{dc}, and the oscillator power P_{RF} generated by the active device, i.e.,

$$P_d = P_{dc} - P_{RF} = V_{dc} I_{dc} - P_{RF} \quad . \qquad (2.4)$$

An estimate of the junction temperature at steady state ($dT/dt = 0$) can be obtained from the device thermal resistance and dissipated power at the junction as

$$T_f = T_a + R_{th} \cdot P_d \quad . \qquad (2.5)$$

The maximum bias current that can be used for a safe operating condition of the device is limited by the maximum allowed junction temperature. Normal operating bias current is constrained by the maximum bias current and the required reliability which decreases with the increasing operating device temperature.

Low Frequency "Bias Circuit" Equation

In the absence of RF oscillations, the dc voltage across the IMPATT diode is given by

$$V_{dc} = V_B(T) + I_{dc}(t)R_{sc} \quad , \qquad (2.6)$$

where $V_B(T)$ is the temperature-dependent breakdown voltage, $I_{dc}(t)$ is the dc bias current, and R_{sc} is the space charge resistance.

The ionization rates of electrons and holes decrease with increasing temperature.[4] Thus, for an IMPATT diode with a given doping profile, the breakdown voltage will increase with increasing temperature. The space charge effect is the variation of electric field in the depletion region due to the generated carrier space charge. This effect gives rise to a positive space charge resistance for the IMPATT diode.

Since the electron and hole ionization rates are highly nonlinear functions of the electric field, the dc voltage is reduced by an amount V_R which depends upon the amplitude of the RF oscillation and bias current level when microwave oscillations are present. The magnitude of this rectification voltage generally increases with increased RF voltage level and decreases with increased current level.[5] Figure 2.2 shows the bias circuit approximation, where the dc voltage is given by

$$V_{dc} = V_B(T) + I_{dc}(t)R_{sc} + V_R(V_{RF},T,I_{dc}) \quad . \qquad (2.7)$$

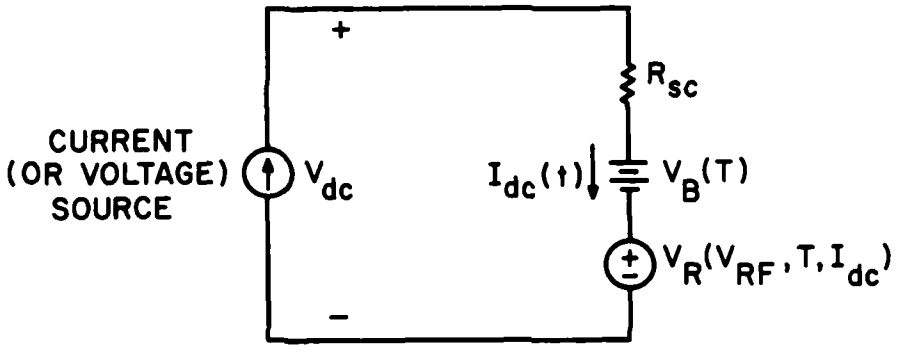

FIG. 2.2 LOW FREQUENCY "BIAS CIRCUIT" EQUIVALENT CIRCUIT.

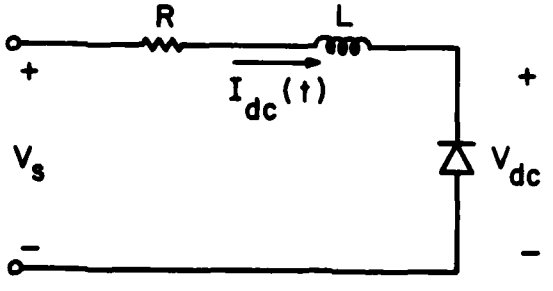

FIG. 2.3 CONSTANT VOLTAGE WITH FINITE IMPEDANCE AS BIAS SOURCE.

Equation 2.7 is the bias circuit equation which describes the relationship between dc voltage and bias current at a different RF voltage level and junction temperature. The bias source applied to the device can be constant current or constant voltage with finite impedance. In the case of a constant voltage source V_s with series resistance R and inductor L as shown in Fig. 2.3, the dc voltage across the device is

$$V_{dc} = V_s - RI_{dc} - L\frac{dI_{dc}(t)}{dt} \quad . \qquad (2.8)$$

2.2 Device and Circuit Parameters Required for the Analysis

To study the transient behavior of a pulsed oscillator, the following device and circuit parameters must be obtained by theoretical calculation or measurement:

1. Device admittance Y_d *which depends on RF voltage* V_{RF}, bias current I_{dc}, optical current I_{op}, oscillation frequency f, and junction temperature T.

2. Circuit admittance which is a function of frequency.

3. Thermal resistance R_{th} which depends on device size, device material, geometry, material of heatsink, bias current pulsewidth, and duty cycle.

4. Thermal time constant which is related to device width.

In this section a more detailed description of these device and circuit properties and their effects on the oscillator behavior is described.

Describing Function $Y_d(V_{RF},I_{dc},I_{op},f,T)$

Describing functions[6] can be used to describe the equivalent circuit of nonlinear devices including IMPATT diodes. Derivation of an appropriate admittance describing function from large-signal behavior

of the active device, and its use in the study of pulsed oscillators will be demonstrated. The admittance describing function Y_d is extremely useful for characterizing static and dynamic effects in oscillators and amplifiers. It can be used to describe the RF properties of the diode under the conditions when the dependent variables are slowly varying in time. Hence, the quasi-static behavior of RF voltage, bias current, optical current, frequency and temperature can be determined in nonequilibrium as well as static situations. Initial analysis to illustrate the turn-on, post turn-on and turn-off transients of a pulsed oscillator has made use of a uniformly doped double-drift region (DDR) IMPATT diode as an example. A DDR diode is chosen because the millimeter-wave output power and efficiency are significantly higher for DDR diodes than for those obtained with the single-drift region (SDR) diodes. The results of the large-signal device admittance obtained are being combined with the RF circuit admittance and bias circuit to study dynamic effects in the pulsed oscillator under different conditions.

Device admittance data obtained from simulation or measurement are discrete. For the purpose of analysis, it is better to express Y_d as a continuous function of V_{RF}, I_{dc}, I_{op}, f and T, since then the natural frequency s can be determined by solving the running oscillation condition given by

$$Y_d(V_{RF},I_{dc},I_{op},s,T) = - Y_c(s) \quad . \qquad (2.9)$$

Analytical expressions for both Y_d and Y_c as functions of frequency are desired. The device conductance G_d is an even function of frequency, while device susceptance is an odd function.[7] These even and odd properties are useful for constructing an approximate expression for Y_d. For certain bias currents, optical currents, and junction

temperatures, Y_d is a function of RF voltage and frequency. Therefore, G_d and B_d can be expressed as shown in Eq. 2.10:

$$G_d = \sum_{k=0}^{R} \sum_{n=0}^{S} A_{kn} V_{RF}^{k} (f^2)^n \qquad (2.10a)$$

and

$$B_d = \sum_{k=0}^{R} \sum_{n=0}^{S} B_{kn} V_{RF}^{k} (f^{2n+1}) \quad . \qquad (2.10b)$$

Values of A_{kn} and B_{kn} can be found in the least mean-squared error sense.

If f is replaced by $s/j2\pi$, Y_d can be represented as a continuous function of V_{RF} and s,

$$Y_d = G_d + jB_d$$

$$= \sum \sum A_{kn} V_{RF}^{k} (-1)^n \left(\frac{s}{2\pi}\right)^{2n} + \sum \sum B_{kn} V_{RF}^{k} (-1)^n \left(\frac{s}{2\pi}\right)^{2n+1} \quad . \qquad (2.11)$$

Large-signal properties including optical effects of millimeter-wave IMPATT diodes have been studied extensively and are given in the accompanying report.[8] Figure 2.4 shows the large-signal device admittance with 60 kA/cm^2 bias current density and 300°K junction temperature. This figure is the plot of Eq. 2.11 after the discrete data are treated as described.

The Circuit Model

To study the dynamic behavior of a pulsed oscillator, it is essential to have a model for the microwave circuit. The most straightforward method of modeling is by means of a lumped equivalent network representing the RF circuit. Although an equivalent circuit of a practical oscillator may be more complex in general, it can be reduced to a simple form over a limited frequency range of interest. The RF circuit can be represented by a lumped RLC series or parallel network

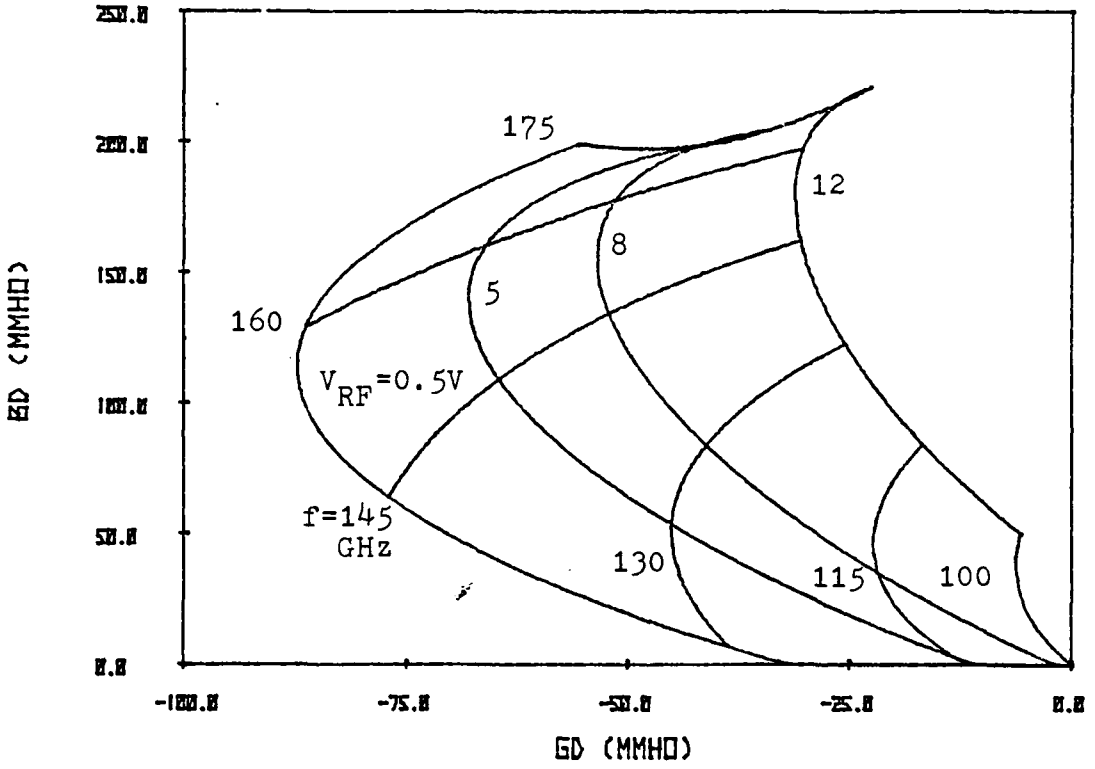

FIG. 2.4 G-B LOCUS FOR DIFFERENT VALUES OF V_{RF}.
(J_{dc} = 60 kA/cm^2, device diameter = 50 μm
and T_j = 300^{o}K)

as shown in Fig. 2.5. These RLC elements are frequency independent, and the circuit admittance presented to the diode is a simple function of frequency.

A millimeter-wave diode can be mounted in a waveguide or microstrip circuit to generate RF power. In many cases the diode is mounted in a reduced height waveguide with a tuning short. This waveguide oscillator circuit consists of an IMPATT diode mounted on a copper heatsink, a rectangular waveguide of reduced height, a movable short, a dc bias post and a waveguide taper. The reduced height portion of the waveguide provides a low impedance necessary for proper matching of the load to the diode. The waveguide taper is for impedance matching between reduced and full height waveguides.

A theoretical analysis of this post-in-waveguide circuit has been studied, and the calculated results can be applied to the circuit design in optimizing the oscillator performance. This more complex equivalent circuit is based on the analysis of Lewin[9] and modified by Chang and Ebert.[10] The results obtained for the RF circuit can then be combined with the device to predict the oscillator behavior.

Thermal Resistance

The maximum dissipated power is determined by the safe operating temperature of the junction (approximately 375°C for Si) and the total thermal resistance which is a measure of how efficiently the heat can be removed. Thermal resistance is related to diode area, diode geometry, and the thermal properties of the semiconductor, diode metallization, and the heatsink. When a Si diode is mounted on a heatsink, and an ideal thermal contact between all the metallic layers is assumed, total thermal resistance R_{th} is given by

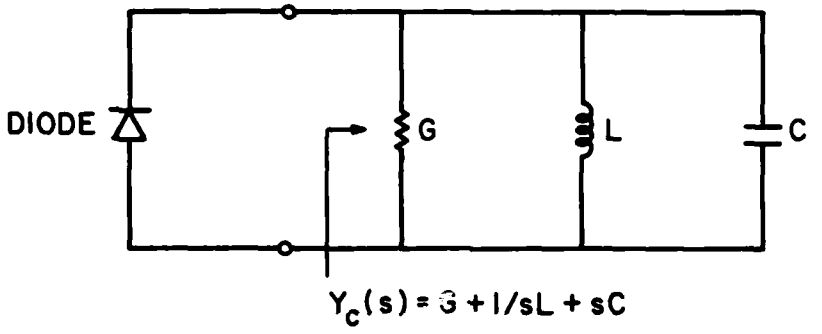

FIG. 2.5 A SIMPLIFIED RF EQUIVALENT CIRCUIT.

$$R_{th} = R_s + R_{HS} \quad ,$$

where R_s is the contribution due to the Si and thin layers of contact metallization, and R_{HS} is the contribution from the heatsink.

For the pulsewidth larger than several thermal time constants, R_s is approximately equal to its CW value, i.e.,

$$R_s = \frac{1}{A} \sum \frac{d_i}{k_i} \quad ,$$

where A is the diode area, k_i is the thermal conductivity of the ith layer, and d_i is the material thickness of the ith layer.

For a pulsed oscillator, heat is supplied to the surface of the heatsink in periodic pulses. Thermal resistance contributed from the heatsink R_{HS} can be calculated for an avalanche diode under periodic pulses. The diode is under a periodic heating and cooling cycle caused by the bias pulses. In an actual diode, the heat generation is confined primarily to the active layer close to the diode junction. This generated heat flows through the semiconductor before reaching the heatsink. R_{HS} depends on the pulsewidth t_1 and duty cycle ($d = t_1/T$), where T is the period of successive pulses. R_{HS} is given by[11]

$$R_{HS} = \frac{d^{\frac{1}{2}}(\alpha t_1)^{\frac{1}{2}}}{(\pi R^2)k} \left[\frac{2}{(\pi d)^{\frac{1}{2}}} \left(1 - e^{-R^2/4\alpha t_1} \right) + I \right.$$

$$\left. + \frac{R}{d^{\frac{1}{2}}(\alpha t_1)^{\frac{1}{2}}} \operatorname{erfc} \left[\frac{R}{2(\alpha t_1)^{\frac{1}{2}}} \right] \right] \quad .$$

where R is the radius of the diode, d is the duty cycle, t_1 is the pulsewidth and I is given by

$$I = \frac{2}{\pi d} \int_o^\infty \frac{e^{-dx^2}\left[e^{-(1-d)x^2} - e^{-x^2}\right]\left[1 - \cos \frac{Rx}{(\alpha T)^{\frac{1}{2}}}\right]}{x^2(1 - e^{-x^2})} dx \quad .$$

For a copper heatsink, the thermal conductivity k is 3.96 W/cm°C, and thermal diffusivity α is 1.14 cm^2/s. Figure 2.6 shows R_{HS} as a function of a pulsewidth at a 40-kHz pulse repetition frequency. Within reasonable limits, a short pulsewidth is more effective (i.e., less thermal resistance R_{HS}) than a low duty cycle in preventing diode damage from overheating.

The thermal conductivity of diamond is greater than that of copper. Thus the thermal resistance of the diode can be reduced with a diamond heatsink and higher power can be handled accordingly. Geometries which distribute the junction area over a much larger heatsink area[12] can also be used to reduce thermal resistance.

Thermal Time Constant

Calculation of the thermal time constant can be carried out for a simplified geometrical configuration[13] such as that shown in Fig. 2.7. It consists of a heat source located at the end of a slab of material of constant cross section A, device width d, thermal conductivity k, specific heat c', and density ρ. The other end is connected to a heatsink of temperature T_a. Heat is stored in the thermal capacitance of the device chip, then passes through the thermal resistance of the semiconductor and the contact metallization to the infinite heatsink. The thermal time constant due to the device-chip capacitance and thermal resistance of the simplified model is given by

$$\tau_{th} = rc = \frac{d}{kA} \cdot c'dA\rho = c'\rho d^2/k \quad ,$$

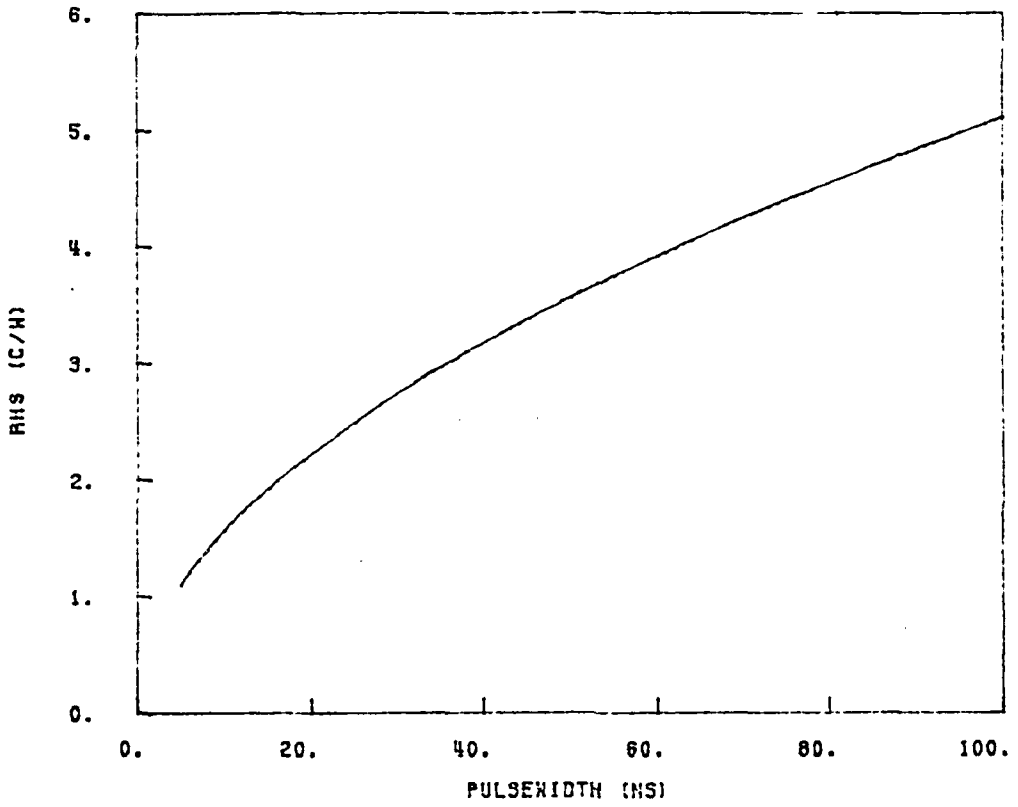

FIG. 2.6 HEAT SINK THERMAL RESISTANCE AS A FUNCTION OF PULSEWIDTH.(Pulse Repetition Frequency = 40 kHz, Device diameter = 50 μm)

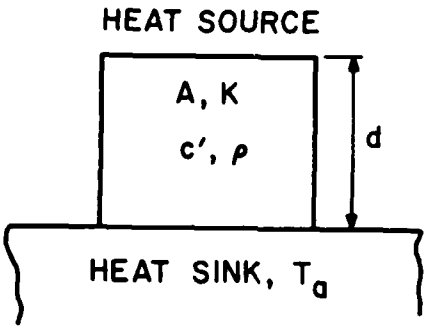

FIG. 2.7 SIMPLIFIED GEOMETRY TO CALCULATE THE THERMAL TIME CONSTANT.

where τ_{th} = the thermal time constant of the diode (s),

r = the thermal resistance of the slab of material (°C/W), and

c = the heat capacity of the slab of material (J/°C).

Silicon is often used in millimeter-wave IMPATT diodes and its properties at 300°K are specific heat c' = 0.7 J/g°C, density ρ = 2.328 g/cm^3, and thermal conductivity k_{Si} = 1.45 W/cm°C.

Figure 2.8 shows the thermal time constant of a Si diode as a function of device width. It can be seen that τ_{th} decreases as the device width decreases. For the double-drift IMPATT diode with an active region width d = 1 μm, τ_{th} is 11.2 ns. Since the active region width of the diode decreases as the desired frequency increases, the thermal time constant is reduced for higher frequency devices. Hence, the temperature rise of pulsed millimeter-wave diodes is faster than that of lower frequency devices.

2.3 Usefulness and Limitations of the Oscillator Model

The oscillator model described in Sections 2.1 and 2.2 is capable of predicting many important effects in CW and pulsed IMPATT oscillators including the following: (1) turn-on transients (oscillation buildup and frequency response) and their dependence on the device (bias current), circuit (bias circuit, RF circuit) and external influences (injection locking, photon injection, ambient temperature); (2) post turn-on transients (frequency chirp, temperature response, and power variation); (3) turn-off transients (device cool-off, and decay of the output power); (4) control of the post turn-on transients; and (5) behavior of varactor/photon tuned oscillators.

The performance of this oscillator model is limited in several respects. Knowledge of these limitations is necessary for the proper

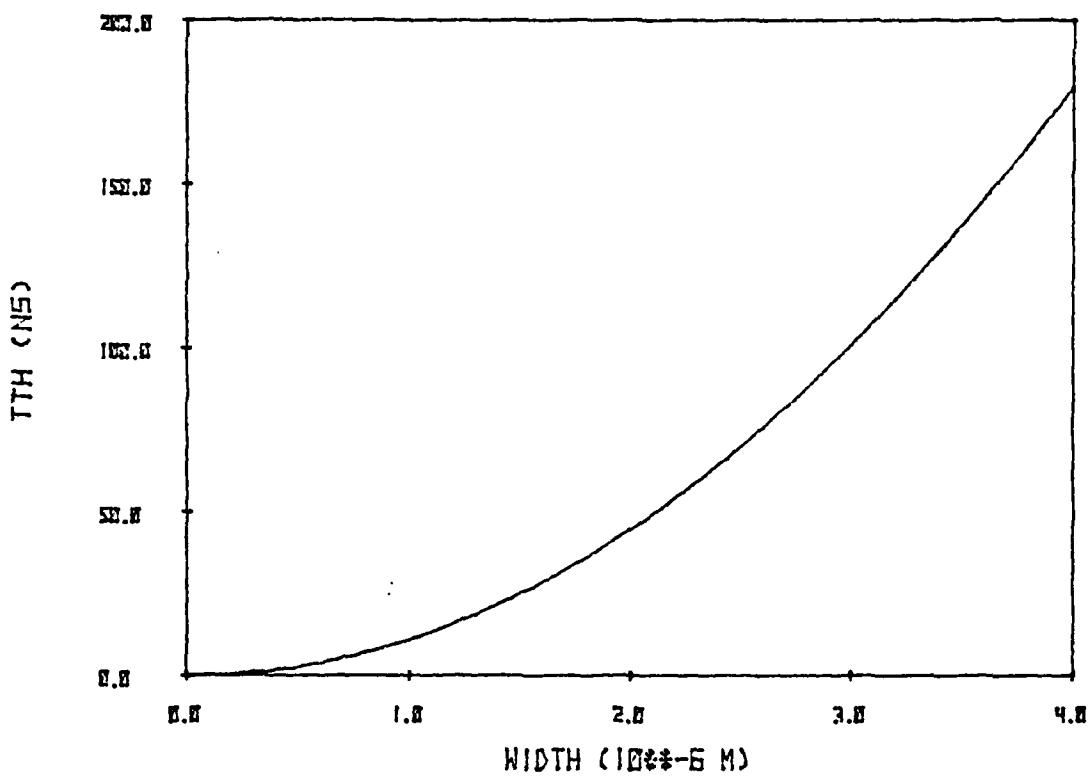

FIG. 2.8 THERMAL TIME CONSTANT AS A FUNCTION OF DEVICE WIDTH.

use of this model. Temperature and photon injection dependence of the microwave circuit are neglected. In the real oscillator circuit, the microwave circuit may be dependent on temperature and photon injection especially when a microstrip circuit is used. The same temperature is assumed throughout the semiconductor layer while the more realistic thermal distribution is dependent on the location. A single thermal time constant is used in the model. The thermal time constant may be dependent on the operating temperature, and several time constants may be involved. The value of τ_{th} for the same semiconductor is approximately 10 ns in the example and that of the heatsink is much larger (on the order of μs). Variation of the device and circuit properties due to aging is not considered.

2.4 An Example of a Pulsed Oscillator which Identifies the Various Effects

Introduction

To study the turn-on, post turn-on, and turn-off transients of pulsed oscillators quantitatively, a quasi-static device model is used in which it is assumed that the microwave admittance of the diode is an instantaneous function of RF voltage, dc current, photon injection level, and junction temperature. This model, which was developed for oscillator analysis, can be used to determine the dynamic and steady-state behavior of the device when interacting with a microwave circuit of known admittance.

A constant bias current pulse is often used in pulsed IMPATT oscillators, such that the oscillator is turned on when adequate current

is passing through the device, and the microwave circuit is properly matched. Rf power builds up as a result of the device-circuit interaction. A significant portion of the dc power is dissipated which results in the temperature rise and a change of the device properties. Thus, oscillation frequency and output power vary. When the bias pulse is turned off, the RF oscillation cannot sustain, output power decreases, and the junction temperature returns to the ambient temperature.

In this section many important effects of a free-running pulsed IMPATT oscillator are demonstrated through an example. In this example, a flat bias current (60 kA/cm^2) pulse with a 40-ns pulsewidth and a 40-kHz pulse repetition frequency (period = 25 μs) is applied to a diode with a 50-μm diameter. Other important device parameters are thermal resistance, R_{th} = 6.7°C/W, and thermal time constant, τ_{th} = 11.24 ns. A simple RLC parallel network represents the passive circuit seen from the device terminals. In this example, G equals 24.9 mmho, L equals 9.39×10^{-13} H, and C = 1.4522 pF.

Turn-On Transients of the Pulsed Oscillator

The device-circuit interaction which results in the buildup of RF oscillation is obtained by using a time-domain computer simulation.

A sudden change in the dc bias current shifts the device admittance from $Y_d(V_{RF},I_d)$ to $Y_d(V_{RF},I_d + \Delta I_d)$. Because of the stored energy requirements of the microwave circuit, the RF voltage cannot change instantaneously. Therefore, immediately after the change in bias current, the circuit constraint $Y_d(s) + Y_c(s) = 0$ can only be satisfied by the growth of the RF voltage to a new value. Such growth takes time, and the delay time between the bias pulse and the output power is related to the amount of current change ΔI_d and the quality

factor Q of the microwave circuit. For constant current pulse, the oscillator turn-on is usually characterized by a rapid decrease in dc voltage across the IMPATT diode.

The natural frequency s which determines the nature of the transient response can be solved by numerical methods. The growth rate σ is the rate of RF voltage growth, given by

$$\frac{1}{V_{RF}} \frac{dV_{RF}}{dt} = \sigma \quad .$$

If σ is negative, then any oscillatory response will be damped out, and the degree of damping depends on the magnitude of σ. An oscillator will be free-running of initially σ is positive. Any disturbance will cause RF voltage to build up. As long as σ remains positive the exponential buildup of the free-running oscillator will continue and the output will eventually stabilize at some amplitude. Since the diode conductance G_d and susceptance B_d are generally dependent on the amplitude of the ac voltage, the dc voltage across the device, and junction temperature, the oscillation frequency and growth rate of the oscillator are time dependent. This is a result of device-circuit interaction. There are large transients in the output frequency during turn-on. This is due to the increase in device susceptance B_d as the RF voltage swing increases so that the oscillation frequency decreases continuously during the buildup until the growth of the oscillation is complete. After steady state is reached, the frequency settling time and the delay time between the bias pulse and full RF power can be determined.

An initial value of RF voltage (V_{RF} = 0.1 V) is used in the calculation. A high growth rate (8.1×10^9) at the start of oscillation and its decrease as the oscillation builds up are illustrated in

Fig. 2.9a. It can be seen that the growth rate approaches zero when the buildup is complete. Figure 2.9b shows that the RF voltage increases from 0.1 to 12 V within 0.8 ns. Since the initial RF voltage is small, the buildup of the RF voltage is not significant until 0.5 ns, although the growth rate is high at t = 0. Build up is faster with a higher initial RF voltage.

Figure 2.9c demonstrates the response of device conductance during turn-on. The magnitude of the device conductance $|G_d|$ decreases as RF voltage increases. This fall of $|G_d|$ is a natural phenomenon common to all negative-resistance diode oscillators and is a result of device nonlinearity. When the negative conductance falls to the same value as the circuit conductance ($G_d + G = 0$), where G is the circuit conductance, stable operation is obtained.

RF power ($P_{RF} = - 0.5\ G_d V_{RF}^2$) is determined by the values of device conductance and RF voltage. Figure 2.9d shows the buildup of output power during turn-on. The delay time between the bias pulse and RF power which depends on the initial RF voltage is approximately 0.6 ns. Since the ionization rates of electrons and holes are higher nonlinear functions of the electric field, dc bias voltage across the diode V_{dc} will decrease as the RF voltage builds up as shown in Fig. 2.9e. Variation of V_{dc} is negligible when the RF voltage swing is small (< 1 V). V_{dc} decreases from 24.9 to 20.2 V as the RF voltage increases from 0.1 to 12 V and remains relatively constant after the oscillator is turned on. A large decrease of dc voltage can be seen when the RF voltage is building up.

The device susceptance B_d increases with increasing RF voltage, i.e., B_d changes from 24 to 126 mmho during turn-on as shown in

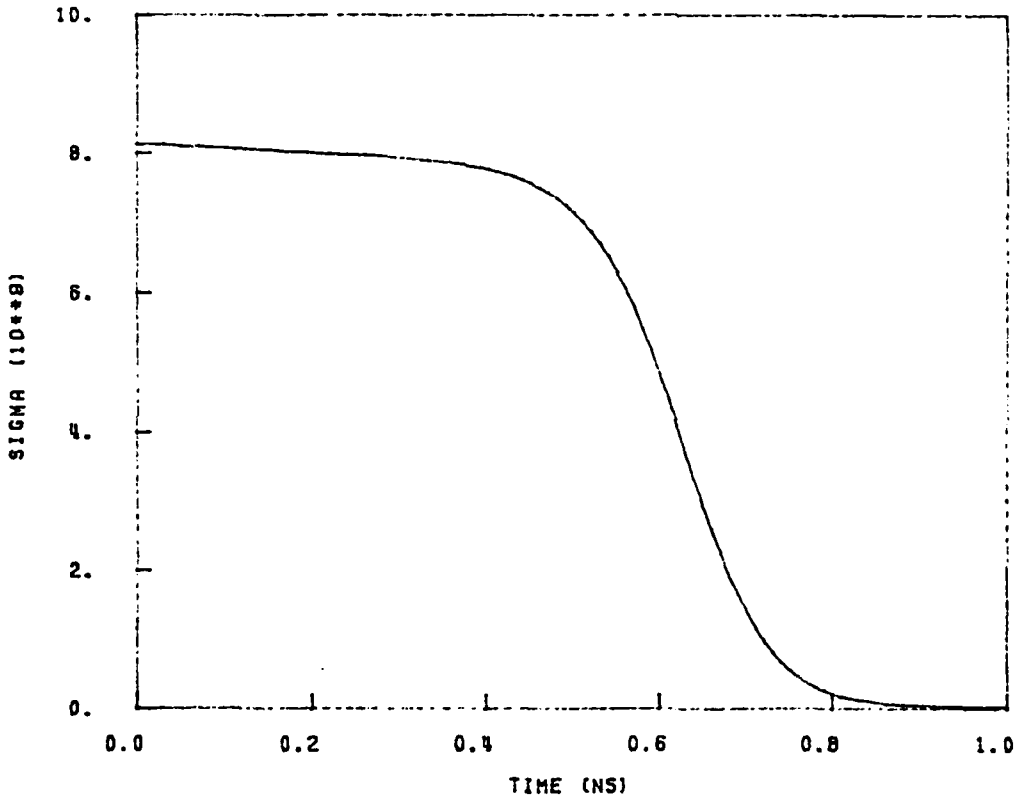

FIG. 2.9a BEHAVIOR OF GROWTH RATE DURING TURN-ON.

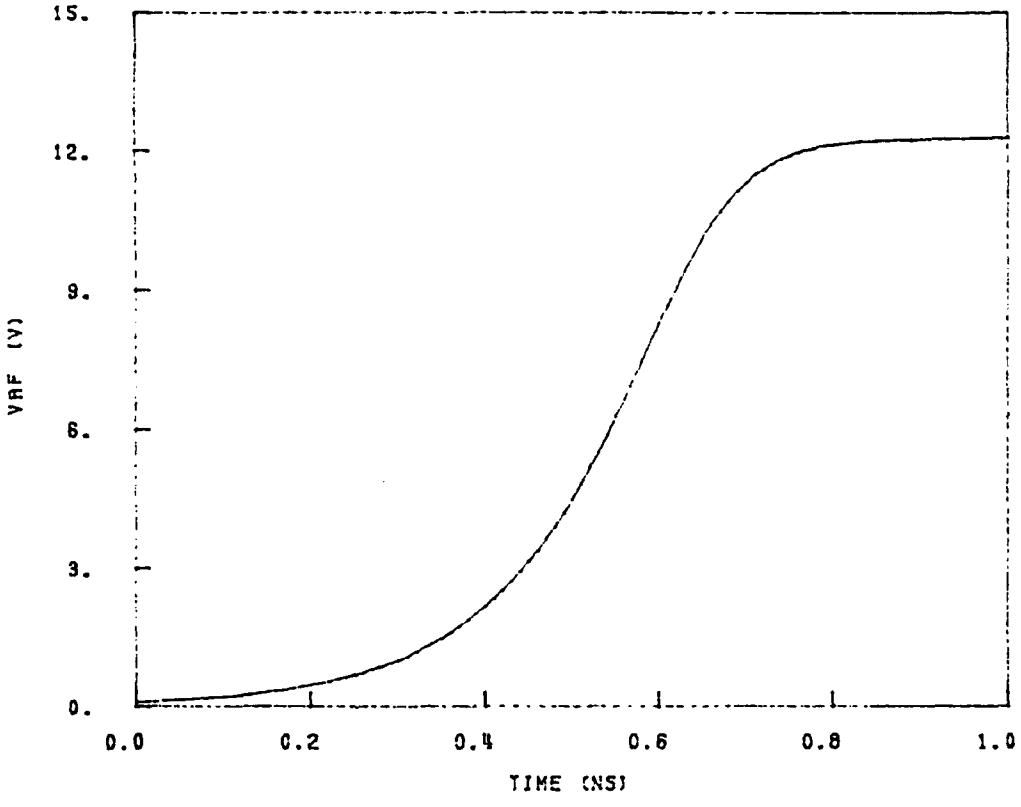

FIG. 2.9b BUILDUP OF RF VOLTAGE DURING TURN-ON.

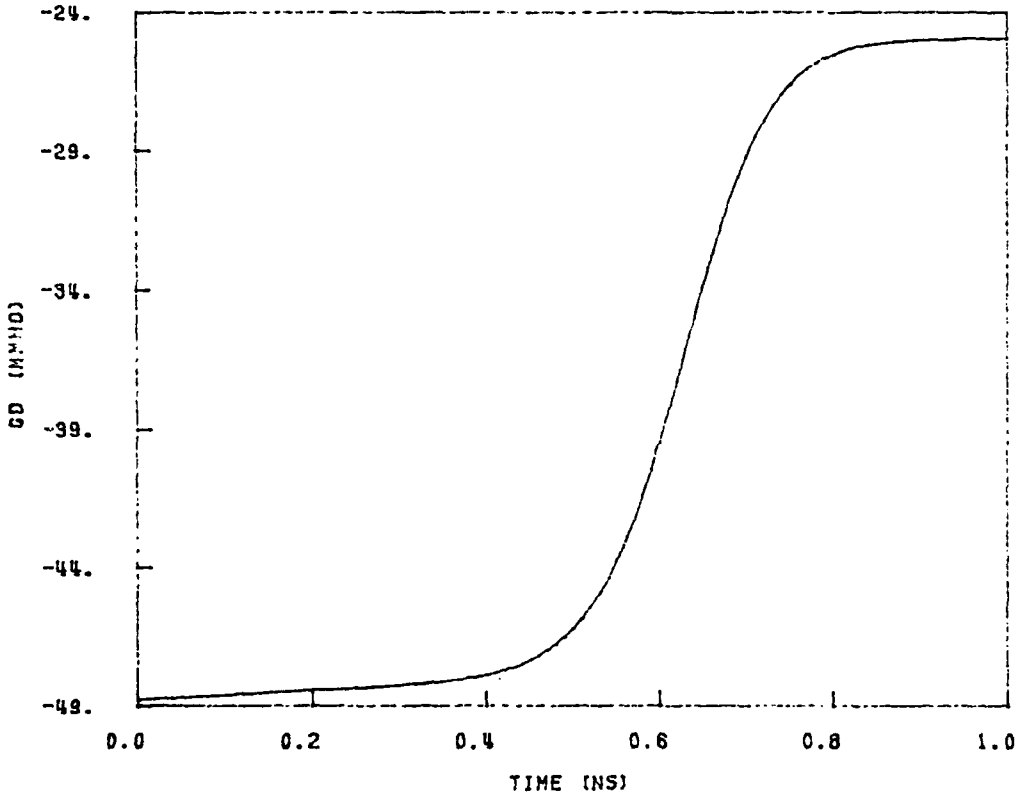

FIG. 2.9c RESPONSE OF DEVICE CONDUCTANCE DURING TURN-ON.

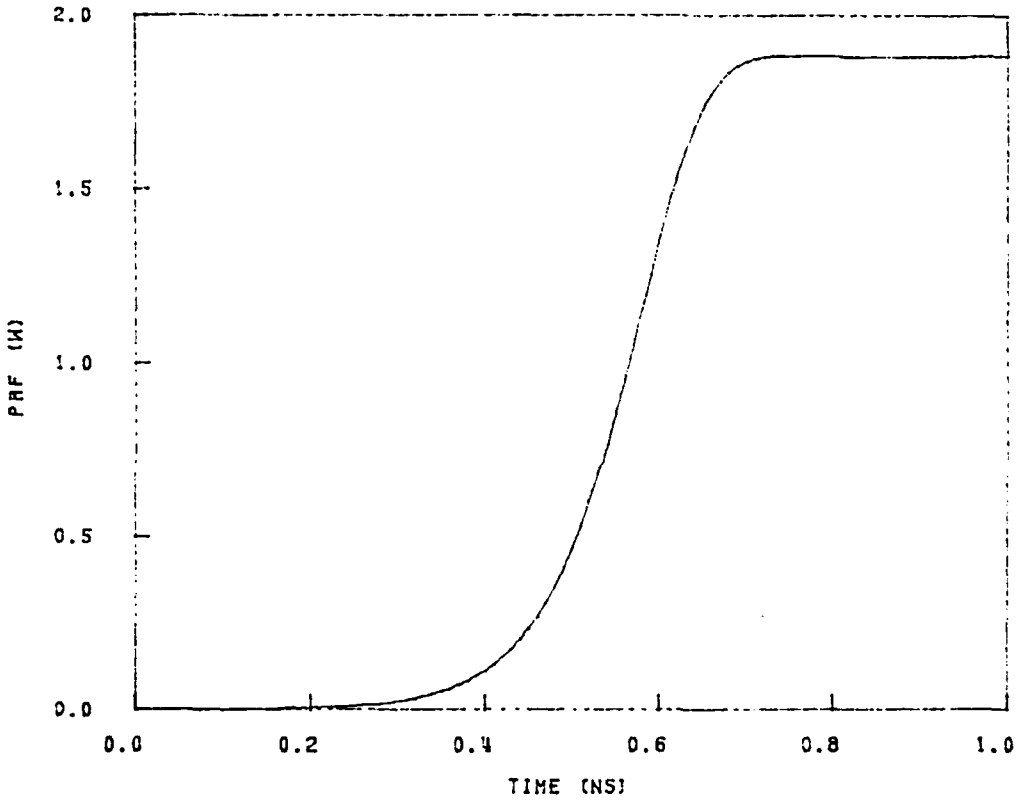

FIG. 2.9d BUILDUP OF RF OUTPUT POWER DURING TURN-ON.

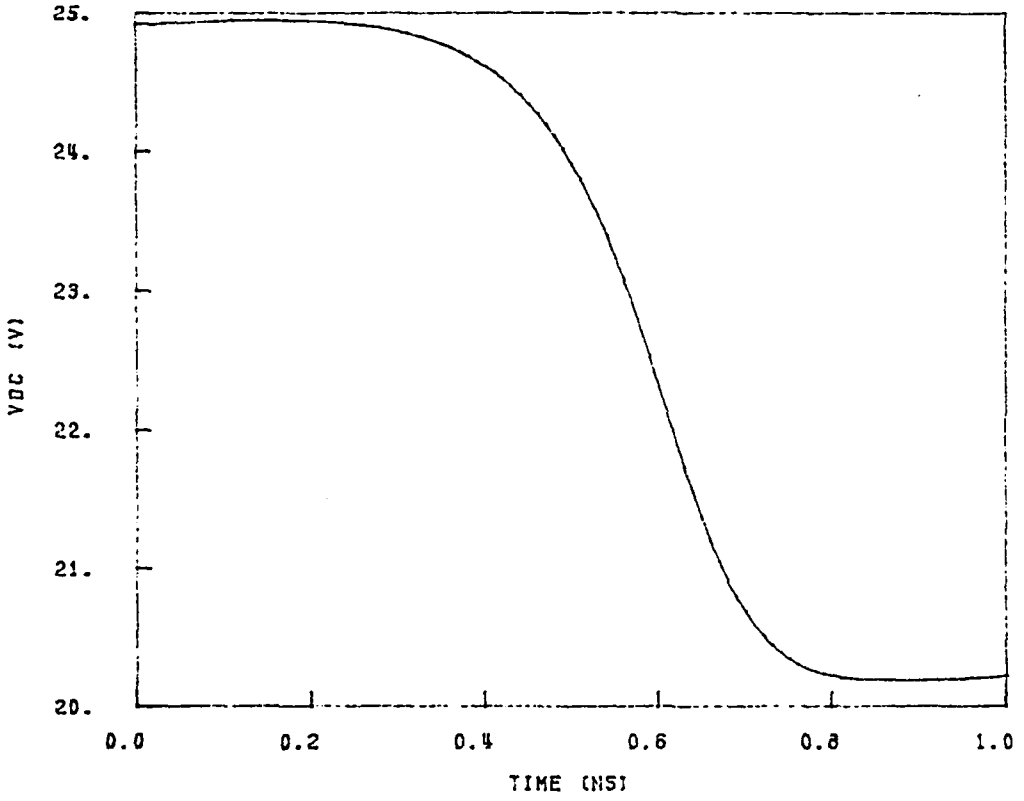

FIG. 2.9e VARIATION OF DC VOLTAGE DURING TURN-ON.

Fig. 2.9f. This increase of device susceptance causes the oscillation frequency to vary from 135 to 129 GHz when oscillation builds up as shown in Fig. 2.9g. Although the device temperature changes from 300 to 315°K during turn-on, it is reasonable to conclude in this example that the turn-on transients are mainly the result of device-circuit interaction. The effect of temperature rise on the oscillator performance shows up after the oscillator is turned on. Figure 2.9h and 2.9i show the turn-on transients in the s-plane and the device admittance plane.

Temperature Response During the Pulse

The device junction temperature, which is determined by ambient temperature, thermal resistance from the junction to heatsink and the dissipated power, is an important parameter affecting the performance of IMPATT oscillators. For a given diode under pulsed operation, the temperature behavior during the pulse depends on bias current, pulse-width, pulse repetition frequency, RF circuit, and ambient temperature.

For low duty cycle operation, the "off" period is much longer than the "on" period and allows the device to cool off to ambient temperature. Therefore the diode junction is nearly at ambient temperature at the beginning of each heating cycle and gradually heats up because of the dissipated power P_d which varies with the dc power and RF oscillation power P_{RF} as

$$P_d = P_{dc} - P_{RF} = V_{dc}I_{dc} - 0.5\,|G_d|V_{RF}^2 \quad ,$$

where V_{dc} = the dc voltage across the device,

I_{dc} = the dc bias current passing through the device,

G_d = the device admittance, and

V_{RF} = the RF voltage across the device.

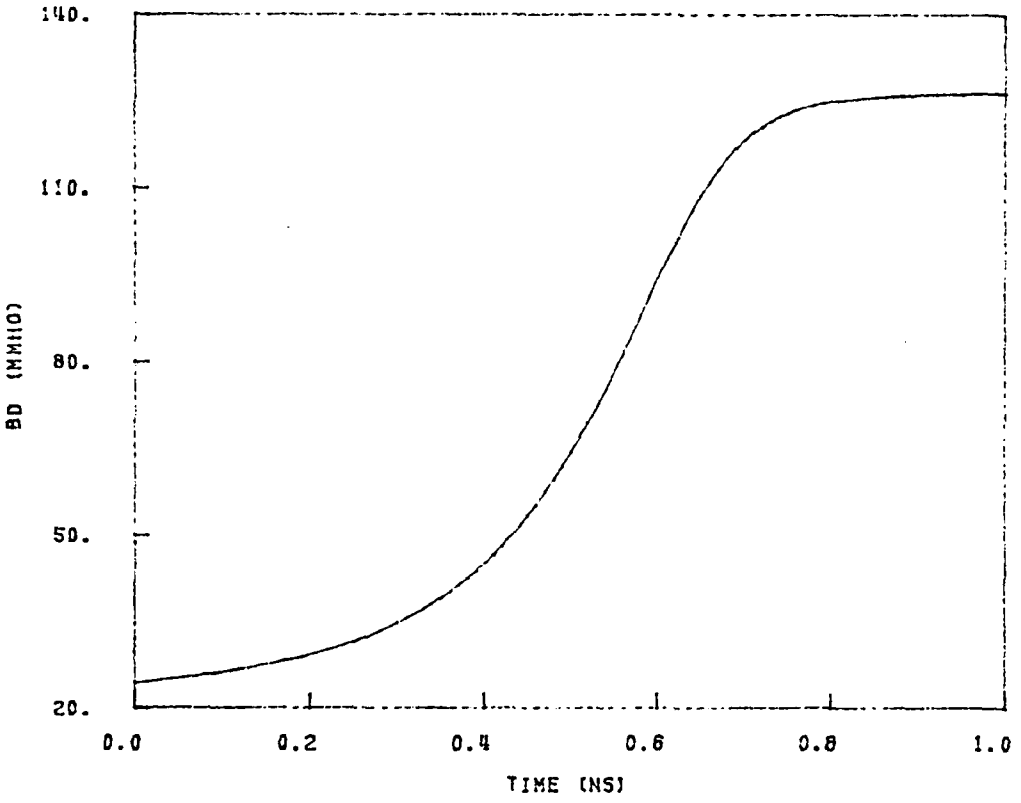

FIG. 2.9f INCREASE OF DEVICE SUSCEPTANCE DURING TURN-ON.

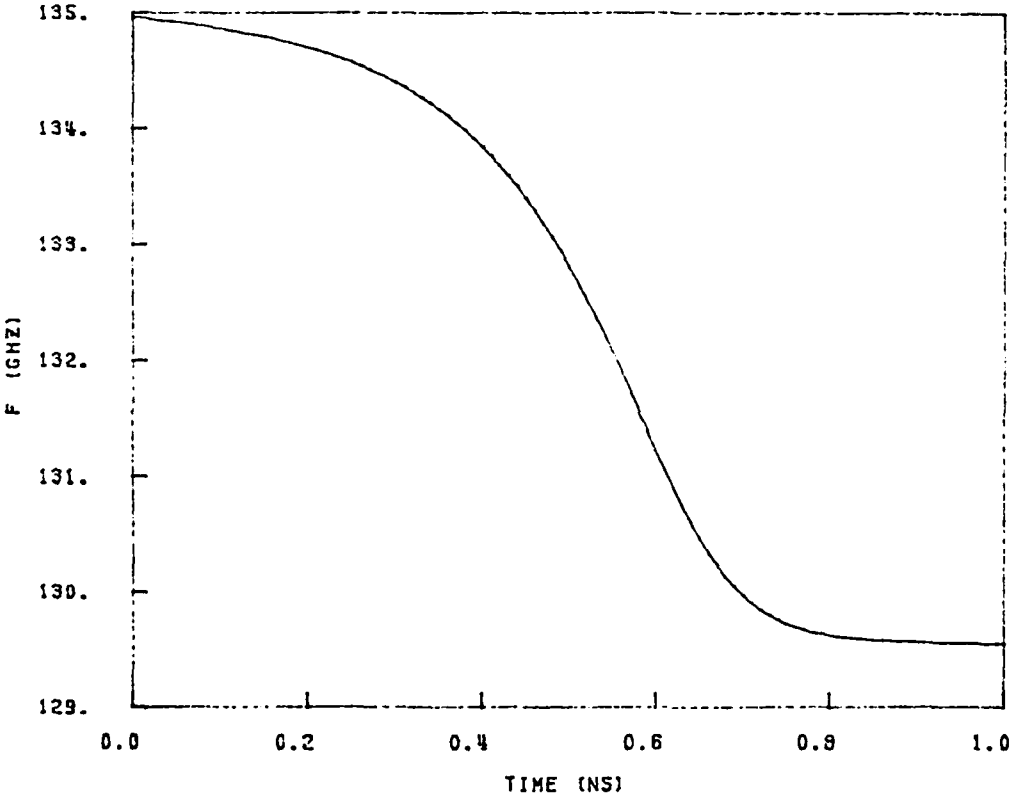

FIG. 2.9g DECREASE OF OSCILLATION FREQUENCY DURING TURN-ON.

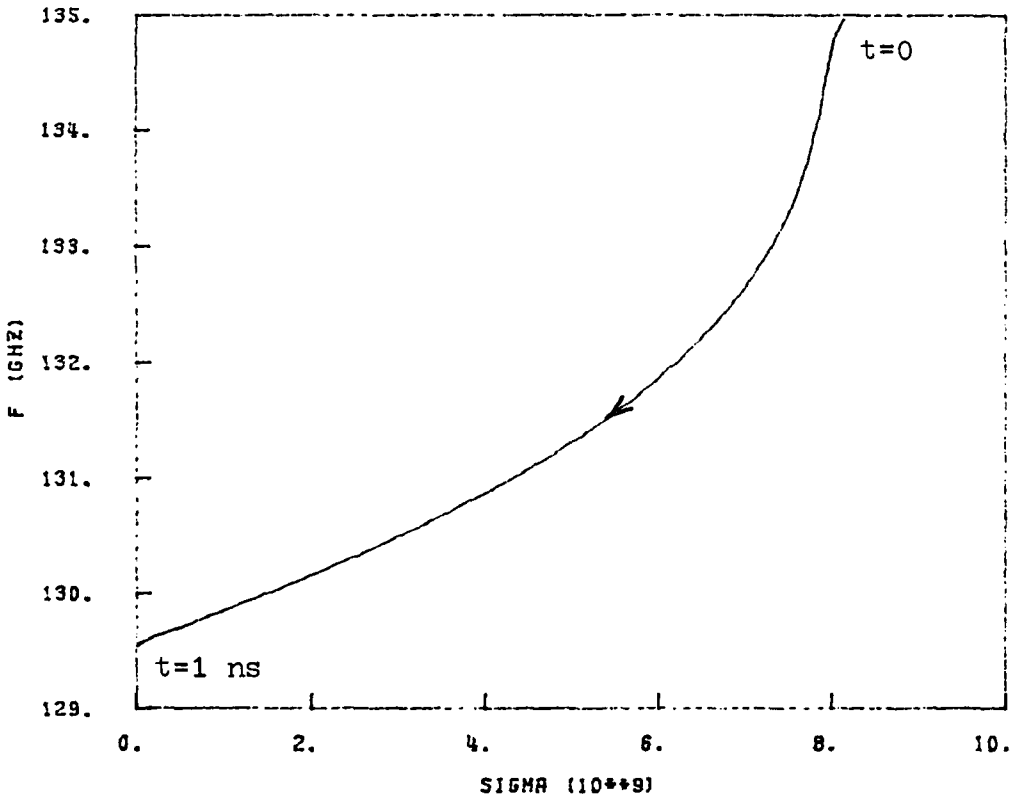

FIG. 2.9h TURN-ON TRANSIENT ON S PLANE.

ARROWHEAD REPRESENTS THE INCREASE OF TIME.

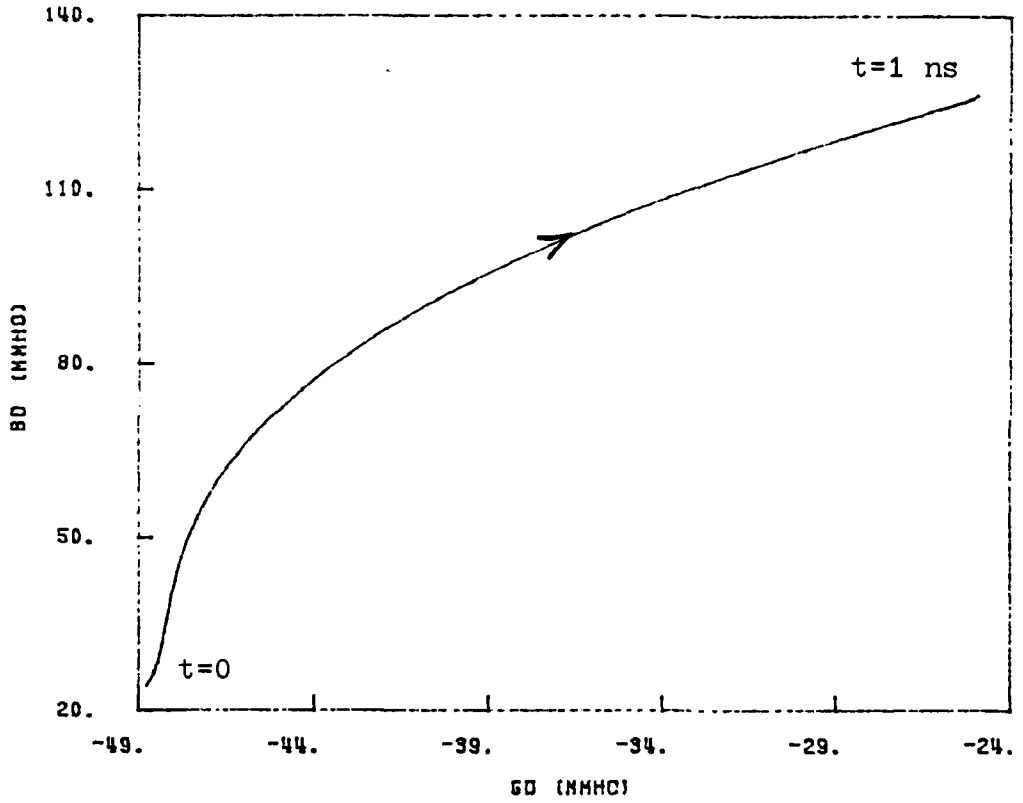

FIG. 2.9i TURN-ON TRANSIENT ON DEVICE ADMITTANCE PLANE.

ARROWHEAD REPRESENTS THE INCREASE OF TIME.

The maximum temperature rise of the diode ΔT is related to the dissipated power at the junction P_d and the thermal resistance of the device R_{th} by

$$\Delta T = P_d R_{th} .$$

Given the input bias power, the thermal resistance determines the maximum temperature rise. The actual temperature rise during the pulse is approximately equal to the maximum temperature rise ΔT when pulsewidth is longer than several thermal time constants τ_{th}.

Semiconductor devices including IMPATT diodes are temperature sensitive. Oscillator performance during the pulse is primarily determined by the temperature dependence of the device properties providing that the temperature dependence of the microwave circuit is negligible. The effect of temperature on the small-signal device admittance has been studied by Schroeder and Haddad.[14] With increasing diode temperature the small-signal negative conductance was found to increase and the region of negative conductance was shifted toward lower frequencies. This may be caused by several temperature-dependent physical parameters including saturated velocity, dielectric constant, and ionization rates. Intrapulse performance of the oscillator can be obtained from the temperature dependence of large-signal device properties. For the diode used as an example, the following conclusions which are useful for the intrapulse analysis can be drawn:

1. The absolute value of the device conductance decreases with increasing RF voltage and increases with increasing temperature.

2. The device susceptance has a tendency to increase with RF voltage and operating temperature.

3. Breakdown voltage increases with operating temperature.

Junction temperature increases from 300 to 470°K during the 40-ns pulsewidth as shown in Fig. 2.10. As the junction temperature rises, the ionization rates and scattering-limited velocities of electrons and holes decrease. Both effects tend to increase breakdown voltage and dc voltage across the device. Figure 2.11 illustrates the increase of dc voltage from 20.2 to 25.1 V during the pulse. The positive temperature-coefficient property of the breakdown voltage can be used to prevent the thermal runaway when the diode is biased under constant voltage operation.

Frequency Drift During the Pulse

The variation of oscillation frequency due to the change of temperature ΔT can be estimated[15] from the oscillation conditions. The oscillation conditions can be expressed as

$$G_d(V_{RF},I_{dc},f,T) + G_c(f,T) = 0$$

and

$$B_d(V_{RF},I_{dc},f,T) + B_c(f,T) = 0 \quad ,$$

where G_d = the device conductance,

G_c = the circuit conductance,

B_d = the device susceptance, and

B_c = the circuit susceptance.

To obtain analytic results the following additional assumptions are made:

1. G_c is a constant independent of temperature and frequency.
2. Frequency dependence of G_d is negligible.

The change of G_d to T must be compensated by that due to the change in RF voltage V_{RF} and dc current I_{dc} to maintain the oscillation conditions, i.e.,

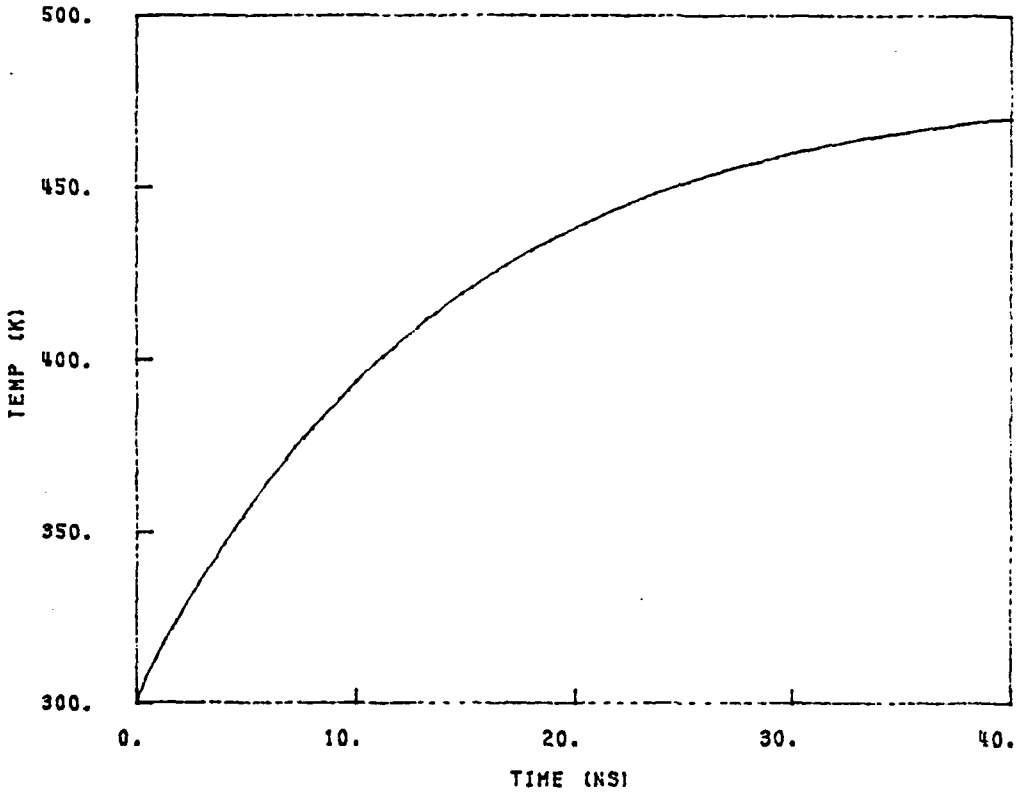

FIG. 2.10 JUNCTION TEMPERATURE RESPONSE DURING THE PULSE.

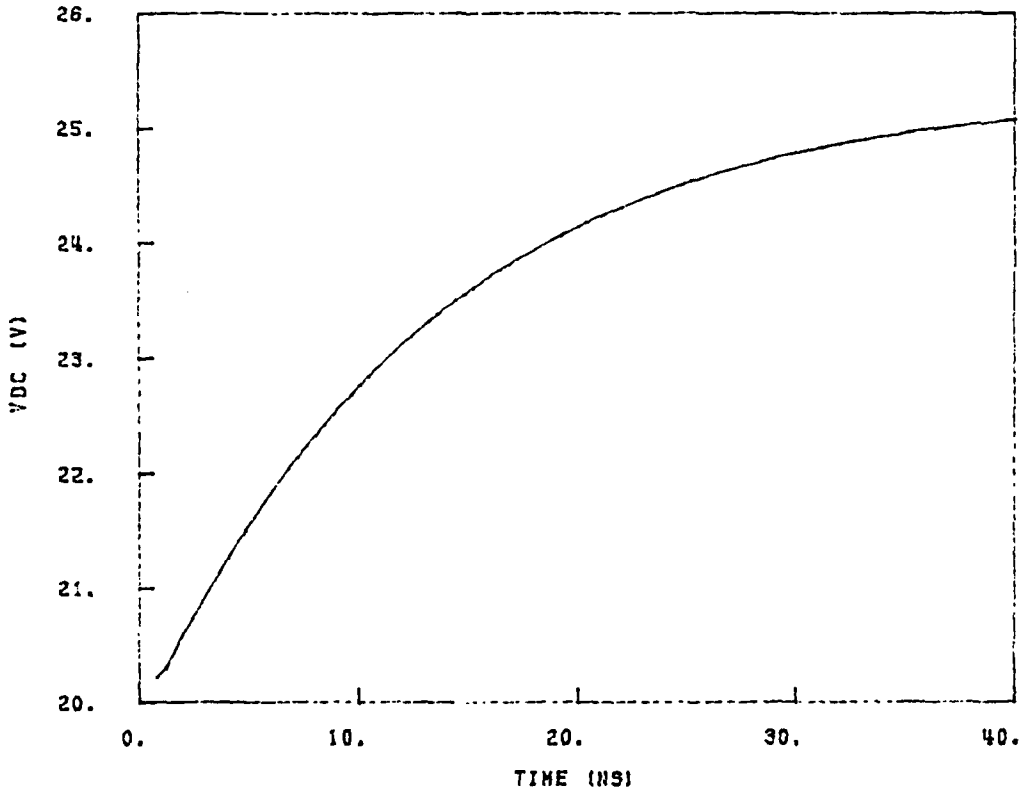

FIG. 2.11 DC VOLTAGE RESPONSE OF POST TURN-ON.

$$\frac{\partial G_d}{\partial V_{RF}} \Delta V_{RF} + \frac{\partial G_d}{\partial I_{dc}} \Delta I_{dc} + \frac{\partial G_d}{\partial T} \Delta T = 0$$

and

$$\frac{\partial B_d}{\partial V_{RF}} \Delta V_{RF} + \left(\frac{\partial B_d}{\partial T} + \frac{\partial B_c}{\partial T}\right)\Delta T + \left(\frac{\partial B_d}{\partial f} + \frac{\partial B_c}{\partial f}\right)\Delta f + \frac{\partial B_d}{\partial I_{dc}} \Delta I_{dc} = 0 \quad .$$

From these equations, Eq. 2.12 is derived,

$$\left[\frac{\partial (B_d + B_c)}{\partial f}\right]\Delta f = A_1 \Delta T + A_2 \Delta I_{dc} \quad , \qquad (2.12)$$

where

$$A_1 = \frac{\partial B_d}{\partial V_{RF}} \frac{1}{\partial G_d / \partial V_{RF}} \frac{\partial G_d}{\partial T} - \frac{\partial (B_d + B_c)}{\partial T}$$

and

$$A_2 = \frac{\partial B_d}{\partial V_{RF}} \frac{1}{\partial G_d / \partial V_{RF}} \frac{\partial G_d}{\partial I_{dc}} - \frac{\partial B_d}{\partial I_{dc}} \quad .$$

Frequency drift due to ΔT is related to the circuit admittance and large-signal device properties of IMPATT diodes. For constant current operation ($\Delta I_{dc} = 0$) the oscillation frequency decreases with positive temperature change when A_1 is negative. The sign of A_1 is determined by the values of $\partial B_d/\partial V_{RF}$, $\partial G_d/\partial V_{RF}$, $\partial G_d/\partial T$ and $\partial (B_d + B_c)/\partial T$. The temperature dependence of circuit admittance is assumed to be negligible, i.e., $\partial B_c/\partial T = 0$ and $\partial G_c/\partial T = 0$. The large-signal properties including temperature dependence of an IMPATT diode have been studied and the results are summarized as follows:

1. Device susceptance B_d increases with RF voltage ($\partial B_d/\partial V_{RF} > 0$).

2. Device conductance G_d increases with RF voltage and this is one of the criteria to achieve stable oscillation ($\partial G_d/\partial V_{RF} > 0$).

3. G_d decreases (more negative G_d) with temperature ($\partial G_d/\partial T < 0$).

4. B_d increases with temperature ($\partial B_d/\partial T > 0$).

5. B_d increases with frequency ($\partial B_d/\partial f > 0$).

6. Circuit susceptance B_c has to increase with frequency to obtain stable oscillation ($\partial B_c/\partial f > 0$).

The sign of A_1 determined from 1. to 4. is negative. Thus the frequency drifts downward as junction temperature increases. This conclusion is in good agreement with the investigation of Fong and Kuno.[16] Equation 2.12 can be modified when the loaded oscillator quality-factor Q_L is introduced. Q_L is defined by

$$Q_L = \frac{f_o}{2G_c} \left.\frac{\partial(B_d + B_c)}{\partial f}\right|_{f=f_o} ,$$

where f_o is the oscillation frequency of the oscillator. Equation 2.12 becomes

$$\Delta f = \frac{f_o}{2G_c Q_L} (A_1 \Delta T + A_2 \Delta I_{dc}) .$$

For a given diode, higher loaded circuit quality-factor $Q_{L,C}$ means higher Q_L. Accordingly, frequency drift Δf decreases with higher $Q_{L,C}$, where

$$Q_{L,C} = \frac{f_o}{2G_c} \left.\frac{\partial(B_c)}{\partial f}\right|_{f=f_o} .$$

During the post turn-on period, device susceptance B_d increases from 126 to 152 mmho and oscillation frequency decreases from 129.5 to 128.5 GHz as shown in Fig. 2.12. This frequency drift (1.3 GHz) is smaller than the drift during the turn-on period (5.5 GHz), since the increase of B_d caused by temperature rise (26 mmho) is smaller than that caused by the oscillation buildup (102 mmho).

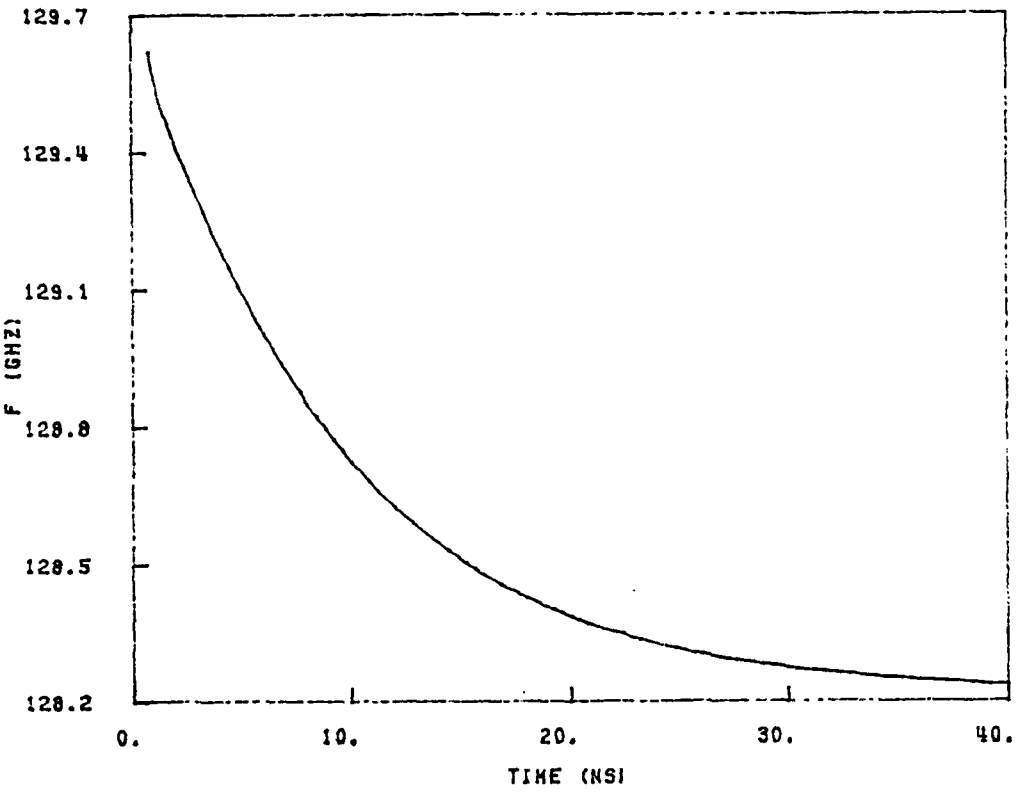

FIG. 2.12 FREQUENCY DRIFT DURING POST TURN-ON.

RF Voltage and Power Variations During the Pulse

For the diode used in the example, the drift region is not quite punched through at 300°K, and consequently a thin layer of high-resistivity Si (typically 1 Ω-cm) appears as a parasitic loss element. This undepleted layer degrades the oscillator efficiency. A nonpunch-through diode has been shown[17] to be more temperature sensitive than a punch-through diode. The reduced ionization rates of electrons and holes with increasing temperature have important effects on the electric field profile. Since a higher electric field is required to maintain the same bias current, the space charge region widens, the parasitic series resistance is appreciably reduced, and efficiency increases at a higher junction temperature.

For a constant current pulse, the RF voltage and output power continue to increase with increasing junction temperature. The output power increases for two reasons. The first is because as the breakdown voltage increases with temperature, the power input at a constant current source bias increases, and if the efficiency remains constant, the output power must also increase. Secondly, it has been shown that the efficiency actually increases with temperature, so the output power would increase even if the breakdown voltage remains constant.

Figures 2.13 and 2.14 show the RF voltage and the output power variations of post turn-on transients. The RF voltage increases from 12 to 15.6 V, and the output power increases from 1.8 to 3 W.

Turn-Off Transient of the Pulsed Oscillator

When the bias current pulse is turned off at t = 40 ns, the bias current density decreases from 60 kA/cm^2 to 0 and the device admittance changes. The circuit constraint $Y_d(s) + Y_c(s) = 0$ can only

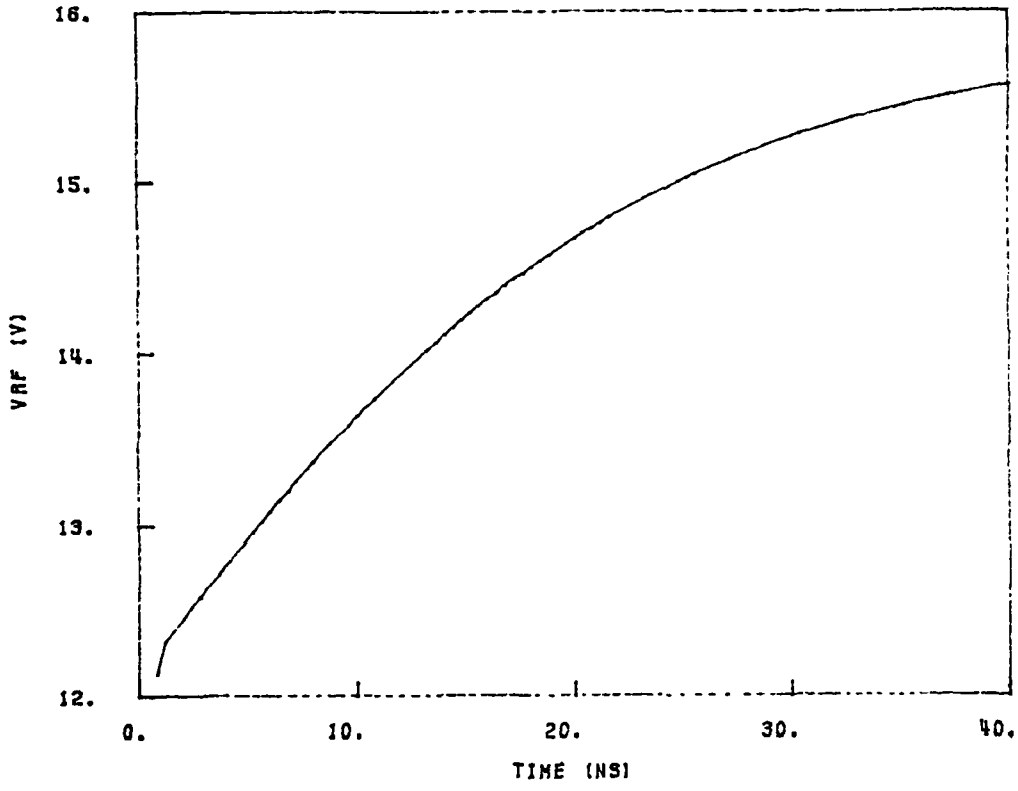

FIG. 2.13 RF VOLTAGE VARIATION DURING POST TURN-ON.

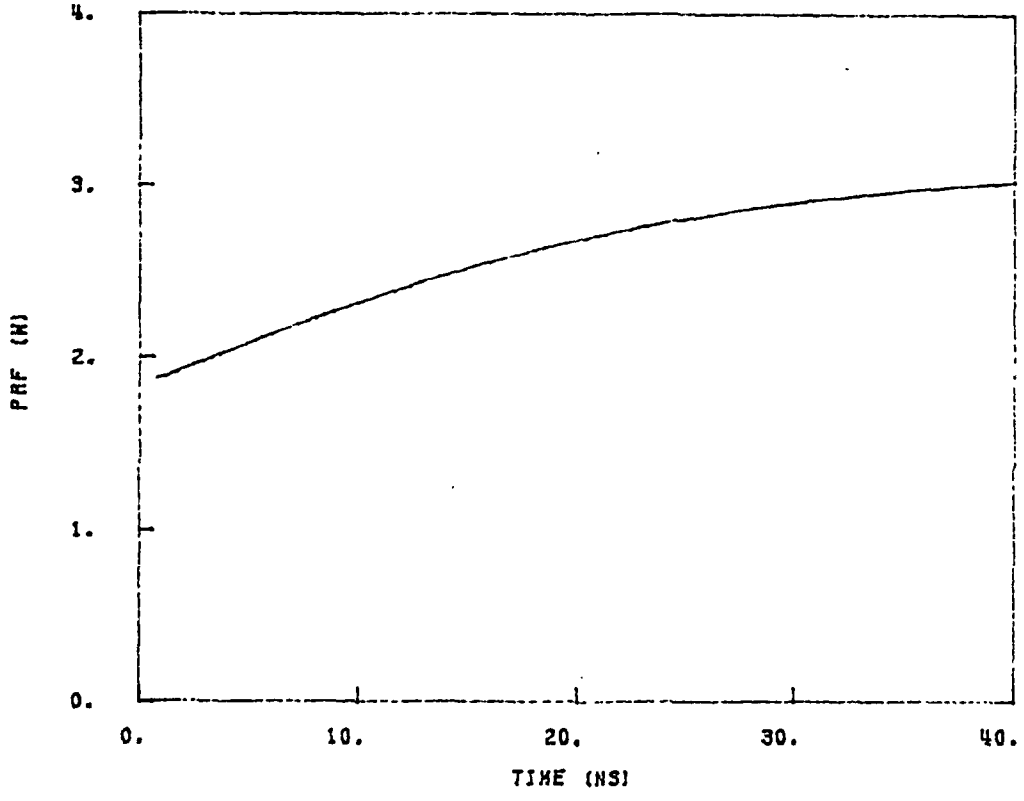

FIG. 2.14 OUTPUT POWER VARIATION DURING POST TURN-ON.

be satisfied with $\sigma < 0$. Therefore, the RF oscillation cannot be sustained, and the RF voltage will decrease. Decrease of RF voltage is proportional to the produce of RF voltage and the magnitude of the decay rate. RF voltage decreases drastically from 15.6 to 0.1 V within 0.2 ns as shown in Fig. 2.15. The turn-off time (0.2 ns) is smaller than the turn-on time (0.8 ns) as expected since both the RF voltage (15.6 V) and the decay rate ($\sigma = -1.5 \times 10^{10}$) at $t = 40$ ns are large. Since the "off" period ($\cong 25$ μs) is much larger than the "on" period (40 ns), the junction temperature will cool off from 470 to 300°K during the long "off" period.

2.5 Separation of Short- and Long-Term Effects

Short-term (turn-on) and long-term (post turn-on) effects are well separated when the delay time between the applied bias pulse and output power is smaller than the thermal time constant of the diode as illustrated in Section 2.4. The short-term effect is mainly the result of device-circuit interaction, and the long-term effect is caused by the device temperature rise.

However, in some cases the distinction between short- and long-term effects is not so well defined. Two of them will be described briefly:

1. If the circuit Q is large, as in the cavity stabilized oscillator, a longer time is needed to store the required energy, and the device temperature rises at the same time. When the turn-on time is larger than the pulsewidth, short- and long-term effects cannot be separated.

2. If the magnitude of the device conductance G_d is too small ($G_d + G_c > 0$) at ambient temperature, the oscillator is not turned on immediately after the bias pulse is applied. Then, the input dc power

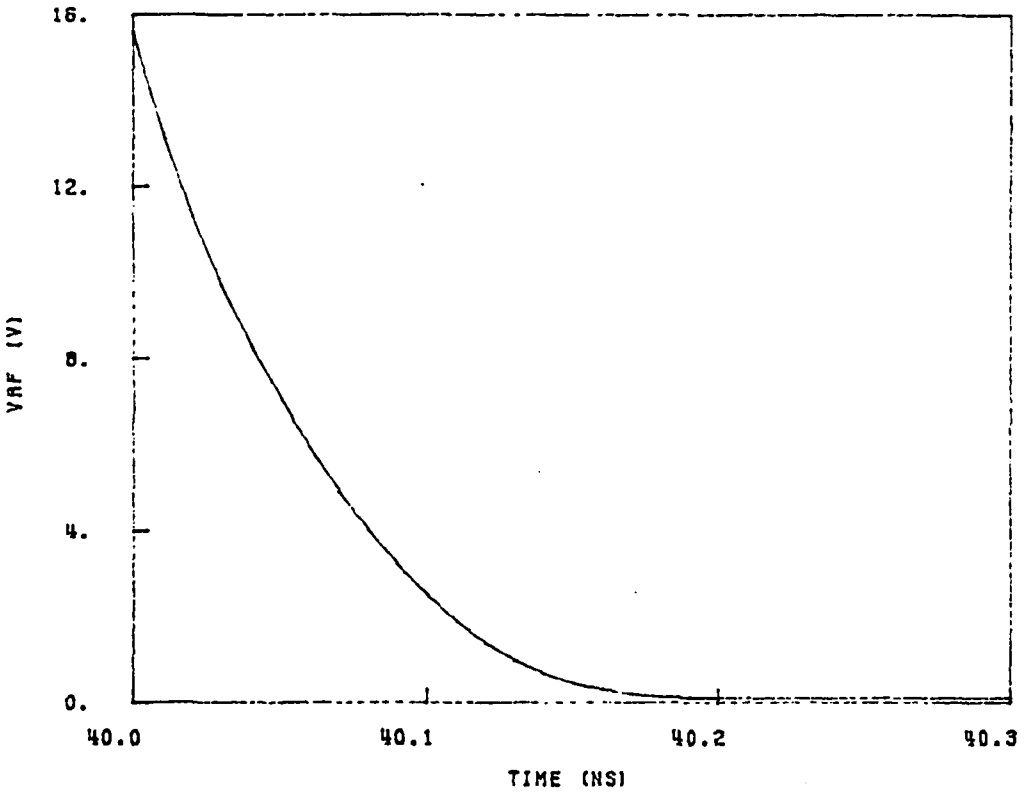

FIG. 2.15 DECREASE OF RF VOLTAGE DURING TURN-OFF.

converts into heat, and the device temperature keeps increasing. After the device temperature increases to a certain value, $|G_d|$ is large enough, and the entire circuit will not be stable. This delay-start phenomenon is a consequence of the temperature increase. Therefore, the short-term effect is not always caused by the sudden increase of bias current, and the long-term effect may not be the consequence of temperature rise.

SECTION 3. DEPENDENCE OF OSCILLATOR TURN-ON TRANSIENTS ON DEVICE AND CIRCUIT PARAMETERS

3.1 Introduction

The turn-on transient of a free-running or injection-locked IMPATT oscillator can be analyzed by solving for the RF voltage $V_{RF}(t)$ and phase $\theta(t)$, given the initial RF voltage $V_{RF}(0)$ and phase $\theta(0)$. Detailed analysis has shown that the transient response is sensitive to many device and circuit parameters.

From the condition for free-running oscillation $Y_d(s) = - Y_c(s)$, a great deal of insight into oscillator turn-on transients can be obtained from a complex plane representation (device-circuit diagram) of the device admittance Y_d together with the negative locus of the circuit admittance vs. frequency, $- Y_c(f)$. Y_d is a function of RF voltage, frequency, junction temperature, bias current, and photon injection, while $Y_c(f)$ is the frequency response of the circuit seen from the device terminals.

The approximate magnitude of the initial growth rate at $t = 0$ is proportional to the distance between the device admittance curve and the circuit (negative) curve, while the imaginary parts of the device and the circuit admittance determine the frequency response of the free-running oscillator. Details of the turn-on transient can be obtained through a simulation program.

In this section the turn-on transients (growth rate decrease, RF voltage buildup, output power increase, dc voltage decrease, oscillation frequency decrease, device admittance change, etc.) and their dependence on device and circuit parameters are obtained from

the oscillator model developed in the previous chapter. This oscillator model is used to predict many important turn-on transients of millimeter-wave IMPATT oscillators including the following: (1) turn-on time and oscillation frequency as a function of bias current, (2) turn-on time and frequency response as a function of circuit Q, (3) effects of various bias circuits, (4) influence of injection locking, (5) effects of photon injection under different bias conditions, (6) starting jitter in the leading edge envelope of the output power, and (7) turn-on time as a function of ambient temperature.

3.2 Effect of Bias Current

In this section simulation results of the turn-on transient of an IMPATT oscillator at various bias current densities are demonstrated. In order to understand the bias current dependence of turn-on transients, it is essential to know the device properties as a function of bias current. At the start of oscillation, RF voltage across the device terminals is small. Thus the small-signal device admittance is very important at the beginning of turn-on ($t = 0$). The small-signal properties of IMPATT diodes studied by Misawa[18] can be summarized as follows:

1. The avalanche frequency is proportional to the square root of the dc bias current [$f_a \alpha (I_{dc})^{\frac{1}{2}}$].

2. The magnitude of the device conductance $|G_d|$ increases with bias current.

3. The device susceptance B_d decreases with bias current.

4. The magnitude of the device Q decreases with bias current where the device Q is defined as the angular frequency times the ratio

of the average stored energy to the energy dissipation per unit time. Since power is generated in an IMPATT diode, the Q is negative.

In addition to the small-signal device properties, the large-signal device properties which determine the efficiency and output power of an oscillator are also important. Efficiency and output power increase with bias current before the space charge effect deteriorates the output power. From the small- and large-signal device properties, turn-on transients of the IMPATT oscillators can be predicted qualitatively.

The small-signal Q of the device gives information about the threshold condition and the initial growth rate of a pulsed oscillator. Since the magnitude of the device Q decreases with bias current, there exists a threshold current for the onset of oscillation. Therefore, higher growth rate at t = 0, larger output power, and higher oscillation frequency at steady state can generally be obtained by operating the device at a higher bias current.

To illustrate the bias current dependence of turn-on transients, a fixed tuned oscillator in which the microwave circuit is represented by a simple RLC parallel network (G = 24.9 mmho, L = 9.39 x 10^{-13}) H, and C = 1.4522 pF) is assumed, and the current density J_{dc} varies from 20 to 60 kA/cm^2. Figure 3.1 shows the variation of output power of this fixed tuned oscillator at various bias current levels. When the current density is smaller than the threshold value ($\cong$ 20 kA/cm^2), the output power does not build up within 1 ns. When the current density is 30 kA/cm^2 or more, the output power and RF voltage at steady state increase as the bias current increases. Turn-on time remains approximately the same (0.7 ns) although the initial growth rate may

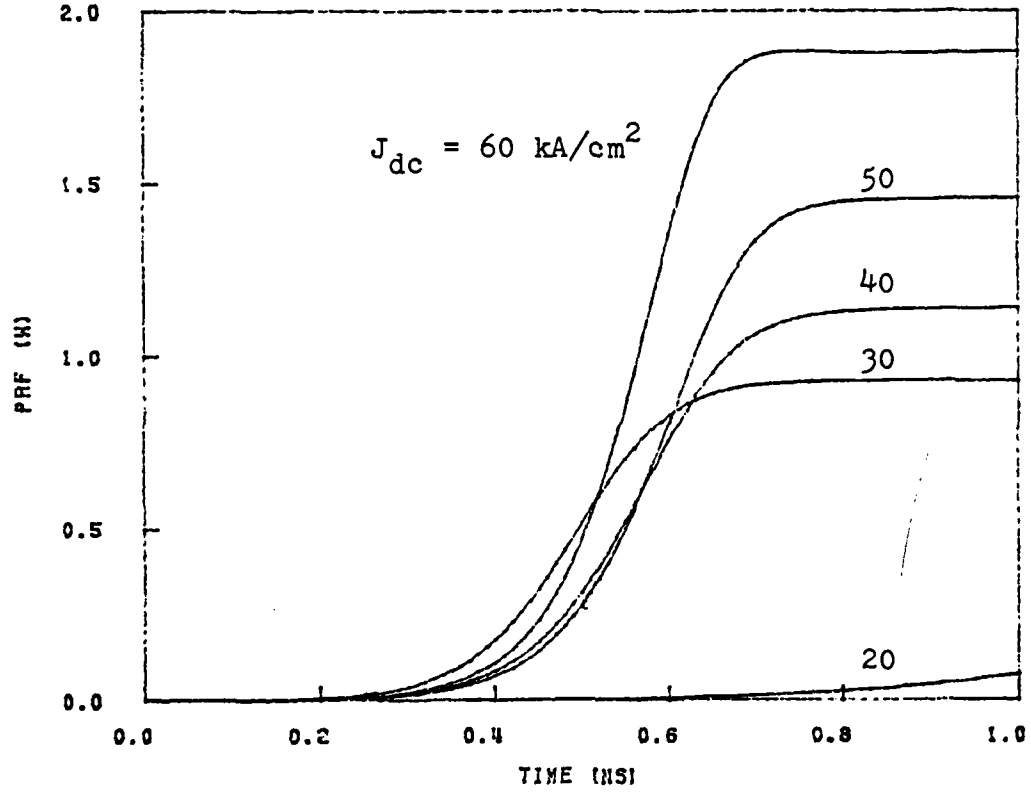

FIG. 3.1 OUTPUT POWER BUILDUP OF A FIXED TUNED OSCILLATOR AT VARIOUS CURRENT DENSITIES.

be larger at a higher current. Figure 3.2 shows the frequency response during turn-on at various current levels. Oscillation frequency at steady state increases with current density as expected. Since the RF voltage swing increases with bias current, the amount of frequency decrease during turn-on increases accordingly.

3.3 RF Circuit Dependence

During turn-on, the amplitude of the RF oscillation increases exponentially, and the growth rate of RF voltage is related to the circuit Q. Thus if the diode is placed in a low Q circuit, substantial frequency decrease and faster turn-on would be expected. However, in a high Q circuit, smaller frequency decrease and slower turn-on would be obtained. Of course to predict the turn-on of a given oscillator, the impedance presented to the diode by the circuit must be known.

To study the RF circuit dependence of the turn-on transient, it is essential to have a model for the external circuit of an IMPATT oscillator. The most straightforward method of modeling is by means of a lumped equivalent network representing the microwave circuit. In this section, a simple parallel RLC network representing the circuit seen from the device terminals as shown in Fig. 2.5 is combined with the device to study the RF circuit dependence of the turn-on transient.

Turn-on time and output power at steady state of an oscillator are very sensitive functions of the circuit conductance. Circuit conductance G is chosen to be equal to $- G_d(V_o,f)$ where V_o is the RF voltage at steady state, and f is the oscillation frequency at steady state. L and C are chosen such that

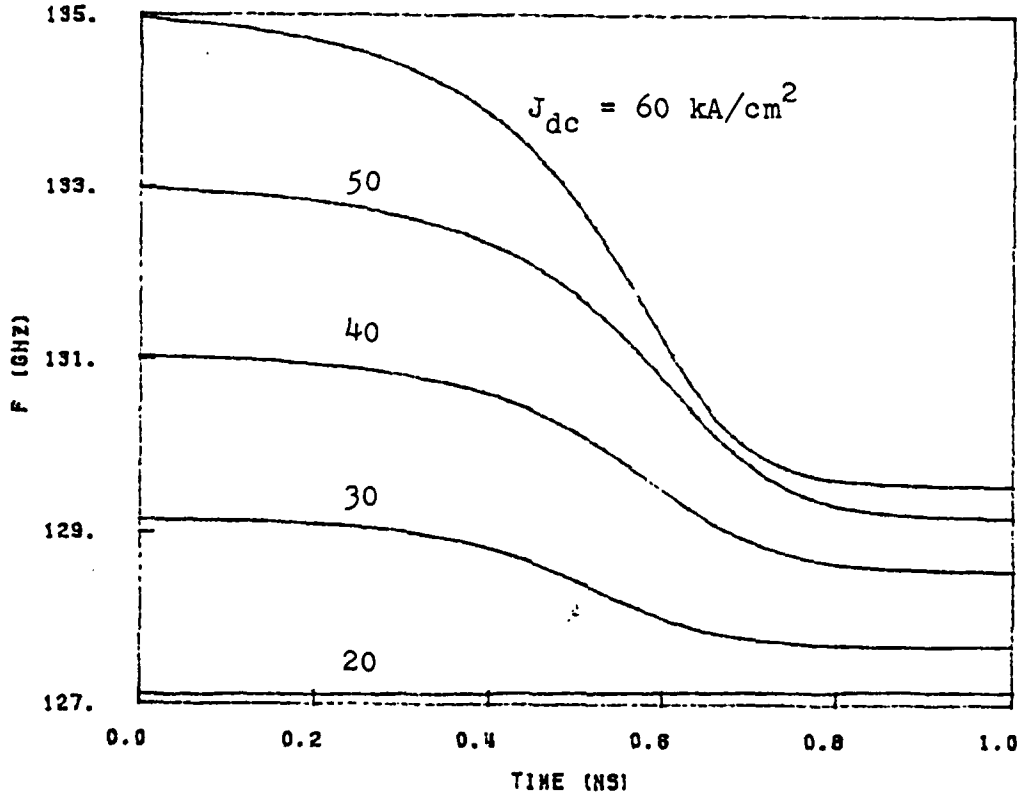

FIG. 3.2 FREQUENCY RESPONSE DURING TURN-ON AT VARIOUS CURRENT DENSITIES.

$$B_d(V_o,f) + B_c(f) = 0 \quad , \quad \text{i.e.,} \quad \omega C - \frac{1}{\omega L} = - B_d(V_o,f) \qquad (3.1)$$

and

$$Q_{L,C} = \frac{\omega}{2G} \frac{\partial B_c}{\partial \omega} = \frac{\omega}{2G}\left(C + \frac{1}{\omega^2 L}\right) \quad . \qquad (3.2)$$

Given the frequency f, $G_d(V_o,f)$, $B_d(V_o,f)$, and loaded circuit quality factor $Q_{L,C}$, then G, L and C can be determined from Eqs. 3.1 and 3.2. To illustrate the RF circuit dependence of the turn-on transient, the following device parameters are used: current density J_{dc} = 60 kA/cm^2, frequency f = 130 GHz, RF voltage V_o = 12 V, device conductance $G_d(V_o,f)$ = - 24.9 mmho, and device susceptance $B_d(V_o,f)$ = 117.6 mmho.

From Eqs. 3.1 and 3.2, L and C are

$$L = \frac{2}{\omega} \frac{1}{2|G_d|Q_{L,C} + B_d} \qquad (3.3)$$

and

$$C = \frac{- B_d + 2|G_d|Q_{L,C}}{2\omega} \quad . \qquad (3.4)$$

In this section G is equal to 24.9 mmho, and L and C for different $Q_{L,C}$ are as follows:

$Q_{L,C}$	L(H)	C(pF)
25	1.7970×10^{-12}	0.69012
50	9.3900×10^{-13}	1.4522
75	6.3555×10^{-13}	2.2143
100	4.8033×10^{-13}	2.9764
125	3.8605×10^{-13}	3.7385

Threshold current, which is defined as the minimum current to trigger the oscillation, increases with increasing circuit conductance.

Various circuit parameters with different $Q_{L,C}$ have been used to demonstrate the RF circuit dependence of the turn-on transient. In the calculation, a current density J_{dc} = 60 kA/cm^2 is applied to the diode. Shown in Fig. 3.3 is the output power buildup of an IMPATT oscillator shortly after the bias pulse is applied. The output power builds up within 0.4 ns for the RF circuit with $Q_{L,C}$ = 25, while the turn-on time is more than 1 ns for the circuit with $Q_{L,C}$ = 75. Growth rate at t = 0 varies from 1.88 x 10^{10} ($Q_{L,C}$ = 25) to 4.81 x 10^{9} ($Q_{L,C}$ = 75). Figure 3.4 shows that a 9-GHz frequency decrease (138.2 to 129.2 GHz) is obtained with $Q_{L,C}$ = 25, while a 5.5-GHz frequency decrease (135.0 to 129.5) is obtained with $Q_{L,C}$ = 50.

3.4 Bias Circuit Dependence

An IMPATT diode is a current-controlled device, and the waveform of the bias current passing through the diode is heavily dependent on the device properties and the bias circuit. This section presents the results of an investigation of the effects of the bias circuit on the turn-on transient. Constant current source, constant voltage source, and constant voltage source with finite internal impedance have been used to represent the different bias circuits. The source impedance is represented by a series of combinations of a resistor R and an inductor L. The rise time of the bias source is adjusted by varying the values of R and L.

Normally under constant current operation, the dc voltage across the diode will drop with increasing RF voltage amplitude. The turn-on transient for the constant current source case has been described in the example in Section 2. Only the constant voltage source and constant voltage source with finite impedance will be discussed in this

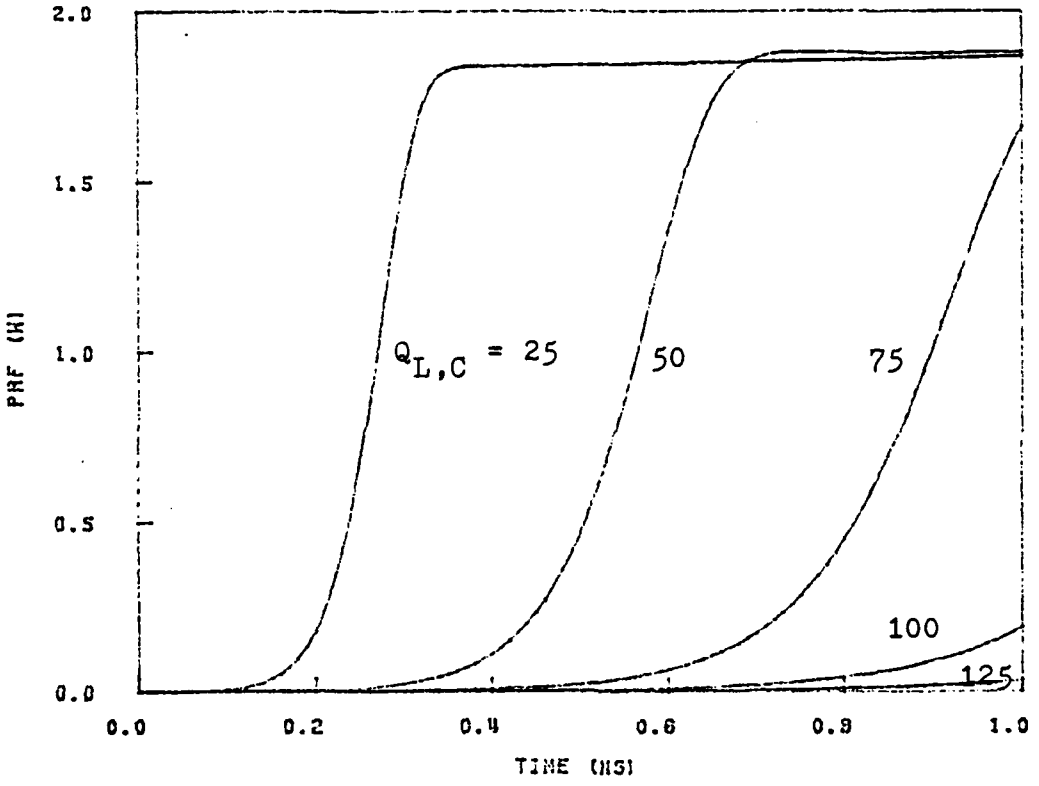

FIG. 3.3 OUTPUT POWER BUILDUP OF IMPATT OSCILLATOR FOR DIFFERENT LOADED CIRCUIT Q.

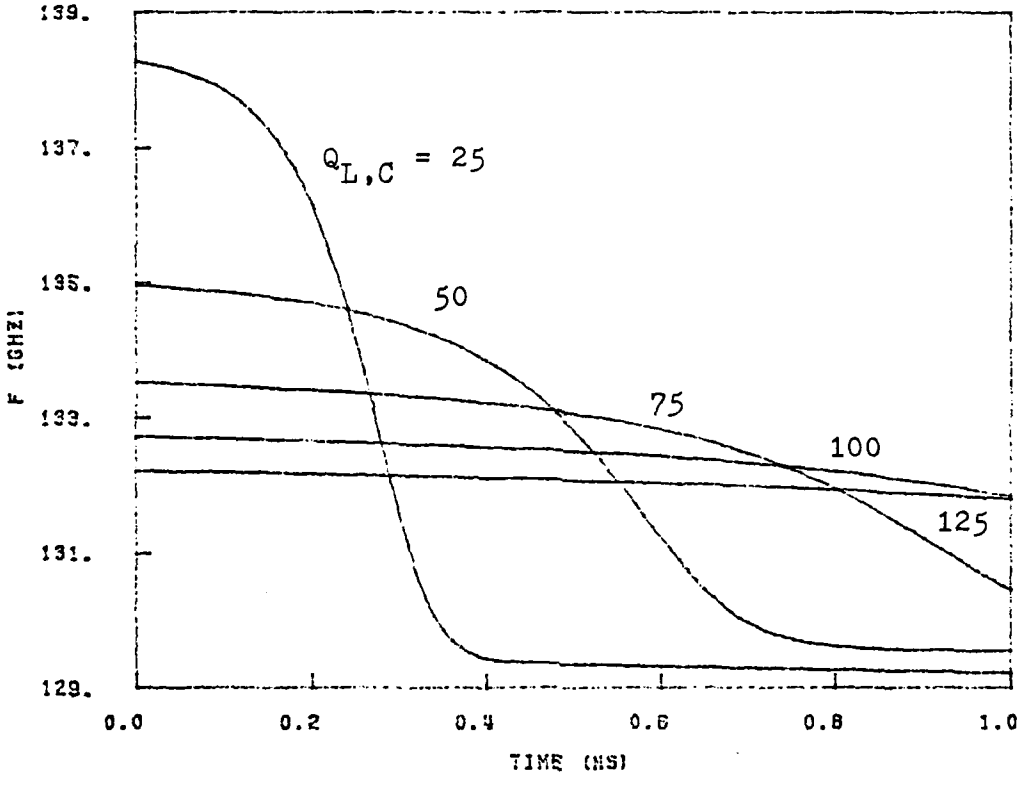

FIG. 3.4 FREQUENCY RESPONSE DURING TURN-ON FOR DIFFERENT LOADED CIRCUIT Q.

section. If the voltage across the diode is held constant, the bias current passing through the diode will increase as the RF voltage increases. When the constant voltage source with finite impedance is used as a bias circuit, the dc voltage and the bias current are not held constant. The dc voltage decreases and the bias current increases as the RF oscillation builds up. This may cause low frequency oscillation.[19]

Low frequency instabilities are serious in millimeter-wave IMPATT diodes, especially DDR diodes which produce the required higher power and efficiency in the millimeter-wave range. The maximum frequency for which low-frequency negative resistance exists in millimeter-wave diodes is several hundred times as large as that in microwave diodes. Thus the suppression of instabilities in higher frequency diodes is more difficult than in lower frequency diodes. Output power will be reduced by low frequency oscillations, and the elimination of low frequency instabilities is essential in the oscillator design.

To illustrate the bias circuit dependence of turn-on transients, a constant voltage source with finite impedance (V_s = 83 V, R = 50 Ω and L = 10 nH) as shown in Fig. 2.3 is used as a bias circuit. Figure 3.5 shows that the current density J_{dc} increases from 0 to 62.8 kA/cm after the step increase of the constant voltage source V_s. Bias current continues to increase until the increase of the junction temperature is significant enough to offset the back-bias effect.

The growth rate σ is negative, and no output power is generated until the current density is greater than 15 kA/cm^2. Then, the rapid increase of bias current causes the growth rate to increase drastically.

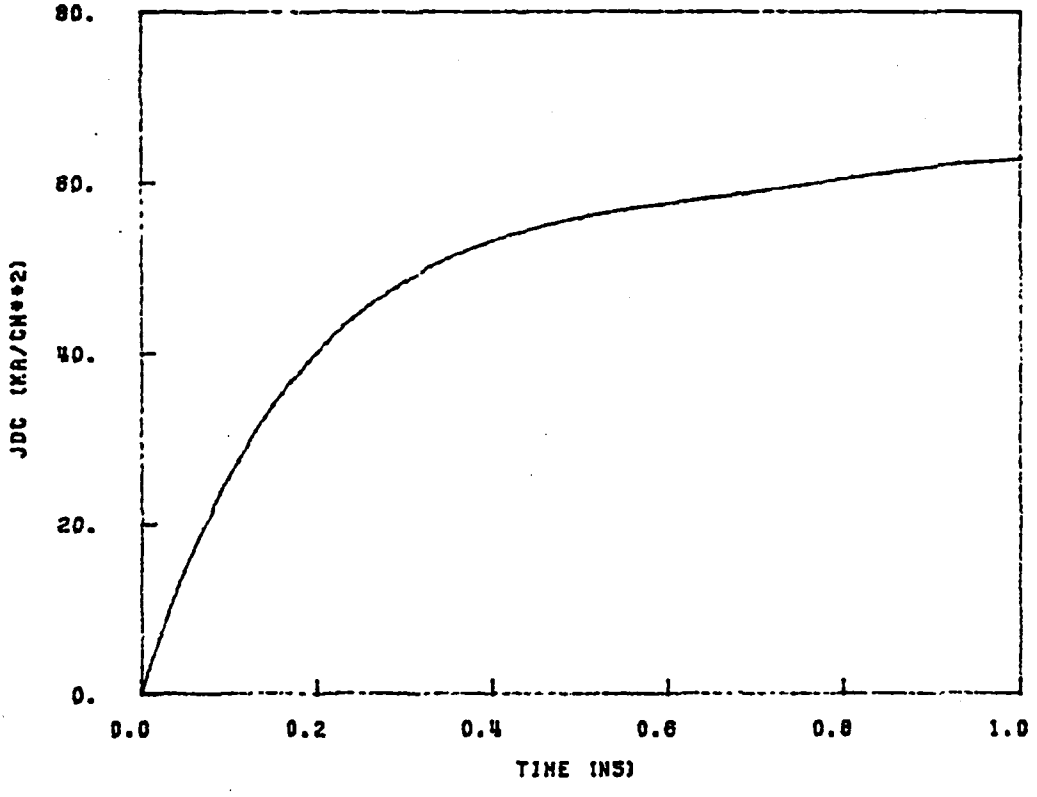

FIG. 3.5 INCREASE OF CURRENT DENSITY FOR CONSTANT VOLTAGE SOURCE WITH FINITE IMPEDANCE.

Consequently, the RF voltage and the output power start to increase. Figure 3.6 shows the increase of output power. The output power builds up to 2 W within 1 ns. The bias current increase and junction temperature rise contribute to the continuous increase of output power after the oscillator is turned on.

Low-frequency negative resistance is determined[20] by the large-signal back-bias effect, the dependence of the device admittance on the RF voltage and dc current, and the oscillator circuit constraint $Y_d(s) + Y_c(s) = 0$. The load for the low-frequency negative resistance is the bias circuit impedance seen from the diode. A low-freqiency bias circuit is stable when

$$R_{sc} + R_{ind} + R > 0 \quad , \tag{3.5}$$

where R_{sc} is the space charge resistance of the diode, R_{ind} is the negative resistance induced by back-bias effect, and R is the bias source resistance.

It can be seen from Eq. 3.5 that low-frequency oscillations can be eliminated by making the bias source resistance R large or by biasing the diode with a constant current source ($R = \infty$). However, at higher frequencies the unavoidable circuit reactances, such as blocking capacitors and bias chokes, introduce time constants that will prevent either constant-current or constant-voltage operation of the diode. Although the space charge resistance has some stabilizing effect, it usually cannot prevent the stable condition from being violated at large RF voltages, and low-frequency oscillations may then appear.

Figure 3.7 shows the behavior of dc voltage across the diode V_{dc} and dc current passing through the diode I_{dc} during turn-on.

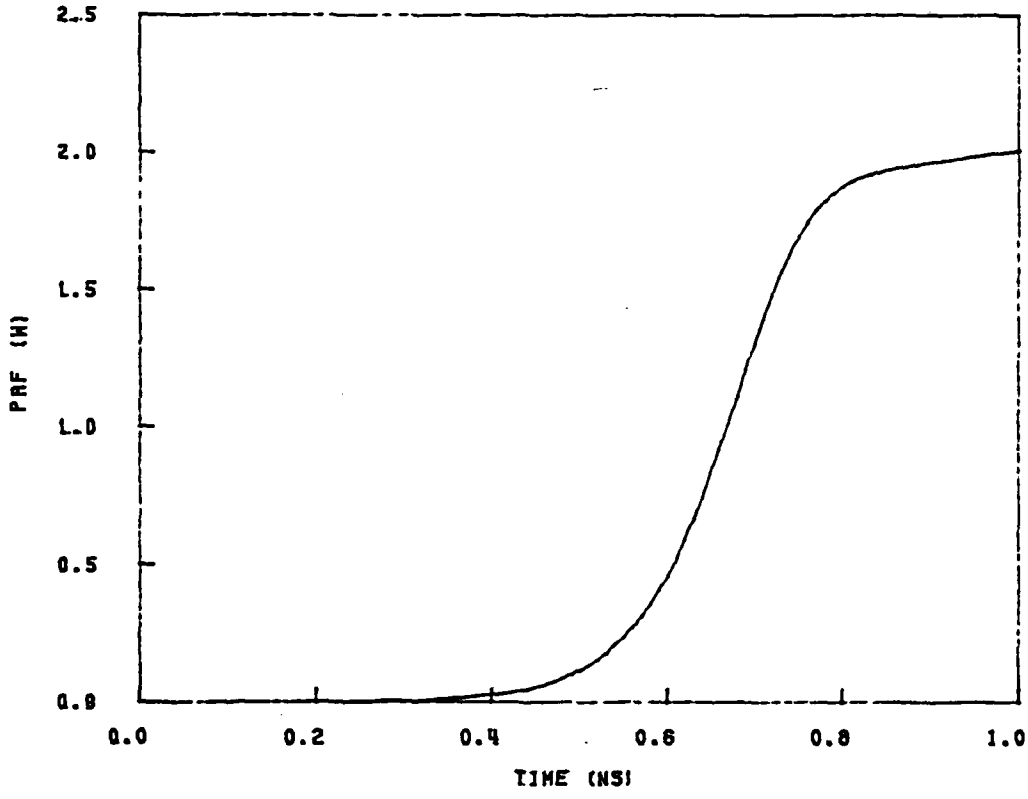

FIG. 3.6 BUILDUP OF OUTPUT POWER FOR CONSTANT VOLTAGE SOURCE WITH FINITE IMPEDANCE.

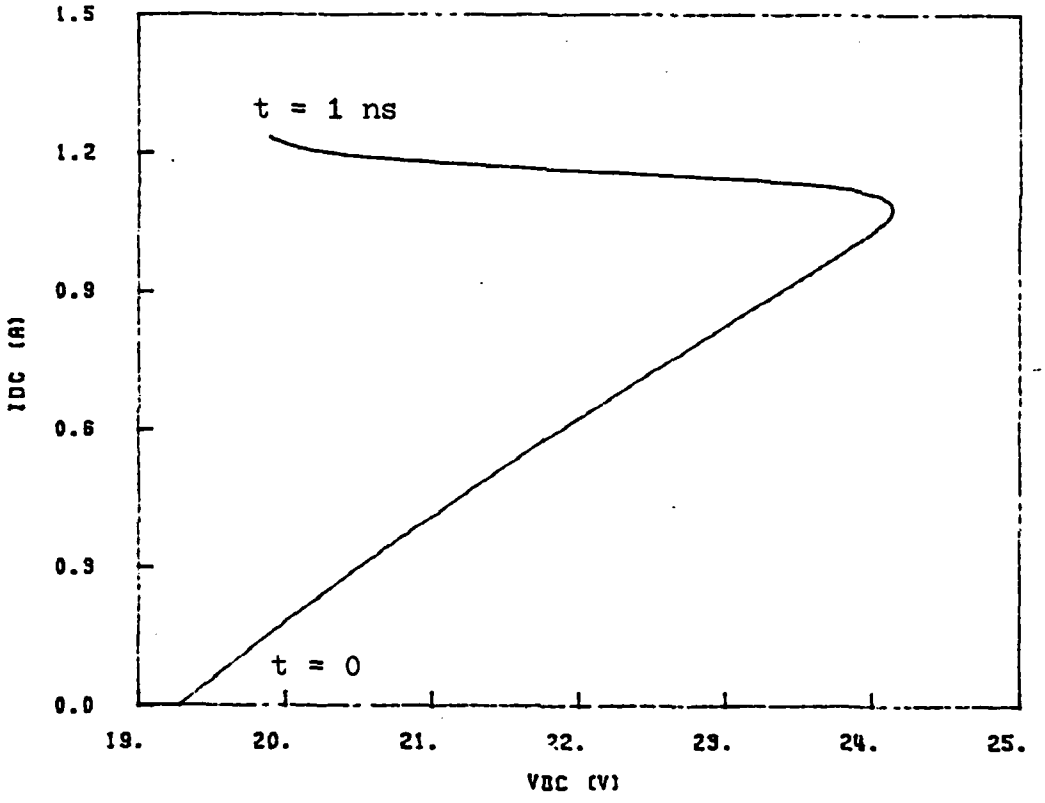

FIG. 3.7 BEHAVIOR OF DC VOLTAGE AND DC CURRENT FOR CONSTANT VOLTAGE SOURCE WITH FINITE IMPEDANCE.

I_{dc} and V_{dc} increase when the RF voltage is small, while I_{dc} increases and V_{dc} decreases when the RF voltage is building up. From positive and negative resistance regions of the dc response, R_{sc} and R_{ind} can be estimated:

$$R_{sc} \cong 4.8\ \Omega \tag{3.6}$$

and

$$R_{ind} + R_{sc} \cong -53.9\ \Omega\ . \tag{3.7}$$

From Eqs. 3.6 and 3.7, it can be seen that the magnitude of R_{sc} is much smaller than that of R_{ind}. To achieve a stable condition at low frequency, $R > 53.9\ \Omega$ is desired. The 50-Ω bias source resistance used here is not large enough to eliminate the low-frequency oscillation.

3.5 Effect of Injection Locking on the Turn-On Transient

Millimeter-wave oscillators can achieve pulse-to-pulse coherency by injection locking to low-level stable oscillators. At $t = 0$, the bias current is negligible, and the IMPATT diode behaves as a capacitor. The device capacitance C_d at $t = 0$ is given by

$$C_d = \frac{\varepsilon A}{d}\ , \tag{3.8}$$

where ε is the dielectric constant of the semiconductor, A is the device area, and d is the device width.

For the Si DDR IMPATT diode used in the calculation, the values are $d = 1\ \mu m$, $A = 1.9635 \times 10^{-5}\ cm^2$, and $\varepsilon = 1.06 \times 10^{-12}\ F/cm^2$, which gives $C_d = 0.208$ pF. $V_{RF}(0)$, which is the RF voltage at $t = 0$, depends on the frequency of the locking signal f_i, RF circuit admittance $(G + jB_c)$, and the injection current I_i:

$$V_{RF}(0) = \frac{I_1}{\sqrt{(\omega_i C_d)^2 + (G^2 + B_c^2)}} \qquad (3.9)$$

and

$$I_1 = \sqrt{8\ GP_{in}}\ , \qquad (3.10)$$

where ω_i is the angular frequency of the locking signal and P_{in} is the injection power of the locking signal.

In this section the effects of the injection locking on the turn-on transient are described. All the other conditions (bias circuit, RF circuit, bias current, etc.) are the same; only the injection frequency, injection power and initial phase angle are varied. Let P_{in} = 0.2 W which is approximately 10 dB below the output power of the free-running oscillator. The oscillator is simulated with the circuit conductance G = 24.9 *mmho*, inductor L = 9.39 x 10^{-13} H, and capacitor C = 1.4522 pF as shown in Fig. 2.5. From Eq. 3.10, the injection current I_1 for the preceeding parameters is I_1 = 0.2 A.

The effects of injection current on the turn-on transient will be studied first while the injection frequency and the initial phase angle are unchanged. An injection frequency of f_i = 129 GHz is used, and the initial conditions for the phase and RF voltage are

$$\theta(0) = 0 \qquad (3.11)$$

and

$$V_{RF}(0) = I_1\ (4.58)\ . \qquad (3.12)$$

To study the effects of injection locking on the pulsed oscillator behavior, the following dynamic equations are used:

$$\sigma = \frac{1}{V_{RF}} \frac{dV_{RF}}{dt} \qquad (3.13)$$

and

$$\dot{\theta} = \omega - \omega_i \quad . \tag{3.14}$$

Therefore, the RF voltage and phase at different times can be calculated:

$$V_{RF}(t + dt) = V_{RF}(t) + dV_{RF} \tag{3.15}$$

and

$$\theta(t + dt) = \theta(t) + d\theta \quad , \tag{3.16}$$

where dV_{RF} equals $(\sigma V_{RF})dt$, $d\theta$ equals $(\omega - \omega_i)dt$, and dt is the time step used in the calculation. The current values of σ and ω are obtained by solving the oscillator equation in the presence of the locking signal, as indicated in Fig. 2.1.

Effect of Injection Current on the Turn-On Transient

The free-running oscillator (FRO) was found to have a fast growth rate and a turn-on time of less than 1 ns with $V_{RF}(0) = 0.1$ V. The dynamics of the pulsed injection locked oscillator (PILO) have been studied. Figure 3.8 shows the output power buildup of the PILO in the time domain for different injection current levels I_1. I_1 varies from 0.04 to 0.1, i.e., $V_{RF}(0)$ varies from 0.183 to 0.458. As the injection current I_1 is increased, the level from which RF oscillation is initiated, $V_{RF}(0)$, increases. The turn-on time increases or decreases depending on the initial phase angle and injection frequency. For a given initial phase angle $\theta(0) = 0$ and injection frequency $f_i = 129$ GHz, the initial growth rate of the PILO remains the same (7×10^{10}) for different injection currents and is much larger than that of the FRO (8×10^{9}). Thus, the output power builds up faster with injection

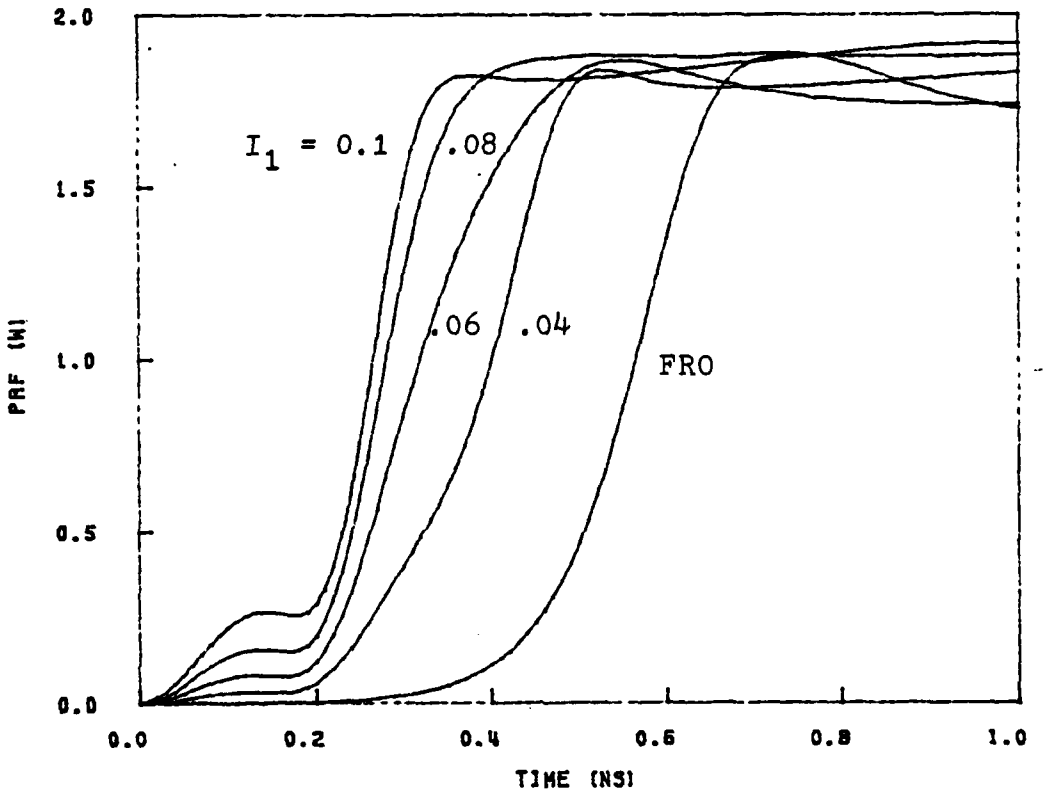

FIG. 3.8 BUILDUP OF OUTPUT POWER FOR DIFFERENT INJECTION CURRENTS I_1.

locking, and the decrease of turn-on time as the injection current is increased is mainly caused by the increase of $V_{RF}(0)$.

The change of the phase angle is proportional to the difference between the oscillation frequency and the injection frequency. For f_i = 129 GHz, the phase angle increases continuously. The large frequency decrease of the FRO during turn-on has been described. The frequency drift of the PILO during turn-on is about the same as that of the FRO. A large amount of frequency drift causes the phase angle to vary drastically. For I_1 = 0.1, the phase angle increases from 0 to 8.84 rad in 1 ns. The RF voltage of the PILO can increase or decrease depending on the value of the phase angle.

Effect of Initial Phase Angle on the Turn-On Transient

To study the effect of the initial phase angle on the turn-on transient of a PILO, both the injection frequency and the injection current were held constant while the initial phase angle $\theta(0)$ was varied from 0 to $7/4\ \pi$. The following conditions were used in the simulation: f_i = 129 GHz, I_1 = 0.06 A, i.e., $V_{RF}(0)$ = 0.2745 V, and $\theta(0)$ = 0 to $7/4\ \pi$ rad.

When a signal is injected, the initial growth rate at t = 0 increases or decreases (relative to that of the FRO) depending on whether $-\pi/2 < \theta(0) < \pi/2$ or $\pi/2 < \theta(0) < 3/2\ \pi$. Figure 3.9 shows the output power buildup of the PILO for different $\theta(0)$. It can be seen that turn-on time is smallest when $\theta(0) = 3/2\ \pi$, although the initial growth rate is not the maximum. The maximum initial growth rate (7×10^{10}) occurs when $\theta(0) = 0$. This phenomenon is caused by the large variation of the phase angle during turn-on.

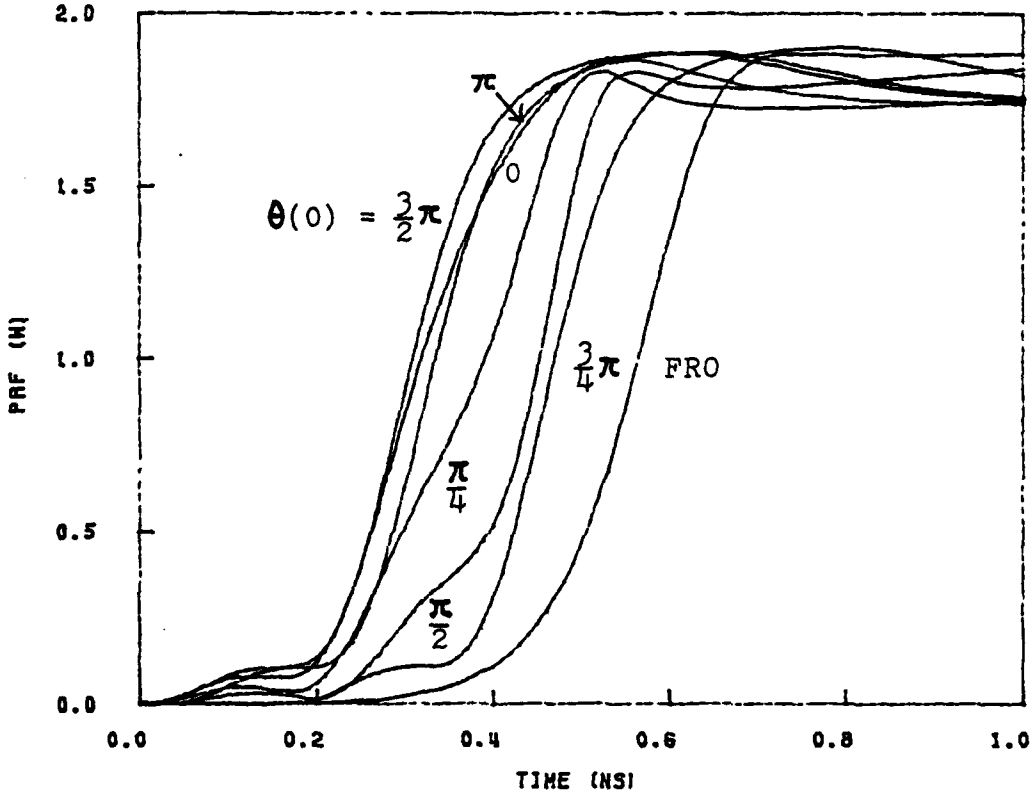

FIG. 3.9 BUILDUP OF OUTPUT POWER FOR DIFFERENT INITIAL PHASE ANGLES.

Effect of Injection Frequency on the Turn-On Transient

To study the effect of injection frequency on the turn-on transient of a PILO, an injection current $I_1 = 0.06$ and an initial phase angle $\theta(0) = 0$ were used. The injection frequency f_i and initial RF voltage $V_{RF}(0)$ are as follows:

f_i (GHz)	$V_{RF}(0)$
129	I_1 (4.575) = 0.2745
129.5	I_1 (4.691) = 0.2815
130	I_1 (4.805) = 0.2883
131	I_1 (5.023) = 0.3014

The major influence of injection frequency on the turn-on transient is the response of the phase angle. When there is no injection signal, frequency decreases from 135 to 129.5 GHz during turn-on. The variation of the phase angle is minimum for $f_i = 131$ GHz and is maximum [$\theta(0)$ varies from 0 to 12.5 rad] for $f_i = 129$ GHz. Figure 3.10 shows the frequency responses of a PILO for various injection frequencies. It can be seen that the frequency variation is minimum during turn-on when $f_i = 131$ GHz.

3.6 Effect of Photon Injection on the Turn-On Transient

The influences of photon injection on IMPATT oscillators can be understood in terms of the effect photon injection has on the device admittance Y_d, assuming negligible optical dependence of the microwave circuit admittance. Photon injection effectively increases reverse saturation current I_o, and this increase results in the variation of device properties. Misawa has shown that an increase in reverse saturation current leads to a premature buildup of the avalanche current and reduces the phase delay associated with the avalanche

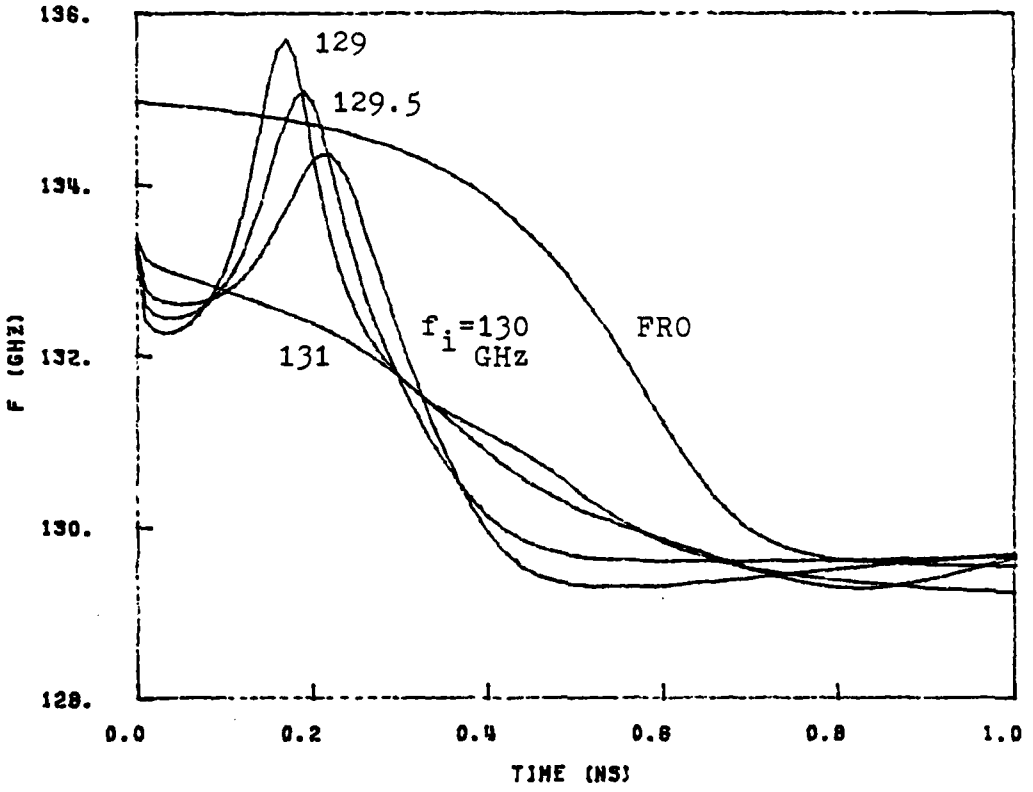

FIG. 3.10 FREQUENCY RESPONSES OF PILO FOR VARIOUS INJECTION FREQUENCIES.

process, which in turn severely reduces the generated output power and efficiency. If the phase delay is reduced sufficiently, the negative conductance will be insufficient to overcome the circuit losses, and RF oscillation will cease at high-level photon injection.

Figure 3.11 shows the buildup of output power at various optical current densities (J_{op} varies from 0 to 875 A/cm^2) when the diode is biased with a constant current source (J_{dc} = 60 kA/cm^2). It can be seen that output power decreases with increasing optical current. Output power decreases from 1.9 to 1.5 W when J_{op} = 500 A/cm^2. The small-signal negative conductance, and hence the initial growth rate of the RF oscillation, are changed by photon injection. The initial growth rate of the IMPATT oscillator decreases, and the turn-on time increases, with photon injection. The oscillator is turned on within 0.7 ns when there is no photon injection, and the buildup is not completed in 1 ns when J_{op} = 875 A/cm^2. Initial growth rate at the start of turn-on is maximum (8.1×10^9) when J_{op} = 0 and is minimum (5×10^9) when J_{op} = 875 A/cm^2.

Another important parameter is the oscillator frequency, determined by the resonance of the circuit-supplied inductive susceptance with the diode-supplied capacitive susceptance. The capacitive susceptance of the diode decreases with photon injection level. This in turn leads to an increase in operating frequency. The simulation result shows that the operating frequency f_o at steady state increases with increasing optical current. The operating frequency f_o increases from 129.5 GHz (J_{op} = 0) to 130 GHz (J_{op} = 500 A/cm^2). This resulting frequency shift, which depends heavily on the circuit Q, is less than 0.5 percent with J_{op} = 5 A/cm^2. RF voltage at steady state, and hence

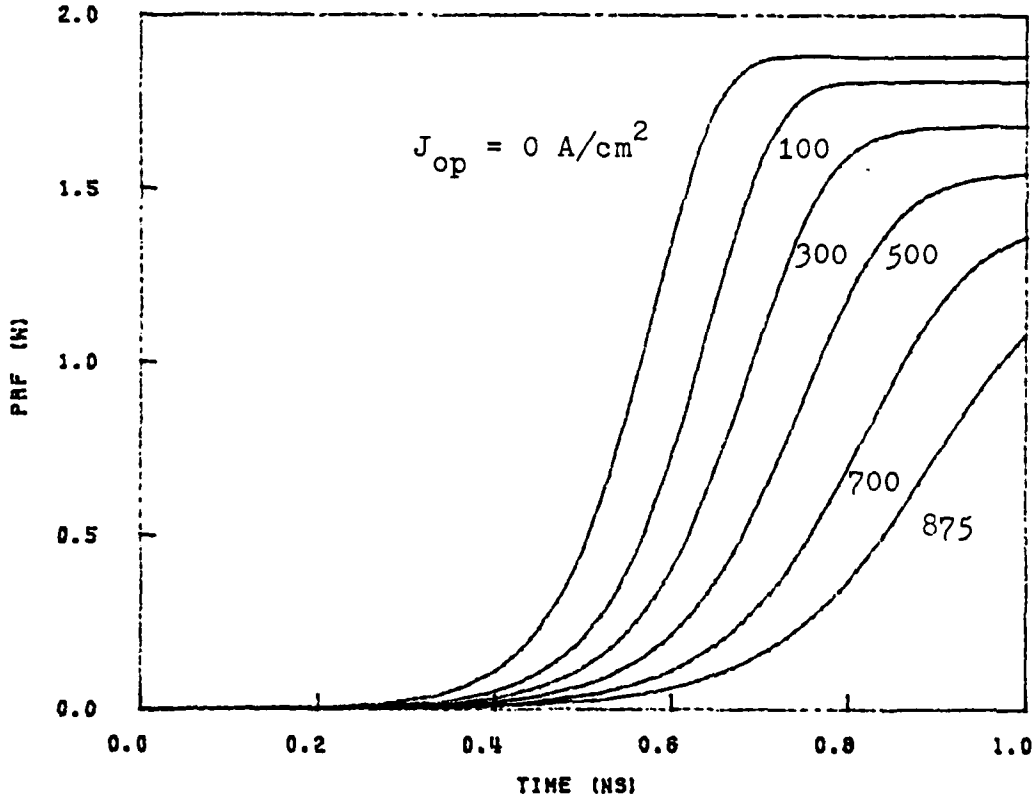

FIG. 3.11 BUILDUP OF OUTPUT POWER AT VARIOUS OPTICAL CURRENT DENSITIES WHEN THE DIODE IS BIASED WITH A CONSTANT CURRENT SOURCE(J_{dc} = 60 kA/cm^2).

the amount of frequency decrease during turn-on, decreases with increasing optical current.

With an appropriate bias circuit, photon injection can be used to trigger RF oscillation. To illustrate this phenomenon, a constant voltage source (20.6 V) with finite impedance (0.5-Ω bias resistor and 0.2-nH bias inductor) is used as the bias circuit. The microwave circuit parameters are G = 22.4 mmho, L = 3.04×10^{-12} H, and C = 0.22 pF. Figures 3.12 and 3.13 show the bias current and output power responses in the time domain when the diode is exposed to various photon injection levels at t = 0.1 ns. Without photon injection, the IMPATT diode cannot generate RF power since the bias current is below the threshold value (J_{dc} = 15 kA/cm^2). When the diode is exposed to an external optical source, the breakdown voltage and the dc voltage across the diode decrease. To offset this decrease of dc voltage the bias current increases. The degree of current increase depends on the injection level and bias circuit configuration. Bias current and output power increase with increasing optical current. With J_{op} = 875 A/cm^2, J_{dc} increases to 35 kA/cm^2, and 0.6 W output power is obtained at t = 0.1 ns. Low bias resistance is required to trigger RF oscillation by photon injection. When the bias resistance is large, the current increase is too small to turn on the oscillator.

3.7 Turn-On Jitter

Turn-on jitter is the variation of the leading edge of the output power with respect to the time the bias current pulse is applied to the diode. Pulsed IMPATT oscillators show detectable turn-on jitter. RF power displayed on an oscilloscope shows a blurred front edge jitter. All exponentially growing systems including pulse

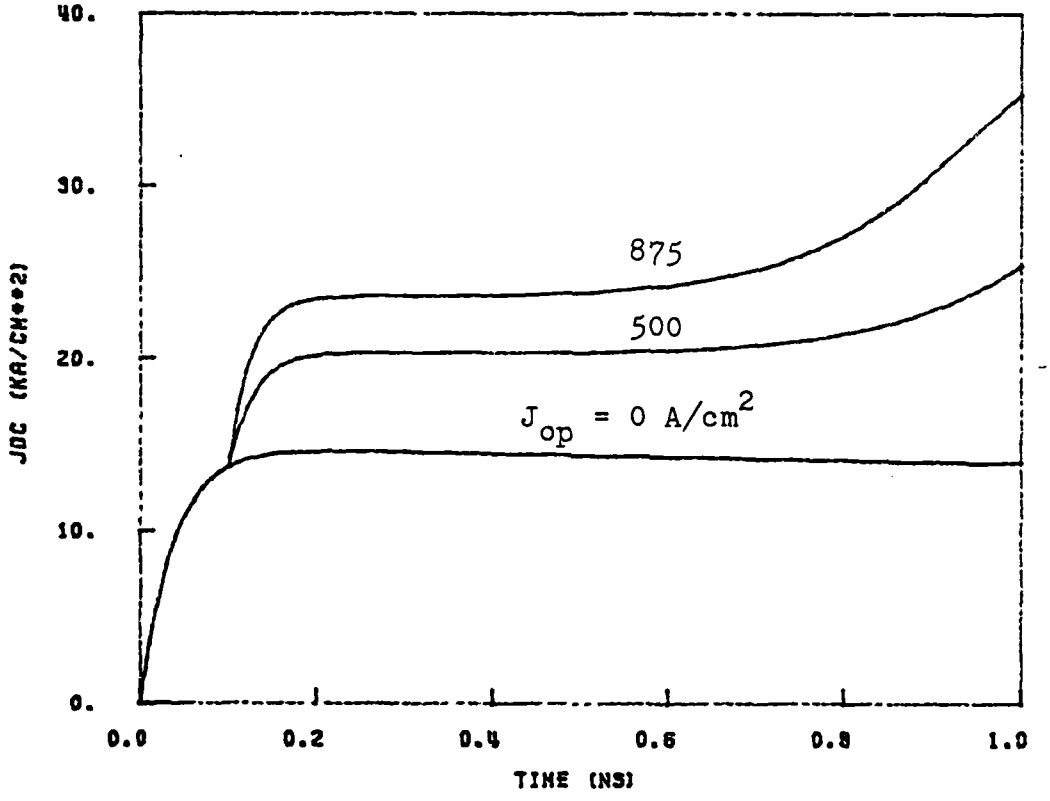

FIG. 3.12 BIAS CURRENT RESPONSE WITH VARIOUS PHOTON INJECTION LEVELS APPLIED AT TIME = 0.1 NS.

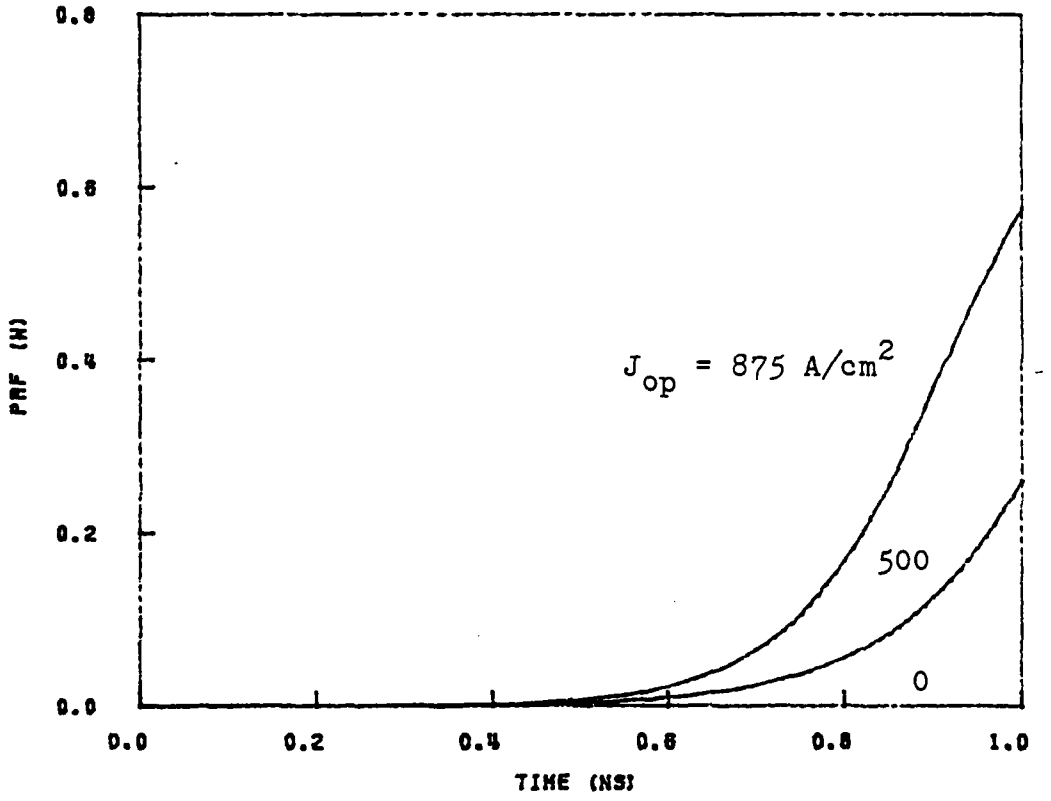

FIG. 3.13 OSCILLATOR TURN-ON BY PHOTON INJECTION. VARIOUS PHOTON INJECTION LEVELS APPLIED AT TIME = 0.1 NS.

oscillators must start from a finite amplitude if they are to build up to a larger amplitude in a finite time. In the case of the free-running IMPATT oscillator, the starting level is generated by the high frequency component of the noise voltage. The time-dependent RF voltage of the oscillator has an amplitude which can be described by[21]

$$V_{RF}(t) = V_{RF}(0)e^{\sigma(t)t} ,$$

where $\sigma(t)$ is the time-dependent growth rate of the RF voltage, and $V_{RF}(0)$ is the initial amplitude of the RF voltage at $t = 0$, when the bias pulse is applied to the diode.

Since $V_{RF}(0)$ is noise generated, its amplitude may vary from pulse to pulse. The higher the initial RF voltage the sooner steady state is reached. Therefore, turn-on jitter which represents a deviation from the perfect infinite pulse train, will occur. Figure 3.14 illustrates the simulated turn-on jitter with initial RF voltage varying from 0.04 to 0.14 V. All the other device (J_{dc} = 60 kA/cm^2) and circuit parameters are unchanged. It can be seen that jitter time is approximately 0.2 ns.

For a given diode and pulse generator, the bias circuit and microwave circuit can be optimized to achieve the minimum turn-on jitter of a free-running oscillator. With an external injection signal or optical injection, the successive pulses start from relatively constant $V_{RF}(0)$. Thus the jitter can be greatly reduced.

3.8 Effect of Ambient Temperature

In this section the effect of ambient temperature on the turn-on transient will be described. Reliability of a semiconductor device is a function of its operating junction temperature T_j. In order to

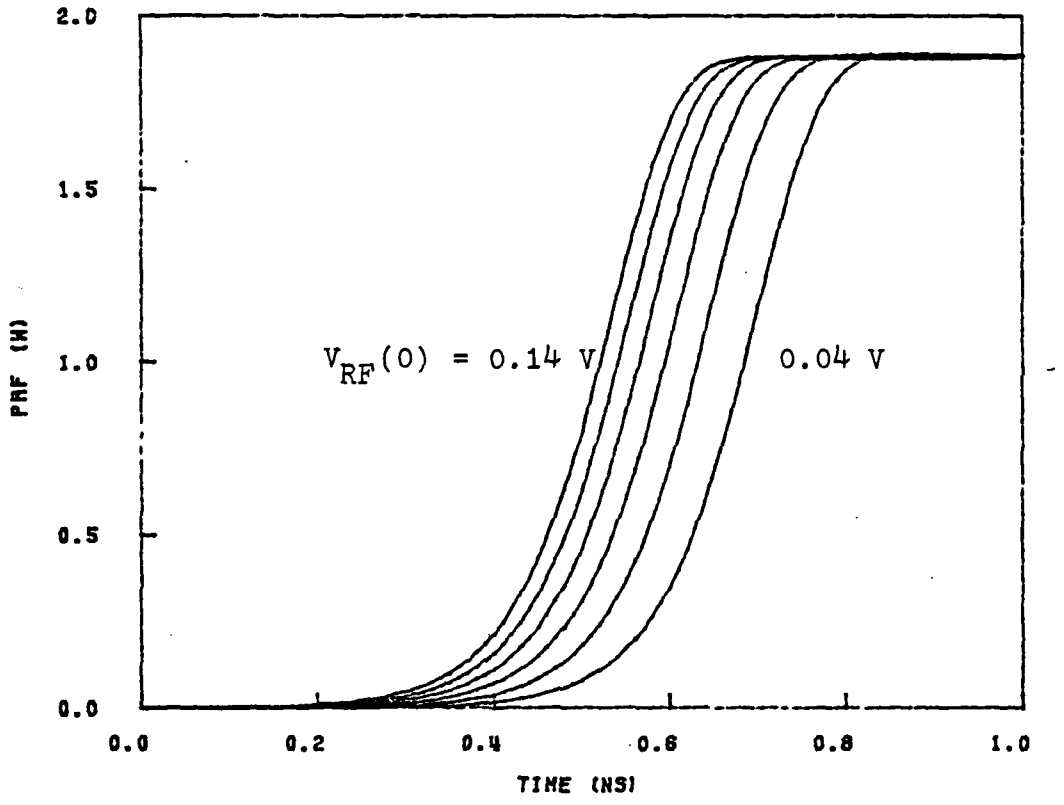

FIG. 3.14 TURN-ON JITTER WITH INITIAL RF VOLTAGE VARYING FROM 0.04 TO 0.14 V.

maintain the desired reliability, the maximum junction temperature $T_{j,max}$ is constrained, as is the allowed junction temperature increase $\Delta T = T_{j,max} - T_a$, where T_a is the ambient temperature. An oscillator operated under high ambient temperature (smaller ΔT) generates less output power since the bias current is limited by ΔT. IMPATT diodes can be operated at lower bias current to improve reliability at the expense of reduced output power. Devices operated at a lower T_a may generate additional power by applying more bias current.

For $J_{dc} = 60$ kA/cm^2, the magnitude of the small-signal G_d at 300°K is larger or smaller than the magnitude at 500°K depending on whether oscillation frequency is $f > 134$ GHz or < 134 GHz, respectively. Figure 3.15 shows the buildup of RF power as a function of ambient temperature. T_a varies from 270 to 330°K. Since oscillation frequency at $t = 0$ is 135 GHz, the initial growth rate decreases, and the turn-on time increases with increasing ambient temperature. Output power at steady state increases with ambient temperature as expected.

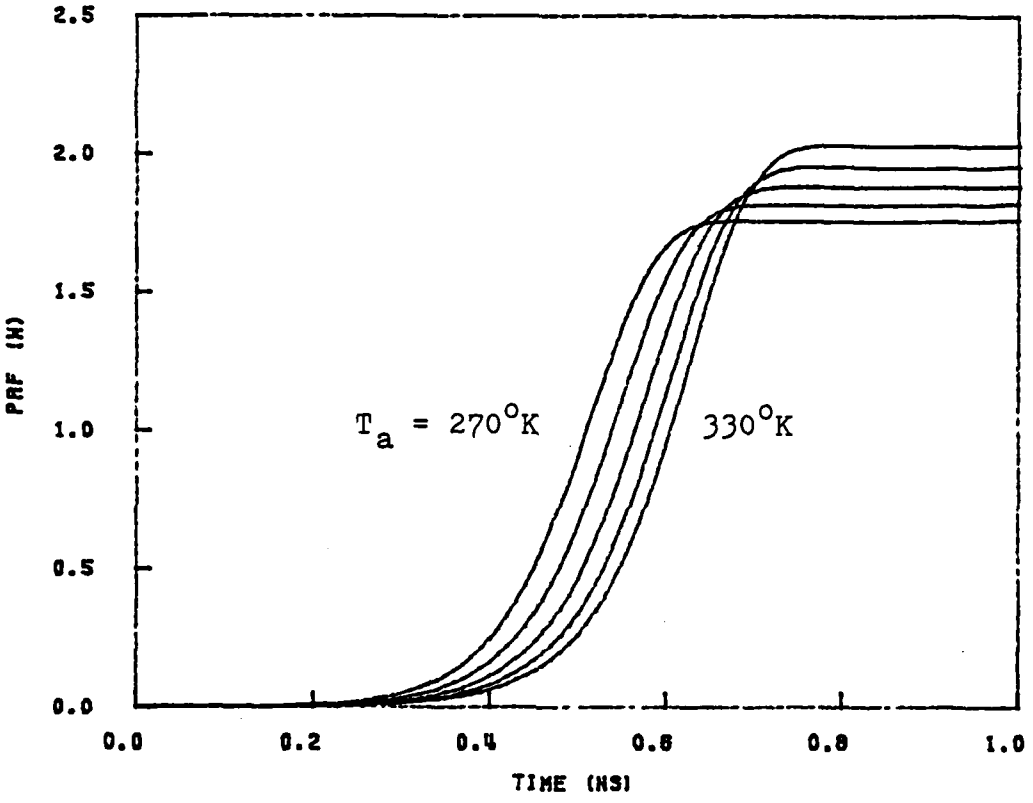

FIG. 3.15 BUILDUP OF OUTPUT POWER AS A FUNCTION OF AMBIENT TEMPERATURE.

SECTION IV.

CONTROL OF THE POST TURN-ON TRANSIENT

4.1 Introduction

Millimeter-wave oscillators can have a wide range of duty cycles (continuous wave, short pulse, and long pulse). One of the problems in millimeter-wave pulsed IMPATT oscillators is the frequency drift caused by the temperature rise of the diode during the bias pulse. The high bias current required for high power oscillation results in a negative frequency drift of several percent during the pulse as described in Section 2.4.

For some systems, post turn-on frequency drift is acceptable. For others the combination of frequency drifts caused by device temperature rise and ambient temperature variation may take the oscillation frequency out of the receiver bandwidth or compromise some other system parameters. It is, therefore, often desirable to reduce or eliminate the post turn-on frequency drift. To improve the post turn-on frequency drift of pulsed oscillators, a number of techniques are available[22,23] including the following: (1) varying the dc bias voltage of a varactor diode located near the IMPATT diode; (2) high Q circuit; (3) using a CW oscillator followed by a microwave switch (such as PIN diode); (4) capacitor with negative temperature coefficient; (5) shaping the bias current waveform; (6) applying a time-dependent optical injection while the bias current remains constant, and (7) injection locking. These techniques have various advantages and disadvantages. The first four techniques are discussed briefly here and others are described in the following sections.

Varactor Compensation

By inserting a varactor diode $n\lambda_g/2$ away from the diode, a small but useful amount of electronic tuning can be obtained. The frequency in a pulsed solid-state oscillator has an almost exponential dependence with time as shown in Fig. 2.12. By applying a nonlinear upward voltage biasing V(t) to the varactor [V(t) increases with time during the pulse], the susceptance of the varactor decreases with time. Therefore, the frequency of the oscillator can be adjusted to increase during the pulse by almost the same magnitude as the frequency drop caused by device heating.

High Q Circuit

Post turn-on frequency drift can be improved by using a high Q circuit as shown in Section 2.4. A smaller drift value ($\Delta f/\Delta t$) can be achieved by this method. However, the delay time between the output power and the bias pulse increases with circuit Q.

Microwave Switch

When a CW oscillator is followed by a microwave switch, the low drift pulsed oscillator can be realized, and the problem of turn-on transient may also be avoided by turning on and off the microwave switch appropriately. This technique reduces the frequency drift during the pulse but at the expense of less peak power and an extra component (microwave switch). The peak power of the oscillator is limited to the maximum output power under CW condition.

Capacitor with Negative Temperature Coefficient

A simple frequency stabilization method using a ceramic dielectric has been demonstrated by Kondo.[24] The increase of diode capacitance causes the oscillation frequency to shift lower when the bias current is

held constant, and the cavity expansion due to the temperature rise also invites the same result on frequency response. When a ceramic capacitor C with a negative temperature coefficient (C decreases with temperature) is loaded in parallel with the diode package, the susceptance changes of the diode and cavity are compensated, and the oscillator would have less post turn-on frequency drift. Advantages of this technique are simplicity and low cost.

4.2 Bias Current Compensation

Since the device admittance is dependent on the bias current, the amount of post turn-on frequency drift can be controlled by shaping the waveform of bias current pulse applied to the diode. Device conductance G_d and susceptance B_d of the IMPATT diode both decrease with an increase of the bias current. The influence of of the bias current shaping on the frequency drift can be understood qualitatively from Eq. 4.1 which has been derived in Section 2.4:

$$\frac{\partial(B_d + B_c)}{\partial f} \Delta f = A_1 \Delta T + A_2 \Delta I_{dc} \quad , \tag{4.1}$$

where

$$A_2 = \frac{\partial B_d}{\partial V_{RF}} \frac{1}{\partial G_d / \partial V_{RF}} \frac{\partial G_d}{\partial I_{dc}} - \frac{\partial B_d}{\partial I_{dc}} \quad . \tag{4.2}$$

Both the first and the second terms ($\partial B_d / \partial I_{dc}$) of Eq. 4.2 are negative, so that the sign of A_2 has to be determined quantitatively. To evaluate the current coefficient A_2, the following parameters estimated at the operating point when $T_j = 300°K$ and $J_{dc} = 60$ kA/cm^2 are used for the millimeter-wave IMPATT:

$\partial B_d / \partial V_{RF} = 1.09 \times 10^{-2}$ mho/V,

$\partial G_d / \partial V_{RF} = 2.1 \times 10^{-3}$ mho/V,

$\partial G_d/\partial I_{dc} = -1.83 \times 10^{-2}$ mho/A, and

$\partial B_d/\partial I_{dc} = -1.14 \times 10^{-1}$ mho/A.

When these parameters are substituted into Eq. 4.2, the value of A_2 is obtained as

$$A_2 = -9.5 \times 10^{-2} + 1.14 \times 10^{-1} = 1.9 \times 10^{-2} \text{ mho/A} .$$

It has been demonstrated that frequency decreases with temperature ($A_1 < 0$). The calculated result ($A_2 > 0$) suggests that an appropriate bias current waveform can be used to compensate the variation of the device admittance due to the thermal effect and provide an improvement of the frequency drift produced in the pulsed oscillator. In this section a post-in-waveguide circuit is used as the circuit model. The circuit and package parameters are described in the appendix.

An increase of dc current results in more dissipated power and accordingly more temperature rise. To compare the effects of various bias current waveforms on the frequency drift, the temperature rise during the pulse has to be taken into consideration. Figure 4.1 shows the various bias current density waveforms used to study the effects of current shaping on the frequency drift and power variation of pulsed IMPATT oscillators. For curve E, current density J_{dc} increases from 45 to 75 kA/cm^2 linearly during the 40-ns pulsewidth. The current waveforms are chosen to give roughly the same junction temperature rise ΔT which is used in the simulation results.

Figure 4.2 shows the frequency responses of the pulsed oscillator under various current waveforms. When there is no current compensation (curve B), the junction temperature rise is 167.5°C, and the frequency decrease caused by the temperature rise is 3.7 GHz (frequency decreases from 119.1 to 115.4 GHz). The temperature coefficient ($f_d/\Delta T$) is

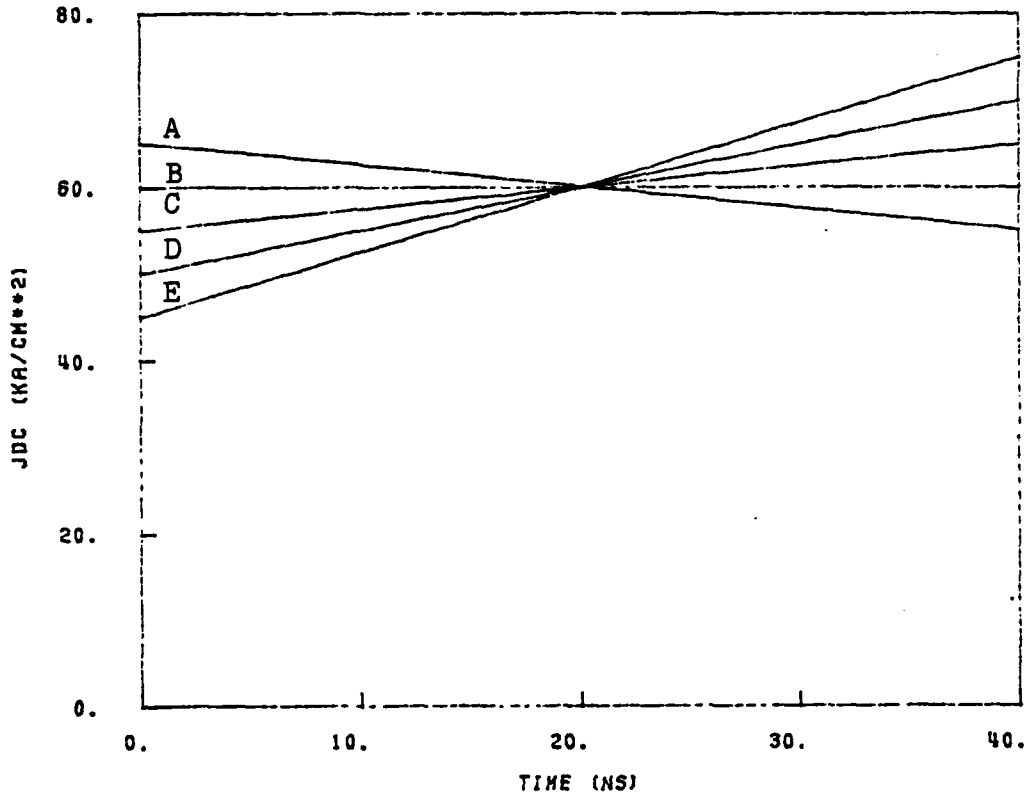

FIG. 4.1 VARIOUS BIAS CURRENT WAVEFORMS USED TO STUDY THE EFFECTS OF CURRENT SHAPING ON THE FREQUENCY DRIFT AND POWER VARIATION OF PULSED OSCILLATOR.

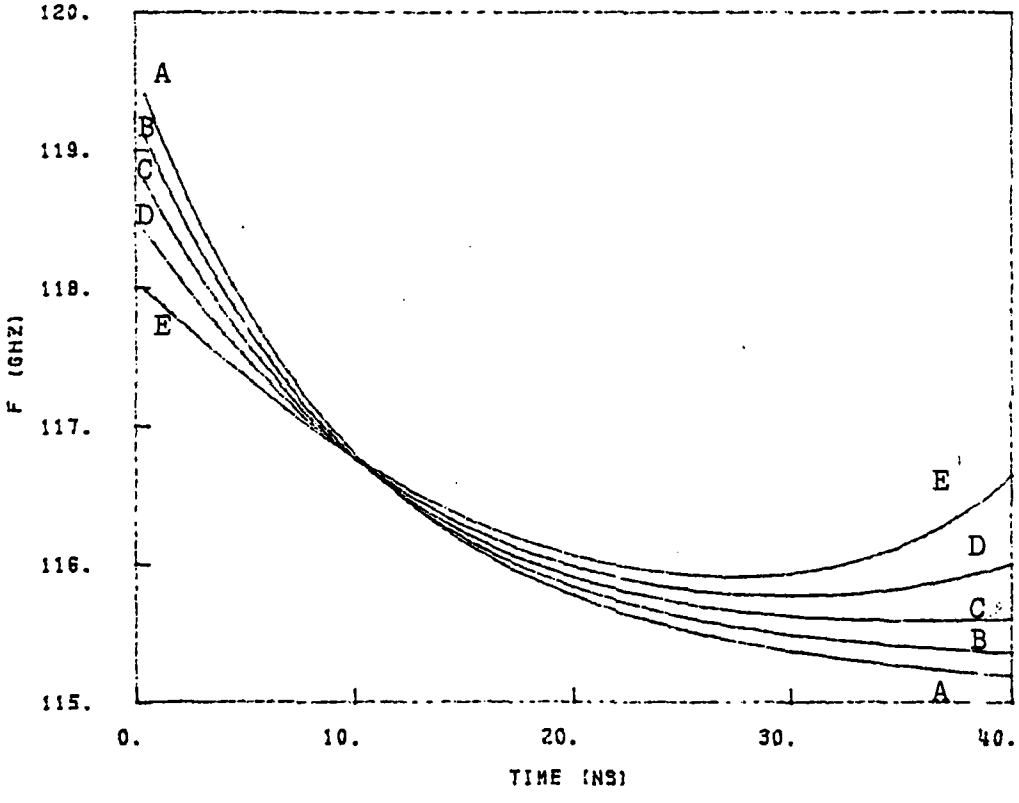

FIG. 4.2 FREQUENCY RESPONSES OF THE PULSED OSCILLATOR UNDER VARIOUS BIAS CURRENT WAVEFORMS.

22.1 MHz/°C, where f_d is defined as the difference between the maximum frequency f_{max} and the minimum frequency f_{min}. The temperature rise of the oscillator with current compensation (curve E) is 187.7°C, and f_d is 2.1 GHz (f_{max} = 118.0 GHz, f_{min} = 115.9 GHz). The temperature coefficient 11.2 MHz/°C is only one-half of that due to the flat current. It can be seen that the frequency drift is varied by biasing the diode with a current pulse having a time-dependent amplitude, and the amount of frequency drift f_d decreases with upward current compensation. For curve E, the oscillation frequency decreases from 118.0 to 115.9 GHz and then increases to 116.6 GHz. The reason for this frequency increase is that the frequency drop caused by the thermal effect is over-compensated by the current increase.

Figure 4.3 shows the power variation of the pulsed oscillator under various bias current waveforms. When there is no current compensation, output power increases from 1.3 to 3.27 W. With upward current compensation (curve E), output power increases from 1.03 to 4.15 W. It can be seen that the amount of power variation increases with an upward current waveform although the frequency drift is improved.

Since the temperature increases and frequency decreases exponentially in the time domain, an exponentially increasing current waveform may achieve less frequency drift than that due to a linearly increasing current waveform. Figure 4.4 shows the exponentially increasing current waveforms used to study the effects of exponentially and linearly increasing current waveforms on the frequency drift. For curve I, current density $J_{dc} = 75 + (45 - 75)e^{-t/\tau_{th}}$ kA/cm^2, where τ_{th} (11.24 ns) is the thermal time constant. Figure 4.5 shows the frequency responses of the pulsed oscillator with exponentially increasing current waveforms. For curve

AD-A112 117 MICHIGAN UNIV ANN ARBOR ELECTRON PHYSICS LAB F/G 9/5
NEAR-MILLIMETER-WAVE SOLID-STATE SOURCES--LIMITATIONS AND CONTR--ETC(U)
JAN 82 D F PETERSON, G I HADDAD, Y S HWANG DAAG29-79-G-0034
UNCLASSIFIED ARO-15951.1-EL NL

2 OF 2
AD A
112117

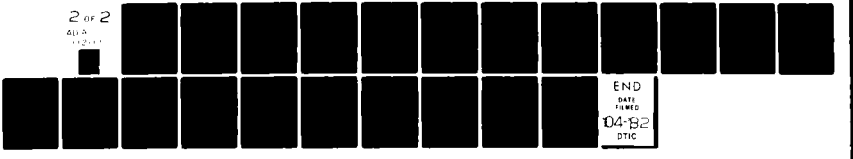

END
DATE FILMED
04-82
DTIC

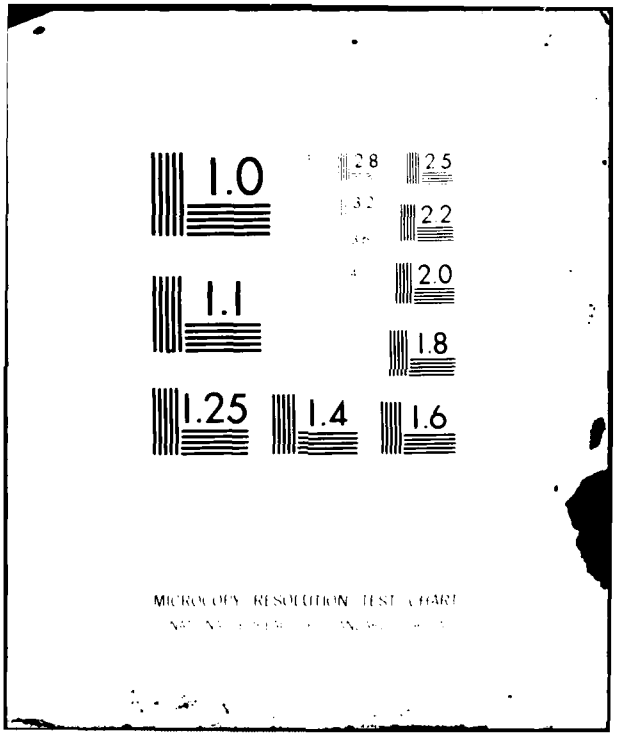
1.0
1.1
1.25
1.4
1.6
2.0
1.8
2.2
2.5
MICROCOPY RESOLUTION TEST CHART

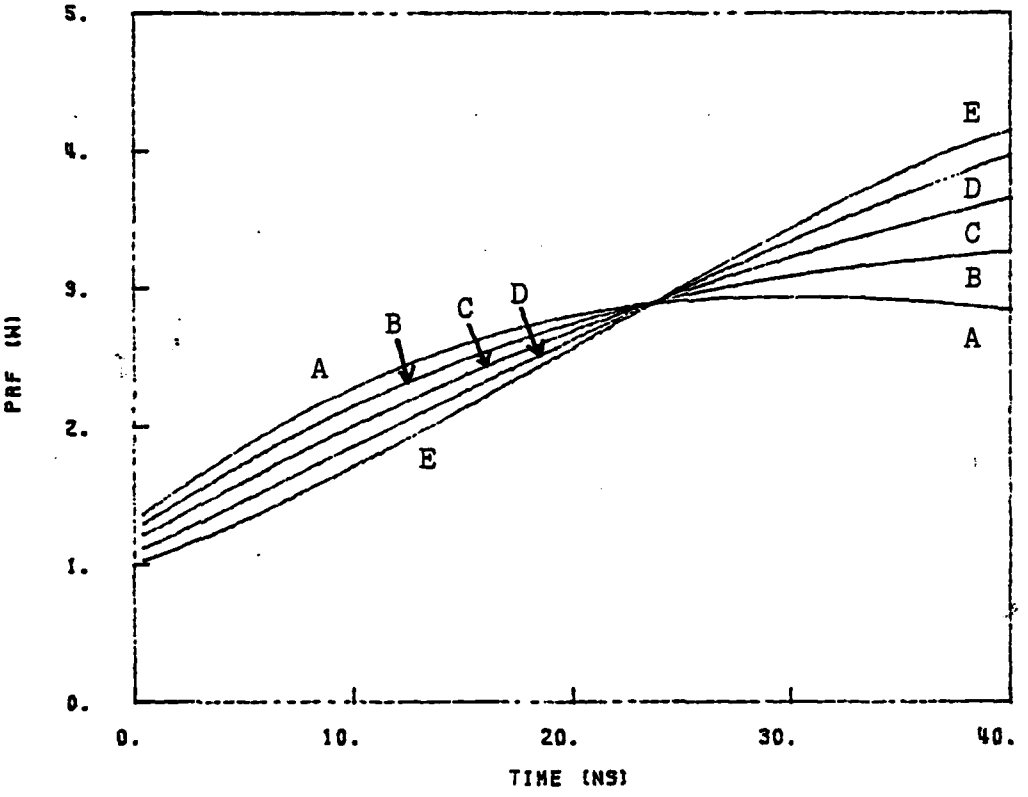

FIG. 4.3 POWER VARIATIONS OF THE PULSED OSCILLATOR UNDER VARIOUS BIAS CURRENT WAVEFORMS.

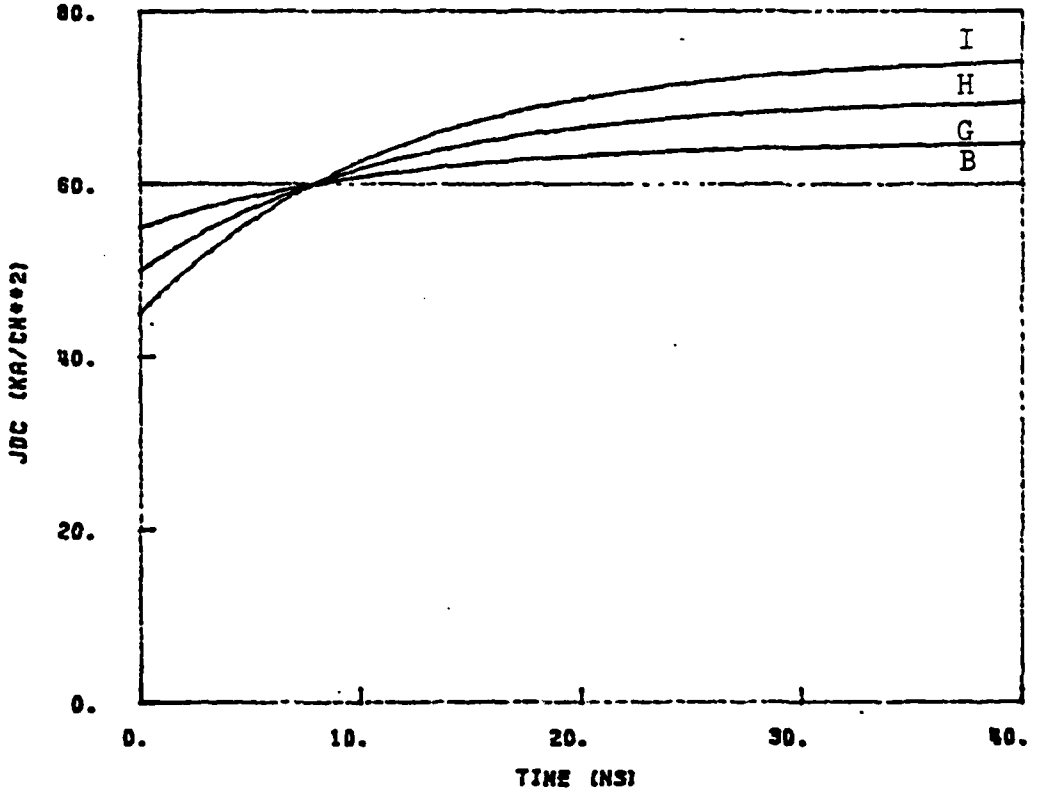

FIG. 4.4 EXPONENTIALLY INCREASING CURRENT WAVEFORMS USED TO STUDY THE EFFECTS OF EXPONENTIALLY AND LINEARLY INCREASING CURRENT WAVEFORMS ON THE FREQUENCY DRIFT.

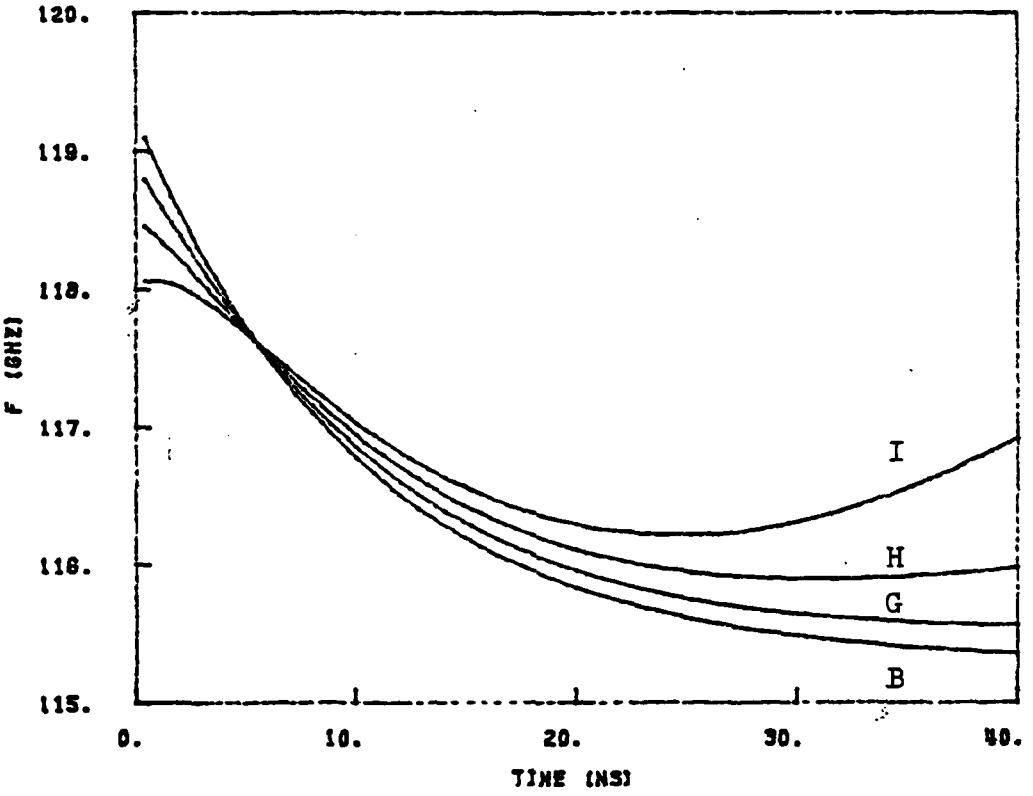

FIG. 4.5 FREQUENCY RESPONSES OF THE PULSED OSCILLATOR WITH EXPONENTIALLY INCREASING CURRENT WAVEFORMS.

I, the temperature rise of the diode is 202°C, and f_d is 1.9 GHz (f_{max} = 118.1 GHz, f_{min} = 116.2 GHz). The temperature coefficient of 9.4 MHz/°C is better than that of curve E (11.2 MHz/°C, J_{dc} increases from 45 to 75 kA/cm^2 linearly).

4.3 Optical Injection Compensation

The current produced by photon injection is subject to multiplication in the same way as the reverse saturation current. A small-signal analysis which describes the primary effects of photon injection on the IMPATT diode has been derived.[25] Photon injection produces an increase in device conductance G_d and a decrease in device susceptance[26-29] B_d. Variation of device admittance with photon injection is strongly frequency dependent, and much greater variation occurs at the lower frequency.[14] Therefore, the output power and oscillation frequency of the IMPATT oscillator can be controlled by photon injection. Injection at high intensity can be used to cease oscillation. Photon injection at low intensity can be used to modulate the amplitude and frequency of an IMPATT oscillator. The amount of modulation also depends on the microwave circuit and the operating condition.

It has been demonstrated that photon injection can be used to control the behavior of TRAPATT oscillators.[30] Frequency drift during the pulse may be eliminated by illuminating the device with an adequately shaped optical pulse. Under constant current bias, the effect of photon injection is to shift the oscillation higher in frequency. The reduction in frequency drift is larger for a time-varying optical pulse that increases more rapidly in intensity.

The influence of optical current shaping on the frequency drift can be described by Eq. 4.3, which is derived in the same way as the

derivation of Eq. 2.12, i.e.,

$$\frac{\partial(B_d + B_c)}{\partial f}\Delta f = A_1\Delta T + A_3\Delta I_{op} \quad , \tag{4.3}$$

where

$$A_3 = \frac{\partial B_d}{\partial V_{RF}} \frac{1}{\partial G_d/\partial V_{RF}} \frac{\partial G_d}{\partial I_{op}} - \frac{\partial B_d}{\partial I_{op}} \quad . \tag{4.4}$$

To evaluate A_3, the device properties are summarized as follows:

1. The device susceptance B_d increases with RF voltage ($\partial B_d/\partial V_{RF} > 0$).

2. The device conductance G_d increases with RF voltage ($\partial G_d/\partial V_{RF} > 0$).

3. The device conductance G_d increases with optical current ($\partial G_d/\partial I_{op} > 0$).

4. The device susceptance B_d decreases with optical current ($\partial B_d/\partial I_{op} < 0$).

The calculated result ($A_3 > 0$) suggests that the frequency drift during the pulse can be reduced with a time-varying optical current waveform.

Under constant current bias (J_{dc} = 60 kA/cm^2), the behavior of the IMPATT oscillator with photon injection has been studied. Figure 4.6 shows the various optical current waveforms used to study the effects of optical current shaping on the frequency drift and power variation of the pulsed IMPATT oscillator. For curve E, optical current density J_{op} increases from 0 to 1750 A/cm^2 linearly during the 40-ns pulsewidth.

Figure 4.7 shows the frequency responses of the pulsed oscillator under various optical current waveforms. The temperature rise of the

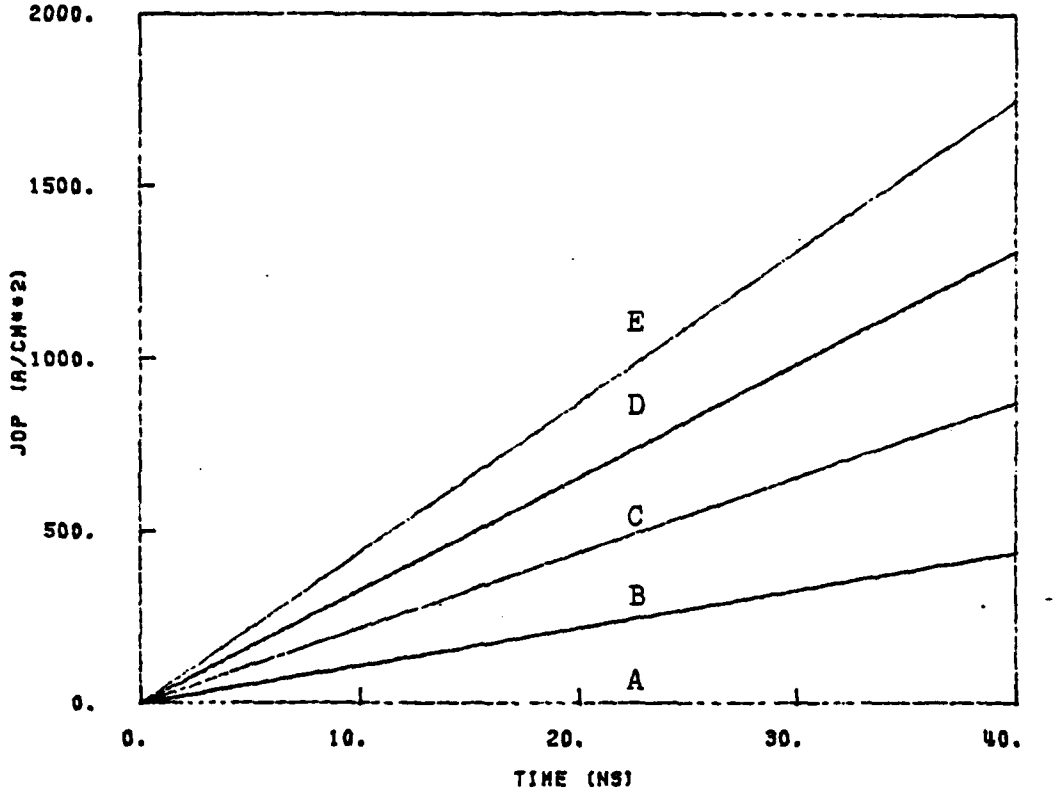

FIG. 4.6 VARIOUS OPTICAL CURRENT WAVEFORMS USED TO STUDY THE EFFECTS OF OPTICAL CURRENT SHAPING ON THE FREQUENCY DRIFT AND POWER VARIATION OF PULSED OSCILLATOR.

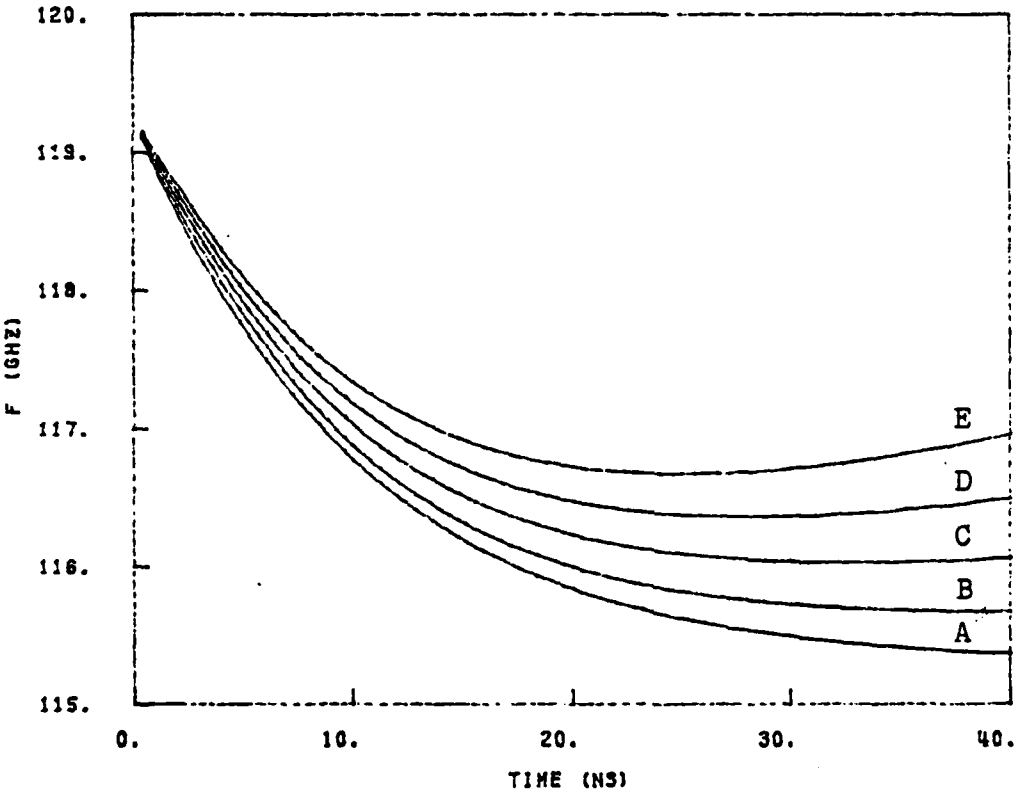

FIG. 4.7 FREQUENCY RESPONSES OF THE PULSED OSCILLATOR UNDER VARIOUS OPTICAL CURRENT WAVEFORMS.

diode with optical compensation (curve E) is 169.1°C, and f_d is 2.5 GHz (f_{max} = 119.2 GHz, f_{min} = 116.7 GHz). The temperature coefficient of 14.8 MHz/°C is smaller than that without compensation (22.1 MHz/°C, curve A). It can be seen that the frequency drift decreases with upward optical compensation. For curve E, frequency decreases from 119.2 to 116.7 GHz and then increases to 117.0 GHz. The reason for this increase is that the frequency decrease caused by temperature rise is overcompensated by optical current.

Figure 4.8 shows the power variation of the pulsed oscillator under various optical current waveforms. When there is no photon injection (curve A) output power increases from 1.3 to 3.27 W. With upward optical compensation (curve E), output power increases from 1.3 to 2.1 W and then decreases to 1.9 W. It can be seen that power variation and the frequency drift are improved with upward optical compensation.

To study the effects of exponentially and linearly increasing the optical current waveforms on the frequency drift, the exponentially increasing optical current waveforms as shown in Fig. 4.9 are used in the simulation. The calculated results indicate that the temperature rise of the diode remains the same. Figure 4.10 shows the frequency responses of the pulsed oscillator with exponentially increasing optical current waveforms. For curve I, the optical current density J_{op} = 1750 $(1 - e^{-t/\tau_{th}})$ A/cm^2 and frequency decreases from 129.3 to 116.9 GHz during the pulse. This frequency drift is the same as that of the linearly increasing optical current waveform (curve E of Fig. 4.7).

4.4 Injection Locking

Injection locking is a conventional technique to stabilize the frequency and tune solid-state oscillators. There are several

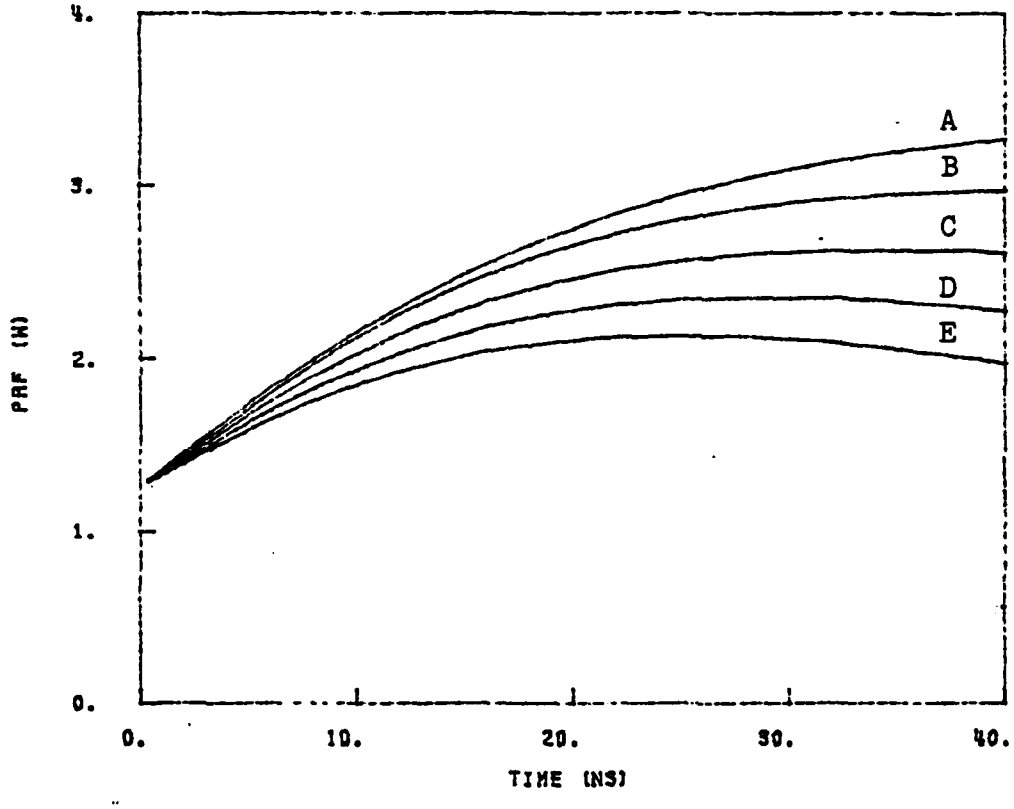

FIG. 4.8 POWER VARIATIONS OF THE PULSED OSCILLATOR UNDER VARIOUS OPTICAL CURRENT WAVEFORMS.

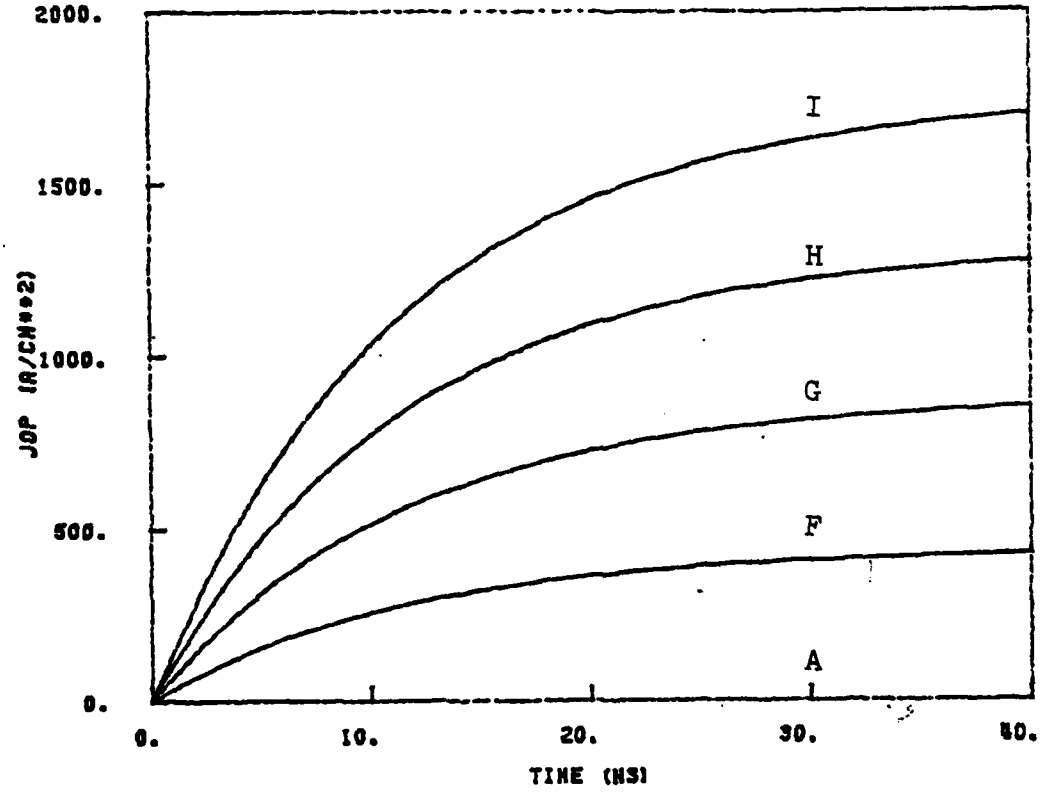

FIG. 4.9 EXPONENTIALLY INCREASING OPTICAL CURRENT WAVEFORMS.

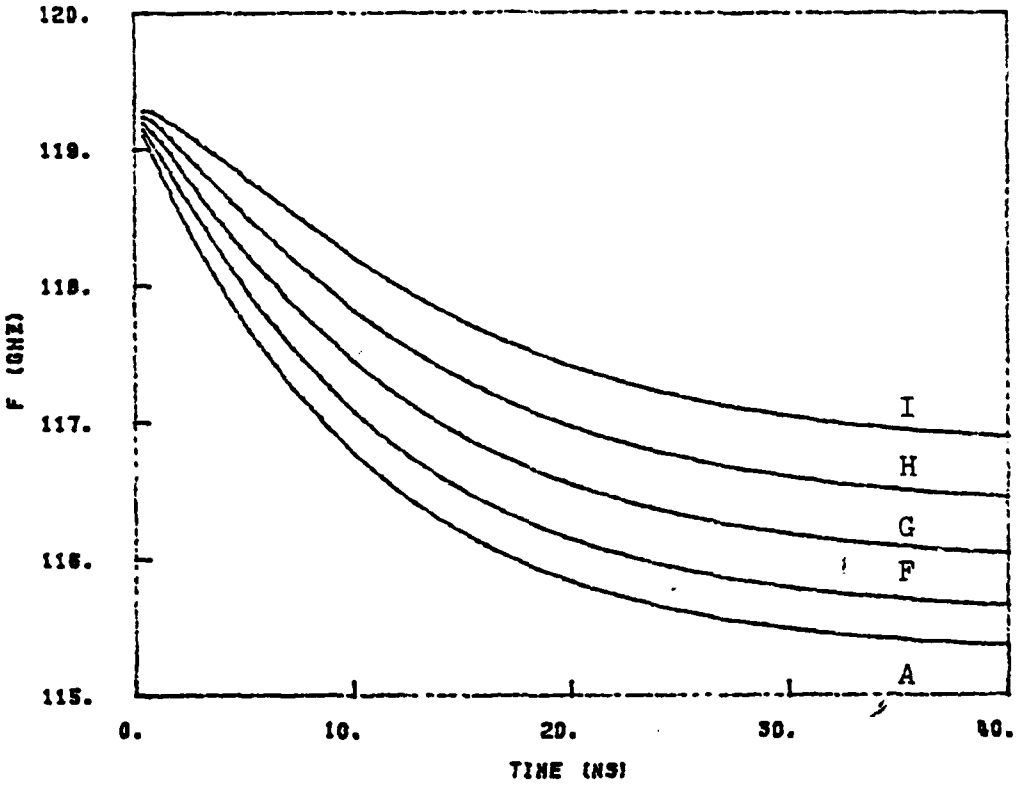

FIG. 4.10 FREQUENCY RESPONSES OF THE PULSED OSCILLATOR WITH EXPONENTIALLY INCREASING OPTICAL CURRENT WAVEFORMS.

types of injection locking:[31]

1. Fundamental frequency injection locking: The injection frequency f_i is nearly equal to the free-running frequency to be locked f_o.

2. Subharmonic injection locking: f_i is nearly equal to $(1/n)f_o$, where n is an integer larger than one. A low frequency signal can be used for injection but the locking bandwidth becomes narrower when n is increased.

3. Sideband-wave injection locking: Two injection frequencies are used; one is a low frequency signal $f_{inj,1}$ and the other with frequency $f_{inj,2} = f_o \pm f_{inj,1}$.

CW and pulsed oscillators can be stabilized in frequency by injection of a low-level signal into the oscillator through a circulator. In the simplest case, the injection frequency is nearly equal to that of a free-running oscillator. When the difference between two frequencies is sufficiently small, the oscillator will be locked and the frequency difference becomes negligible. This section describes the performance of a short pulse (40 ns), low duty cycle, and pulsed injection locked oscillator. The RF voltage and phase transients in the time domain and the effects of the injection power and frequency on the transient behavior can be studied.[32] In the calculation the following parameters are used:

injection frequency f_i = 117 GHz,

injection power P_{in} = 0.2 W (10 dB below the output power of the free-running oscillator),

circuit conductance G = 20 mmho,

circuit susceptance B_c = 117 mmho,

initial phase angle $\theta(0) = 0$,

device capacitance C_d = 0.208 pF, and

injection current $I_1 = \sqrt{8\ GP_{in}}$ = 0.18 A.

For a given injection current and frequency, the intital RF voltage $V_{RF}(0)$ is given by

$$V_{RF}(0) = \frac{I_1}{\sqrt{(\omega_i C_d)^2 + (G^2 + B_c^2)}} = 0.93\ V\ .$$

Without injection locking, the temperature increase causes the frequency to drift under a flat bias current pulse (J_{dc} = 60 kA/cm^2). In the case of an injection locked oscillator, the leading edge portions of the RF oscillation are not locked because of the large frequency transients during turn-on, and the oscillator is locked after the oscillation buildup is accomplished. With injection locking, frequency drift during the pulse is eliminated, and the oscillator is not locked during turn-on as shown in Fig. 4.11. When injection power is decreased, the locked portion of the pulsewidth decreases as shown:

I_1 (A)	Locked Portion (ns)
0.18	2 to 40
0.12	3 to 21
0.06	6 to 15

The oscillator is not locked when t is not within the locked portion.

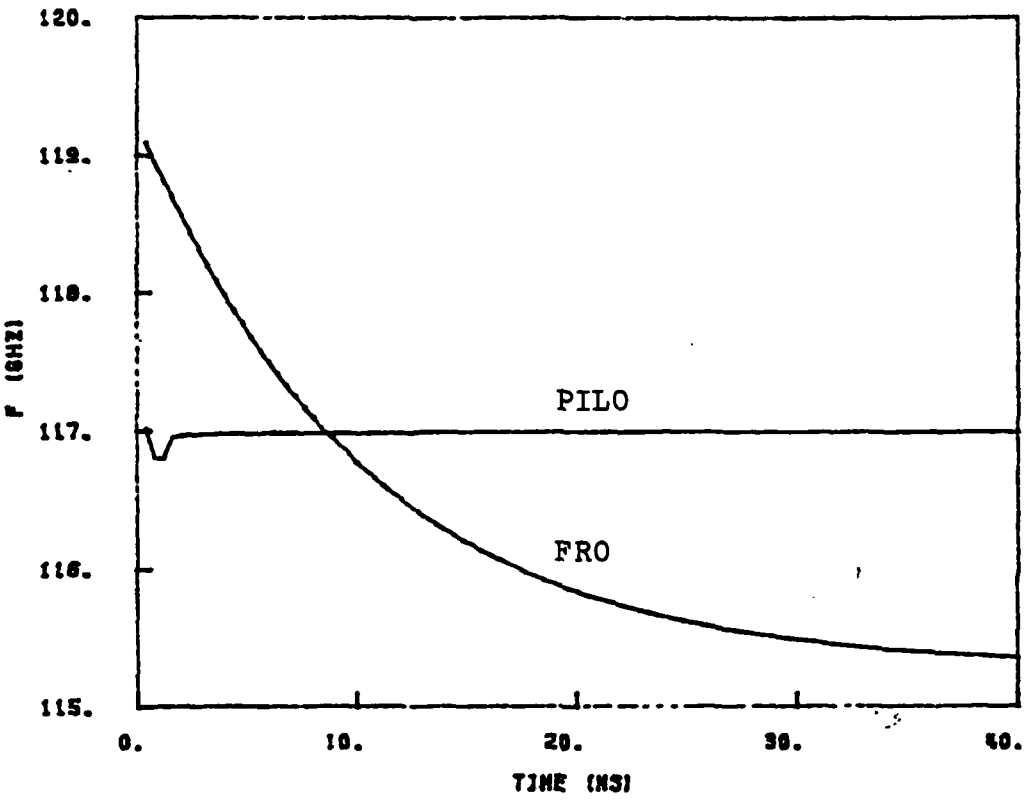

FIG. 4.11 FREQUENCY RESPONSES OF FREE-RUNNING AND PULSED INJECTION LOCKED OSCILLATORS.

SECTION V. SUMMARY

This report has described and given examples of many of the effects which are important in the performance of pulsed millimeter-wave IMPATT-diode oscillators. These effects, which include oscillator turn-on transients, frequency chirp, thermal limitations, bias circuit dynamics, optical injection and injection locking can be studied quantitatively using the device-circuit interactive model developed here to include these phenomena. Based on this model, a better understanding of optical device and circuit properties and optimal control of pulsed millimeter-wave oscillators for radar systems and other applications is possible.

LIST OF REFERENCES

1. Proceedings of the Symposium on Submillimeter Waves, Polytechnic Press of the Polytechnic Institute of Brooklyn, New York, 1970.

2. Kihm, T., Beebe, M., Brenneise, C. and Weglein, R. D., "A W-Band, Coherent, Pulsed-Compression Radar Transceiver Using Linear Frequency Modulation," 1981 IEEE Internal Microwave Symposium Digest, pp. 414-416.

3. Kurokawa, K., "Injection Locking of Microwave Solid-State Oscillators," Proc. of IEEE, vol. 61, No. 10. pp. 1386-1410, October 1973.

4. Sze, S. M., Physics of Semiconductor Devices, John Wiley and Sons, Inc., New York, 1969.

5. Culshaw, B., Giblin, R. A., and Blakey, P. A., Avalanche Diode Oscillator, Taylor & Francis Ltd., London, 1978.

6. Gustafsson, L., Hasson, G.H.B. and Lundstrom, K. I., "On the Use of Describing Functions in the Study of Nonlinear Active Microwave Circuits," IEEE Trans. on Microwave Theory and Techniques, vol. MTT-20, No. 6, pp. 402-409, June 1972.

7. Collin, R. E., Foundations for Microwave Engineering, McGraw-Hill, New York, pp. 155-156, 1966.

8. Burmawi, M.Y., "Optical Effects in Millimeter-Wave IMPATT Diodes and Oscillators," Ph.D. Dissertation, The University of Michigan, Ann Arbor, 1981.

9. Lewin, L., "A Contribution to the Theory of Probes in Waveguides," Inst. of Electrical Engineers Proceedings, vol. 105, pt. c, pp. 109-116, 1958.

10. Chang, K. and Ebert, R. L., "W-Band Power Combiner Design," IEEE Trans. on Microwave Theory and Techniques, vol. MTT-28, No. 4, pp. 295-304, April 1980.

11. Gibbons, G., "Transient Temperature Response of an Avalanche Diode," Solid-State Electronics, vol. 133, No. 8, pp. 799-806, August 1969.

12. DiLorenzo, J. V., Niehaus, W. C., Velerbir, J. R., Jr. and Iglesias, D. E., "Beam-Lead Plated Heat Sink GaAs IMPATT Part I. Performance," IEEE Trans. on Electron Devices, vol. ED-11, No. 8, pp. 509-514, August 1975.

13. Haitz, R. H., Stover, H. L. and Tolar, N. J., "A Method for Heat Flow Resistance Measurements in Avalanche Diodes," IEEE Trans. on Electron Devices, vol. ED-16, No. 5, pp. 438-444, May 1969.

14. Schroeder, W. E. and Haddad, G. I., "The Effect of Temperature on the Operation of an IMPATT Diode," Proc. of IEEE (Lett.), vol. 59, No. 8, pp. 1242-1244, August 1971.

15. Makino, T., "Effect of the Operational Modes on the Temperature Dependence of the Gunn Diode Admittance," Solid-State Electronics, vol. 22, pp. 761-769, 1979.

16. Fong, T. T. and Kuno, H. J., "Millimeter-Wave Pulsed IMPATT Sources," IEEE Trans. on Microwave Theory and Techniques, vol. MTT-27, No. 5, pp. 492-499, May 1979.

17. Chudobiak, W. J., et al., "The Effect of Junction Temperature on the Output Power of a Silicon IMPATT Diode," Proc. of IEEE, vol. 60, pp. 340-341, March 1972.

18. Misawa, T., "Negative Resistance in p-n Junctions Under Avalanche Breakdown Condition, Part I & II," IEEE Trans. on Electron Devices, vol. ED- ,No. 1, pp. 137-151, January 1966.

19. Hirachi, Y., Nakagami, T., Toyama, Y., and Fukukawa, Y., "High-Power 50-GHz Double-Drift Region IMPATT Oscillators with Improved Bias Circuits for Eliminating Low-Freuqency Instabilities," IEEE Trans. on Microwave Theory and Techniques, vol. MTT-24, No. 11 pp. 731-737, November 1976.

20. Bracket, C. A., "The Elimination of Tuning-Induced Burnout and Bias-Circuit Oscillations in IMPATT Oscillators," Bell System Tech. J., vol. 52, No. 3, pp. 271-307, March 1973.

21. Vyse, B., and Levinson, H., "The Stability of Magnetrons Under Short Pulse Conditions," IEEE Trans. on Microwave Theory and Techniques, vol. 29, No. 7, pp. 739-745, July 1981.

22. Howes, M. J. and Morgan, D. V., Microwave Devices, Device Circuit Interactions, Wiley-Interscience, New York, 1976.

23. Morgan, D. V. and Howes, M. J., Microwave Solid State Devices and Applications, Peter Peregrinus Ltd., 1980.

24. Kondo, A., Ishii, T. and Shirahata, K., "Simple Stabilizing Method for Solid-State Microwave Oscillators," IEEE Trans. on Microwave Theory and Techniques, vol. MTT-22, No. 11, pp. 970-972, November 1974.

25. Sanderson, A. C. and Jordan, A. G., "Electron Beam Control of IMPATT Diodes," Solid State Electronics, vol. 15, No. 1, pp. 142-144, January 1972.

26. Gerlach, W. A. and Wellman, R., "The Behavior of a Pulsed Millimeter Wave (70 GHz) IMPATT Diode Oscillator during Laser Illumination," IEEE 1980 Int. Microwave Symposium Digest, pp. 70-72.

27. Kiehl, R. A., "Optical Control of IMPATT Oscillator Dynamics," 1978 IEDM Tech. Digest, pp. 286-289.

28. Forrest, J. R. and Seeds, A. J., "Analysis of the Optically Controlled IMPATT Oscillator," Solid-State and Electron Devices, vol. 3, No. 5, pp. 161-169, September 1979.

29. Sun, H. J., Gutmann, R. J. and Borrego, J. M., "Optical Tuning in GaAs MESFET Oscillators," IEEE 1981 Int. Microwave Symposium Digest, pp. 40-42.

30. Kiehl, R. A. and Eernisse, E. P., "Control of TRAPATT Oscillations by Optically Generated Carriers," IEEE Trans. on Electron Devices, vol. ED-24, No. 3, pp. 275-277, March 1977.

31. Okamoto, H. and Ikeda, M., "Cavity Stabilization and Electronic Tuning of a Millimeter-Wave IMPATT Diode Oscillator by Parametric Interaction," IEEE Trans. on Microwave Theory and Techniques, vol. MTT-26, No. 6, pp. 420-424, June 1978.

32. Parlidis, D., Hartnagel, H. L. and Tomizawa, K., "Dynamic Considerations of Injection Locked Pulsed Oscillators with Very Fast Switching Characteristics," IEEE Trans. on Microwave Theory and Techniques, vol. MTT-26, No. 3, pp. 162-169, March 1978.

APPENDIX

CIRCUIT MODEL USED IN SECTION IV

The circuit model used in Section IV is a post-in-waveguide circuit[16] which has the following circuit and package parameters:

waveguide width = 65 mil,

waveguide height = 15 mil,

radius of the bias post = 11 mil,

bias post position = 32.5 mil,

waveguide short position = 19 mil,

length of the bias coaxial line = 45 mil,

load of the bias coaxial line = 0,

characteristic impedance of the bias coaxial line = 50 Ω,

package parasitic inductor L_p = 0.03 nH, and

package parasitic capacitor C_p = 0.1 pF.

Figure A.1. shows the calculated circuit admittance as a function of frequency seen from the diode chip. In the calculation the package inductance and capacitance are taken into consideration.

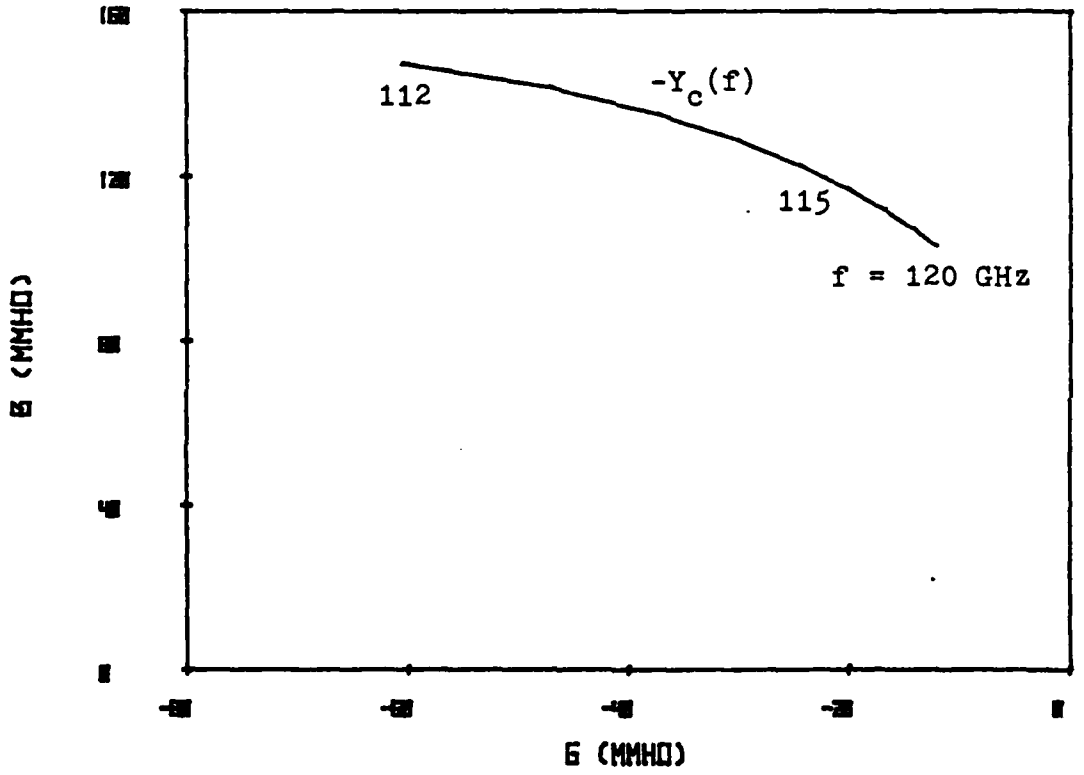

FIG. A.1 NEGATIVE OF CIRCUIT ADMITTANCE AS A FUNCTION OF FREQUENCY SEEN FROM THE DIODE CHIP.

LIST OF PUBLICATIONS AND TECHNICAL REPORTS PUBLISHED

1. M. Y. Burmawi, "Optical Effects in Millimeter-Wave IMPATT Diodes and Oscillators," Technical Report No. 153 and Ph.D. Dissertation, Electron Physics Laboratory, Department of Electrical and Computer Engineering, The University of Michigan, Ann Arbor, October 1981.

2. M. Y. Burmawi, D. F. Peterson, G. I. Haddad, "Optical Control of Millimeter-Wave Silicon IMPATT Diodes," in progress, to be submitted to IEEE Trans. on Electron Devices.

LIST OF SCIENTIFIC PERSONNEL AND ADVANCED DEGREES

Professor D. F. Peterson, Principal Investigator

Professor G. I. Haddad, Senior Investigator

M. Y. Burmawi, Research Assistant, Ph.D., October 1981

Y. S. Hwang, Research Assistant

C. Shiebold, Research Assistant, M.S., January 1980

C. K. Pao, Research Assistant


ATE
LMED
8